



LEHIGH  
UNIVERSITY

Library &  
Technology  
Services

The Preserve: Lehigh Library Digital Collections

# A Mechanistic Study Of The Anomeric Specificity Of Fructose 1,6-bisphosphate Aldolase (e.C.4.1.2.13).

## Citation

WAUD, JOHN MARTIN. *A Mechanistic Study Of The Anomeric Specificity Of Fructose 1,6-Bisphosphate Aldolase (e.C.4.1.2.13)*. 1978, <https://preserve.lehigh.edu/lehigh-scholarship/graduate-publications-theses-dissertations/theses-dissertations/mechanistic-6>.

Find more at <https://preserve.lehigh.edu/>

*This document is brought to you for free and open access by Lehigh Preserve. It has been accepted for inclusion by an authorized administrator of Lehigh Preserve. For more information, please contact [preserve@lehigh.edu](mailto:preserve@lehigh.edu).*

## INFORMATION TO USERS

This material was produced from a microfilm copy of the original document. While the most advanced technological means to photograph and reproduce this document have been used, the quality is heavily dependent upon the quality of the original submitted.

The following explanation of techniques is provided to help you understand markings or patterns which may appear on this reproduction.

1. The sign or "target" for pages apparently lacking from the document photographed is "Missing Page(s)". If it was possible to obtain the missing page(s) or section, they are spliced into the film along with adjacent pages. This may have necessitated cutting thru an image and duplicating adjacent pages to insure you complete continuity.
2. When an image on the film is obliterated with a large round black mark, it is an indication that the photographer suspected that the copy may have moved during exposure and thus cause a blurred image. You will find a good image of the page in the adjacent frame.
3. When a map, drawing or chart, etc., was part of the material being photographed the photographer followed a definite method in "sectioning" the material. It is customary to begin photoing at the upper left hand corner of a large sheet and to continue photoing from left to right in equal sections with a small overlap. If necessary, sectioning is continued again – beginning below the first row and continuing on until complete.
4. The majority of users indicate that the textual content is of greatest value, however, a somewhat higher quality reproduction could be made from "photographs" if essential to the understanding of the dissertation. Silver prints of "photographs" may be ordered at additional charge by writing the Order Department, giving the catalog number, title, author and specific pages you wish reproduced.
5. PLEASE NOTE: Some pages may have indistinct print. Filmed as received.

**University Microfilms International**

300 North Zeeb Road

Ann Arbor, Michigan 48106 USA

St. John's Road, Tyler's Green

High Wycombe, Bucks, England HP10 8HR

7904324

WAUD, JOHN MARTIN  
A MECHANISTIC STUDY OF THE ANOMERIC  
SPECIFICITY OF FRUCTOSE 1,6-BISPHOSPHATE  
ALDOLASE (E.C.4.1.2.13).

LEHIGH UNIVERSITY, PH.D., 1978

University  
Microfilms  
International

300 N. ZEEB ROAD, ANN ARBOR, MI 48106

A MECHANISTIC STUDY OF THE ANOMERIC SPECIFICITY OF  
FRUCTOSE 1,6-BISPHOSPHATE ALDOLASE (E.C.4.1.2.13)

by

John Martin Waud

A Dissertation

Presented to the Graduate Committee  
of Lehigh University  
in Candidacy for the Degree of  
Doctor of Philosophy

in

Molecular Biology

Lehigh University

1978

Approved and recommended for acceptance as a dissertation in partial fulfillment of the requirements for the degree of Doctor of Philosophy.

Keith J. Schray  
Professor in Charge

Accepted: 7/31/38  
Date

Special committee directing  
the doctoral work of John  
Martin Waud

Keith J. Schray  
Dr. Keith J. Schray, Chairman

Ned D. Heindel  
Dr. Ned D. Heindel

Steven Krawiec  
Dr. Steven Krawiec

Jeffrey A. Sands  
Dr. Jeffrey A. Sands

Stephen W. Schaffer  
Dr. Stephen W. Schaffer

### Acknowledgments

I wish to thank Dr. Stephen J. Benkovic for the use of his rapid kinetic equipment and for his technical assistance in using the equipment. I would also like to thank Brian Cunningham, Elizabeth Howell, and Ellen Feldman for their technical assistance.

I am also greatly indebted to Mrs. Claire T. Waud and Mrs. Doris J. Waud for their assistance in preparing the manuscript and for their patient support throughout my graduate education.

Finally, I wish to express my appreciation to Dr. Keith J. Schray without whose advice, encouragement, and support none of the work contained herein would have been possible. I am particularly indebted to Dr. Schray for his ready accessibility and for the many, many hours he spent discussing this work with me.

## Dedication

The author dedicates this work to the memory of his late father, Ira B. Waud who by his encouragement and support, along with that of his mother, Mrs. Claire T. Waud, are largely responsible for any educational success he has attained.

## Table of Contents

	<u>Page</u>
Certificate of Approval	ii
Acknowledgments	iii
Dedication	iv
Table of Contents	v
List of Tables	vi
List of Figures	vii
Abstract	1
Introduction	3
Rationale	33
Experimental Methods	37
Results	82
Discussion	167
Conclusions	211
Bibliography	217
Vita	222

## List of Tables

<u>Table</u>		<u>Page</u>
1	Properties of Some Aldolases	5
2	Aldolase Purification by Procedure of Gracy et al. Starting with 500 gms of Frozen Rabbit Liver	40
3	Aldolase Purification by Procedure of Chappel et al. Starting with 500 gms of Frozen Rabbit Liver	44
4	Aldolase Purification by Procedure of Chappel et al. Starting with 500-800 gms of Fresh Rabbit Liver	47
5	Loading of Polyacrylamide Electrophoresis Gels - Procedure of Ornstein and Davis	76
6	Loading of Polyacrylamide Electrophoresis Gels - Procedure of Reisfeld et al.	77
7	Measurement of the Rate of Liver Aldolase When $\beta$ -FBP is Slowly Generated by PFK	129

## List of Figures

<u>Figure</u>		<u>Page</u>
1	Anomeric Composition of FBP	7
2	Stopped Flow Apparatus	10
3	Rapid Quench Apparatus	13
4	Anomeric Specificity in Glycolysis and Gluconeogenesis	16
5	Anomeric Specificity of the Enzymes Utilizing F6P or FBP as Substrates	18
6	Schematic Representation of the Reactions Involved in the Measurement of the Rate of Liver Aldolase Under Conditions of Slow Generation of FBP by PFK	22
7	Mechanism of Muscle Aldolase	25
8	Lineweaver-Burk Plot for Muscle Aldolase	56
9	Lineweaver-Burk Plot for Liver Aldolase	58
10	Reaction Scheme Used in Computer Simulations	61
11	Simulation of Competitive Formation of the Michaelis Complexes	63
12	Polyacrylamide Gel Electrophoresis Patterns by Procedure of Ornstein and Davis	71
13	Polyacrylamide Gel Electrophoresis Patterns by Procedure of Reisfeld et al.	80
14	Stopped Flow Oscilloscope Traces	84
15	First-order Replot for Muscle Aldolase Stopped Flow Experiment	86
16	First-order Replot for Liver Aldolase Stopped Flow Experiment	89

<u>Figure</u>	<u>Page</u>
17 First-order Replot for Mixed Aldolase Stopped Flow Experiment	92
18 Simulation of Utilization of $\alpha$ -FBP by Liver Aldolase	94
19 Simulation of Utilization of Open FBP by Liver Aldolase	96
20 Simulation of Utilization of $\beta$ -FBP by Liver Aldolase	98
21 Simulation of Mixed Liver Aldolase Plus Muscle Aldolase Experiment with Liver Aldolase Utilization of $\alpha$ - and $\beta$ - FBP	101
22 Simulation of Mixed Liver Aldolase Plus Muscle Aldolase Experiment with Liver Aldolase Utilization of $\alpha$ - FBP	103
23 Simulation of Mixed Liver Aldolase Plus Muscle Aldolase Experiment with Liver Aldolase Utilization of $\beta$ - FBP	105
24 Simulation of Mixed Liver Aldolase Plus Muscle Aldolase Experiment with Liver Aldolase Utilization of Open FBP	107
25 Competitive Inhibition of Liver Aldolase by $\alpha$ - and $\beta$ - Methylfructofuranoside 1,6-bisphosphate	110
26 Competitive Inhibition of Muscle Aldolase by $\alpha$ - and $\beta$ - Methylfructofuranoside 1,6-bisphosphate	112
27 Inhibition of Liver Aldolase by $\alpha$ -2,5- Anhydroglucitol 1,6-bisphosphate	114
28 Competitive Inhibition of Liver Aldolase by Glucitol 1,6-bisphosphate	116
29 Competitive Inhibition of Liver Aldolase by Ribulose 1,5-bisphosphate	119
30 Inhibition of Liver Aldolase by Ribulose 5-phosphate	121

<u>Figure</u>	<u>Page</u>
31 Competitive Inhibition of Liver Aldolase by Ribose 5-phosphate	123
32 Dowex-2 (Cl) Elution Pattern from Measurement of Liver Aldolase Rate with $\beta$ - FBP Generated by PFK - 9 Nano-equivalents of Aldolase Sites	125
33 Dowex-2 (Cl) Elution Pattern from Measurement of Liver Aldolase Rate with $\beta$ - FBP Generated by PFK - 56 Nano-equivalents of Aldolase Sites	127
34 Dowex-2 (Cl) Elution Pattern Using 50mM HCl from $^3\text{H}$ Exchange into DHAP by Liver Aldolase - 2 Minutes of Exchange	131
35 Dowex-2 (Cl) Elution Pattern Using 50mM HCl from $^3\text{H}$ Exchange into DHAP by Liver Aldolase - 4 Minutes of Exchange	133
36 Dowex-2 (Cl) Elution Pattern Using 50mM HCl from $^3\text{H}$ Exchange into DHAP by Liver Aldolase - 10 Minutes of Exchange	135
37 Dowex-2 (Cl) Elution Pattern Using 50mM HCl from $^3\text{H}$ Exchange into DHAP by Liver Aldolase - 90 Minutes of Exchange	137
38 Progress Curve for $^3\text{H}$ Exchange into DHAP by Liver Aldolase	139
39 First-order Replot for $^3\text{H}$ Exchange into DHAP by Liver Aldolase	141
40 Inactivation of Muscle Aldolase by 1-Cl 2,6-dinitrobenzene	144
41 Inactivation of Muscle Aldolase by 1-Cl 2,4-dinitrobenzene	146
42 Inactivation of Liver Aldolase by 1-Cl 2,4-dinitrobenzene	148

<u>Figure</u>	<u>Page</u>
43 Inactivatiin of Liver Aldolase by 4-hydroxymercuribenzoate	151
44 Inactivation of Liver Aldolase by Pyridoxal 5-phosphate	153
45 Log % Activity Remaining vs. Time for PLP Inactivation of Muscle Al- dolase	155
46 Nonintegrated First-order Replot for Inactivation of Muscle Aldolase by 10 $\mu$ M PLP	157
47 Nonintegrated Second-order Replot for Inactivation of Muscle Aldolase by 10 $\mu$ M PLP	159
48 Log % Activity Remaining vs. Time for 10 $\mu$ M PLP Inactivation of Muscle Al- dolase with Zero Activity as Infinite Time Value	161
49 Inactivation of Liver Aldolase by 200 $\mu$ M Pyridoxal 5-phosphate	164
50 Log % Activity Remaining vs. Time for 200 $\mu$ M Pyridoxal 5-phosphate Inactiva- tion of Liver Aldolase	166
51 Schematic Representation of Simulated Competitive Formation of the Michaelis Complex	175
52 Schematic Representation of Simulation of Utilization of $\alpha$ - FBP by Liver Aldolase	178
53 Schematic Representation of Simulation of Utilization of Open FBP by Liver Aldolase	180
54 Schematic Representation of Simulation of Utilization of $\beta$ - FBP by Liver Al- dolase	183

<u>Figure</u>		<u>Page</u>
55	Schematic Representation of Simulation of Mixed Liver Aldolase Plus Muscle Aldolase Experiment with Liver Utilization of $\alpha$ -FBP	185
56	Schematic Representation of Simulation of Mixed Liver Aldolase Plus Muscle Aldolase Experiment with Liver Utilization of $\alpha$ - and $\beta$ -FBP	188
57	Schematic Representation of Simulation of Mixed Liver Aldolase Plus Muscle Aldolase Experiment with Liver Utilization of $\beta$ -FBP	190
58	Schematic Representation of Simulation of Mixed Liver Aldolase Plus Muscle Aldolase Experiment with Liver Utilization of Open FBP	193
59	Structures of Substrate Analogues Employed as Inhibitors	196
60	Plot of $1/k$ Inactivation vs. $1/[PLP]$ for PLP Inactivation of Muscle Aldolase	206

## Abstract

The anomeric specificity of liver aldolase (E.C. 4.1.2.13) has been studied by rapid kinetic techniques and computer simulation. From the rapid kinetic measurements the enzyme has been demonstrated to have a first-order utilization of 100% of the substrate present. This was in contrast to the aldolase isolated from muscle tissue which has been shown to have a biphasic utilization of substrate. The results of the rapid kinetic measurements taken together with the results of computer simulation indicated that liver aldolase utilizes  $\beta$ -FBP, open FBP, or both as its substrate. This conclusion was supported by the results of inhibition studies which employed substrate analogues. Further, by measuring the rate of liver aldolase when  $\beta$ -FBP is slowly generated by phosphofructokinase, it was additionally concluded that the open form of FBP alone is most likely not the substrate of this enzyme.

Some general aspects of the mechanism of liver aldolase were investigated as well. The rate of exchange of  $^3\text{H}$  into DHAP by this enzyme appears to indicate that the rate limiting step for the overall reaction mechanism may not be one of the steps involved in the exchange reaction. The results of these experiments were not clear cut and additional experiments

may be required to fully resolve this question.

By employing group specific inactivating agents such as chlorodinitrobenzene and 4-hydroxymercuribenzoate, it was possible to demonstrate the presence of a cysteine group at the active site of liver aldolase. The inactivation of liver aldolase by pyridoxal 5-phosphate was also studied. It was found that much higher levels of pyridoxal 5-phosphate were required to inactivate liver aldolase than were required to inactivate muscle aldolase.

Five carbon mono- and bisphosphate sugars were studied as probes of the binding interaction between liver aldolase and FBP. It was found that liver aldolase does not appear to have a binding site for the 6-phosphate of FBP.

All of the above findings are discussed in light of their implications to the molecular biology of cellular regulation and evolution.



Class I aldolases have a molecular weight of 150-160,000, are composed of four subunits, and require no metal ion for activity.<sup>2,3</sup> In addition, Class I enzymes are broken down into types according to the source from which the enzyme has been isolated. Type A is isolated from muscle tissue, type B from liver tissue, and type C is isolated from brain tissue. These types are distinct chemical species and as such have distinct chemical properties.

Class II aldolases are those which do not form a Schiff base intermediate, but rather, require a metal ion for catalytic activity, Class II aldolases in general resemble the aldolase isolated from yeast with respect to their chemical properties. Class II aldolases have a molecular weight of about 70,000 and are made up of two subunits.<sup>4,5</sup> The properties of some types of aldolases are summarized in Table I.

#### Rapid Kinetic Techniques to Study Anomeric Specificity

The substrate of aldolase, FBP, is predominantly in a cyclic hemiketal form in aqueous solution. The hemiketal may have two stereochemical forms about the anomeric carbon (the carbon which has the ketone moiety in the open chain form). These stereochemical forms are referred to as the  $\alpha$ -anomer and the  $\beta$ -anomer. See Figure I.

The various types and classes of aldolases have

Table 1

Properties of Some Aldolases

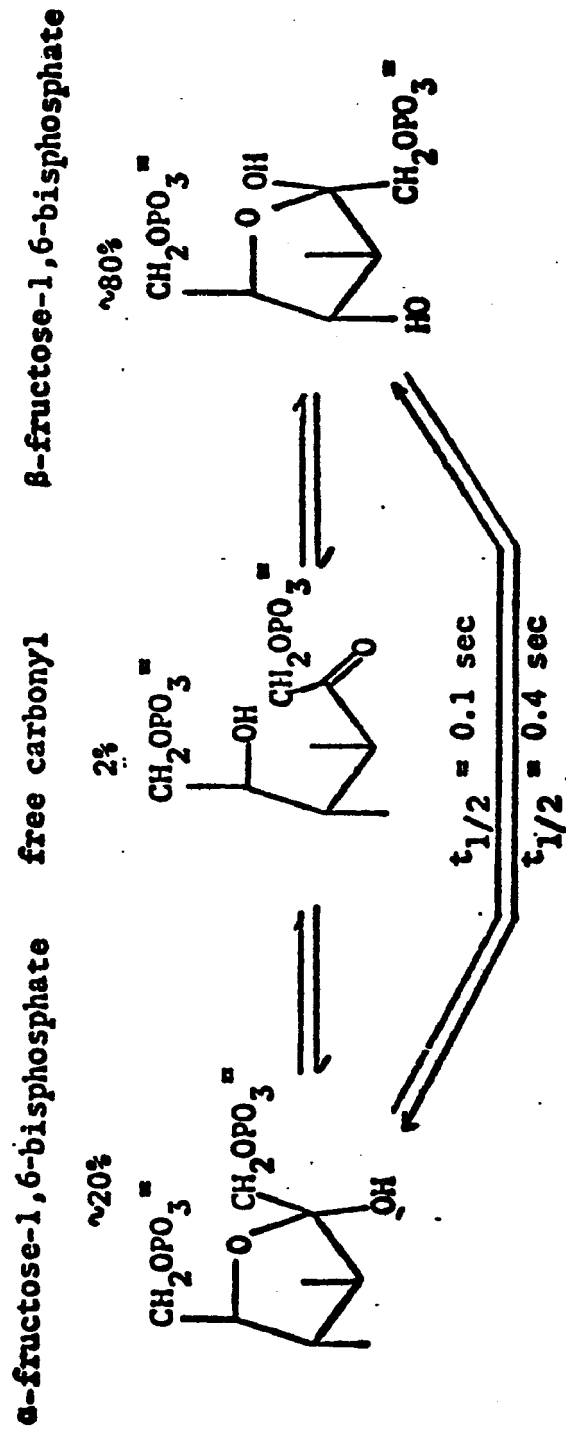
<u>Source</u>	<u>MW</u>	<u>Subunits</u>	<u>Metal</u>	<u>K<sub>M</sub></u>
Rabbit Muscle	160,000	4	None	$2 \times 10^{-5}$
Rabbit Liver	160,000	4	None	$2 \times 10^{-6}$
Yeast	70,000	2	Zinc	$* 4 \times 10^{-4}$

\*William J. Rutter, Federation Proceedings, 23, 1248-1257 (1964)

Figure 1. Anomeric Composition of FBP

At neutral pH, in aqueous solution the anomeric composition of FBP is ca. 80%  $\beta$ -FBP and 20%  $\alpha$ -FBP with 2% or less in the open form.

FIGURE I



varying anomeric specificities, that is varying specificity with respect to their utilization of the  $\alpha$ - or  $\beta$ - form of fructose 1,6-bisphosphate. In addition, yeast aldolase is known to have anomerase activity.<sup>6</sup> Both the anomerase activity and the anomeric specificity are possible key aspects of the overall regulatory mechanism of glycolysis and gluconeogenesis.

The anomeric specificity of muscle aldolase as well as the specificity of the other glycolytic and glyconeogenic enzymes has been studied by numerous investigators, principally by way of rapid kinetic techniques such as stopped flow and rapid quench.

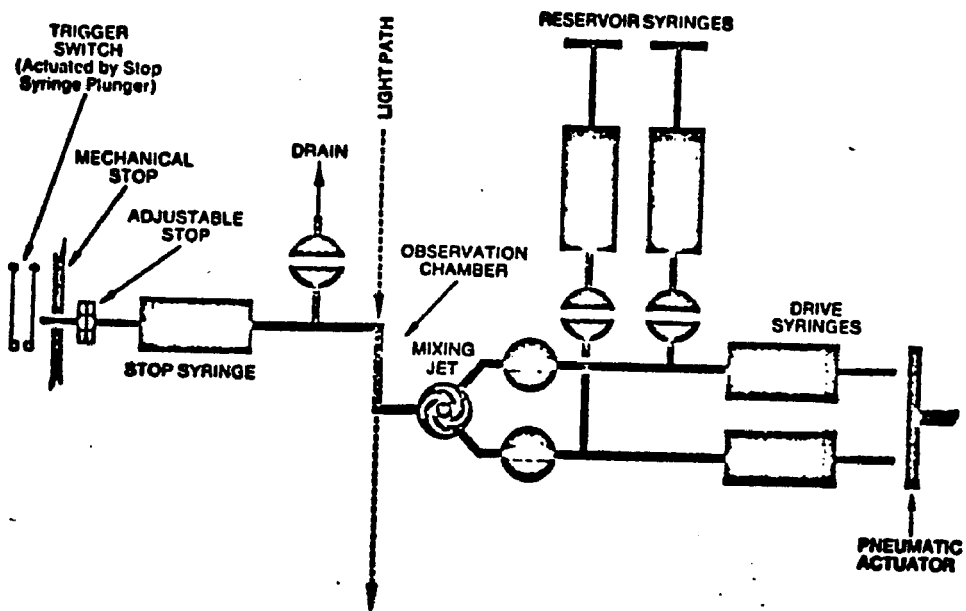
In stopped flow experiments,<sup>7</sup> the enzyme and the substrate are loaded into separate syringes. At time zero, the syringes are driven forward and their contents pass into a mixing chamber. An ultraviolet-visible spectrophotometer is set up to monitor the effluent from this mixing chamber. Downstream of this monitor is a third syringe which is a feedback mechanism to stop the drive mechanism, hence the name, stopped flow. (See Figure 2.) Stopped flow apparatus have typical dead times on the order of 1-3 milliseconds and hence are very useful for studying the early phases of enzymatic reactions.

In the rapid quench experiment,<sup>8</sup> the enzyme and substrate are loaded into separate syringes and at time zero the syringes are driven forward by a pneumatic drive as

Figure 2. Stopped Flow Apparatus

Used by permission of Durrum, Palo Alto, California.

# FIGURE 2



Flow diagram for Durrum stopped flow instrumentation.

in the stopped flow experiment. The contents of the syringes are mixed and the effluent of this mixing chamber passes to a second mixing chamber, where the reaction is quenched by addition of a strong acid or base from a third syringe. The time that the reaction is allowed to proceed (between the mixing chambers) is varied. (See Figure 3). The quenched reaction mixture is later neutralized and then assayed to determine the concentration of reactants, intermediates, and products. This type of apparatus has a dead time of approximately 10-20 milliseconds and hence is also valuable to the study of enzymatic reactions. By studying the very early stages of enzymatic reactions, it is often possible to reveal mechanistic details at the molecular level.

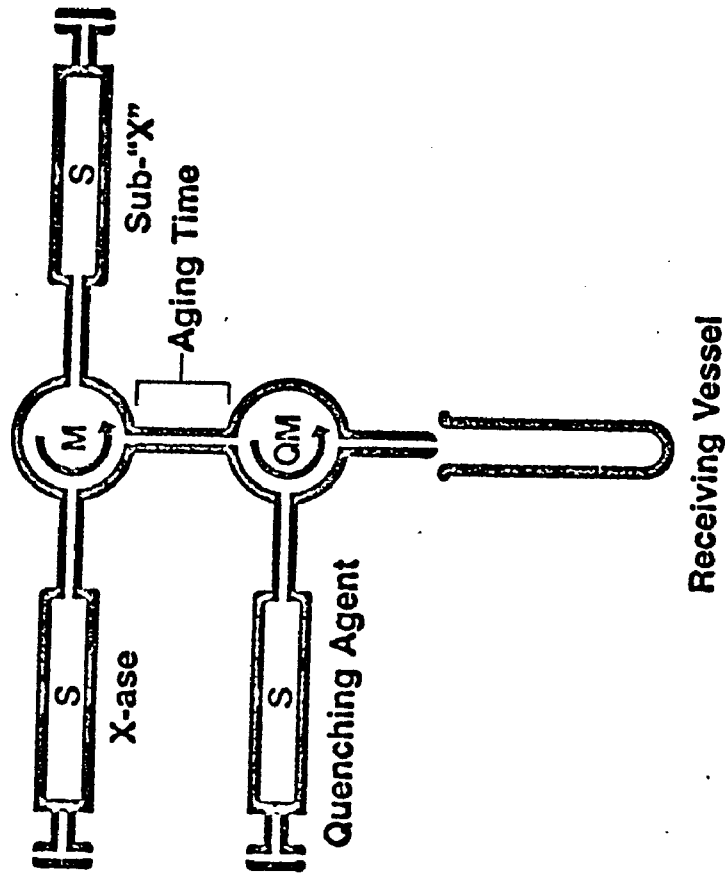
#### Substrate Analogues to Determine Anomeric Specificity

Another less direct approach to determining the anomeric specificity of glycolytic enzymes is the use of substrate analogues. Compounds are prepared which have the stereochemistry of the  $\alpha$ -, the  $\beta$ -, or the open form and which can not anomerize to the other forms. These compounds may act either as competitive inhibitors or as substrates. When they act as substrates, the value of  $V_{\max}$  and  $K_M$  are determined and compared to these values for the normal substrate of the enzyme. In cases where the compounds function as competitive

Figure 3. Rapid Quench Apparatus

Used by permission of Update Instrument, Inc,  
Madison, Wisconsin.

**FIGURE 3**



**Single Syringe-Ram System**

- M** Mixing Chamber
- QM** Quench Mixing Chamber
- S** Syringe

inhibitors, the value of  $K_i$  is determined and used as a measure of the degree of binding for the analogue (and hence presumably for the corresponding anomer). There are, however, many pitfalls in the interpretation of the binding of competitive inhibitors. For example, reduced binding may be due to steric bulk alkyl group in the analogue not found in the substrate, rather than being the result of incorrect anomeric composition. Thus the interpretation of this type of study is less certain than that based on the results of kinetic evaluation.

The anomeric specificity of the glycolytic and gluconeogenic enzymes which have been determined through the types of studies described above are shown in Figure 4. Benkovic and Schray have recently reviewed the anomeric specificity of these enzymes.<sup>9,10</sup> In Figure 5 is shown the portions of these metabolic pathways which involve aldolase directly. Note from Figures 4 and 5 that in general glycolysis occurs via utilization of the  $\beta$ -anomeric forms and gluconeogenesis occurs principally via utilization of the  $\alpha$ -anomeric form of the substrate. As you can see from Figure 5, however, phosphoglucose isomerase (PGI) utilizes the  $\alpha$ -anomer of glucose 6-phosphate as its substrate and produces the  $\alpha$ -anomer of fructose 6-phosphate as its product.<sup>11,12</sup> This is of course the incorrect anomeric form for coupling with

Figure 4. Anomeric Specificity in Glycolysis and  
Gluconeogenesis

**FIGURE 4**

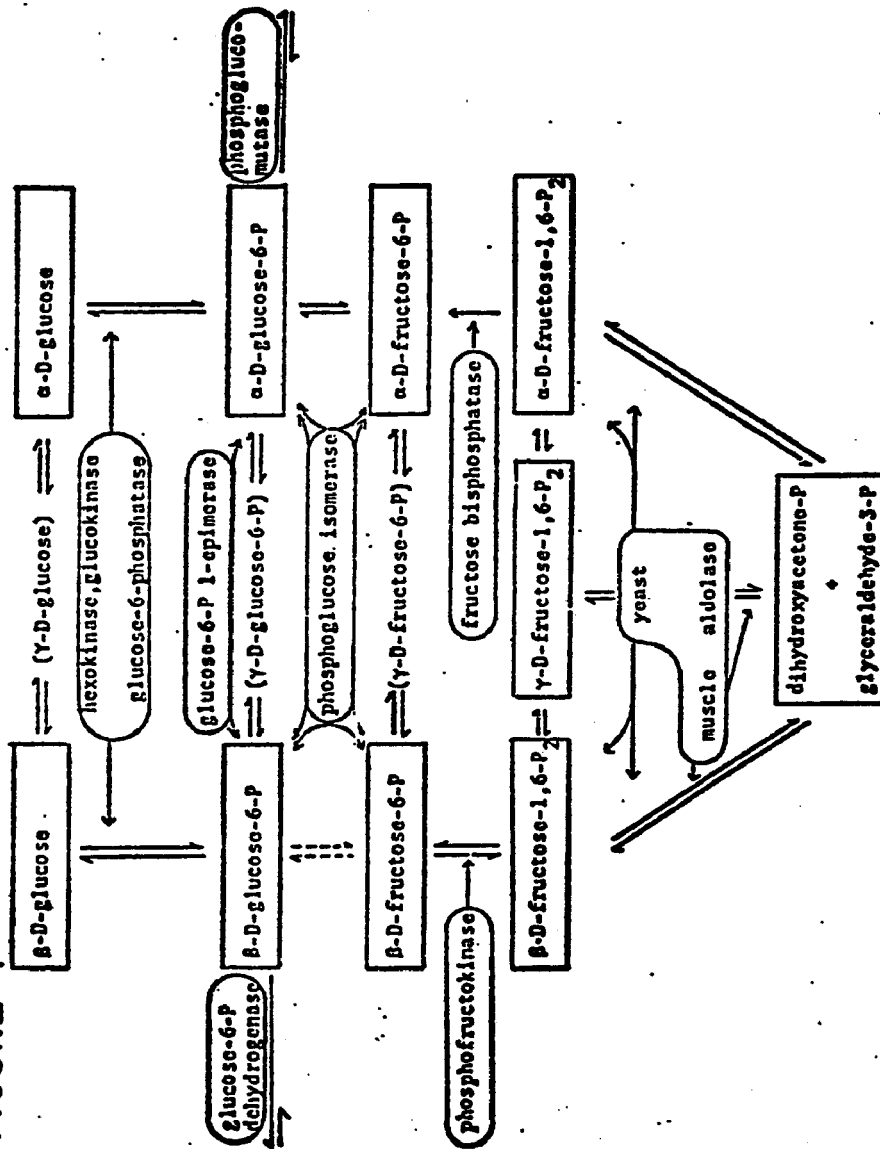
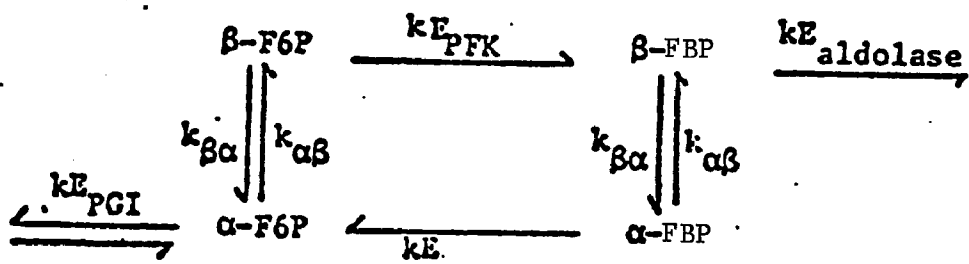


Figure 5. Anomeric Specificity of the Enzymes Utilizing F6P or FBP as Substrate

FIGURE 5



phosphofructokinase during glycolysis. However, the spontaneous  $\alpha$ -F6P  $\rightarrow$   $\beta$ -F6P rate is greater than the overall glycolytic flux rate.<sup>10</sup> Phosphofructokinase (PFK) is specific for the  $\beta$ -anomer of F6P<sup>13,14,15,16</sup> and produces  $\beta$ -FBP. Thus PFK is coupled to aldolase in muscle cells, since muscle aldolase is specific for the  $\beta$ -anomer.<sup>6,17</sup> This means that the muscle aldolase is not coupled to the gluconeogenic pathway. Gluconeogenesis is not an important process in muscle cells. The yeast enzyme, as mentioned above, can utilize both the  $\alpha$ - and  $\beta$ -anomeric form and is known to have anomerase activity.<sup>6</sup> The yeast aldolase, therefore, is coupled both to the glycolytic and gluconeogenic pathways. Fructose biphosphatase (FBPase) is known to utilize the  $\alpha$ -anomer of FBP as its substrate.<sup>14</sup> The  $\alpha$ -F6P produced by fructose biphosphatase is the anomeric form utilized by PGI. Finally, it should be pointed out that FBPase and PFK utilize the opposite anomeric forms. This is particularly important since the PFK-FBPase pair is one of the main regulatory points in the glycolytic-gluconeogenic pathway. If these enzymes were not regulated there would be a futile cycling of F6P and FBP with a corresponding squandering of ATP to phosphorylate F6P!

## The Use of PFK to Slowly Generate $\beta$ -FBP

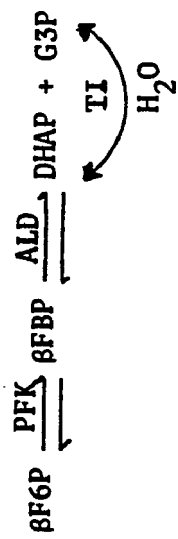
Rose and O'Connell<sup>18</sup> have used slow generation of  $\beta$ -FBP by PFK to study the rate of muscle aldolase at high enzyme to substrate concentration. The reaction was followed by employing a small amount of [5-<sup>3</sup>H]F6P (8 nanomoles) as substrate for PFK. This enzyme then slowly produced only the  $\beta$ - anomer of FBP.<sup>13-16</sup> The reaction rate of muscle aldolase, which was present in vast excess of the level of  $\beta$ - FBP, was measured by coupling the aldolase reaction to triosephosphate isomerase, which quickly exchanges the label out of [2-<sup>3</sup>H]G3P ( initially [5-<sup>3</sup>H]F6P) and into water. The reaction sequence is shown in Figure 6. The rate of the aldolase reaction was then taken to be proportional to:

$$\frac{d\text{FBP}}{dt} \propto \frac{\text{cpm} \quad \text{}^3\text{HOH}}{\text{cpm} \quad \text{FBP} \times \text{time}}$$

Since the muscle aldolase has been demonstrated to bind the cyclic form of the substrate and substrate analogues very tightly,<sup>19,28,22</sup> some predictions were possible with regard to the rate of the reaction on increasing aldolase concentration. If the open form were exclusively the substrate of the reaction, increasing levels of aldolase would have caused increased binding of the  $\beta$ - FBP produced by PFK and, hence, prevent the spontaneous  $\beta$ - to open interconversion. Therefore, the overall

Figure 6. Schematic Representation of the Reactions  
Involved in the Measurement of the Rate of Liver  
Aldolase Under Conditions of Slow Generation of  
FBP by PFK

**FIGURE 6**



rate of the aldolase reaction would have dropped on increasing aldolase concentration. On the other hand, if the  $\beta$ -anomer of the FBP is the substrate for the reaction (with or without the open form also being a substrate), the overall aldolase reaction rate would have risen until it reached the level of the PFK reaction rate. The latter case was observed. It was concluded that  $\beta$ -FBP is the substrate for muscle aldolase. The open form was also concluded to be a substrate in as much as the mechanism of aldol cleavage requires ring opening.

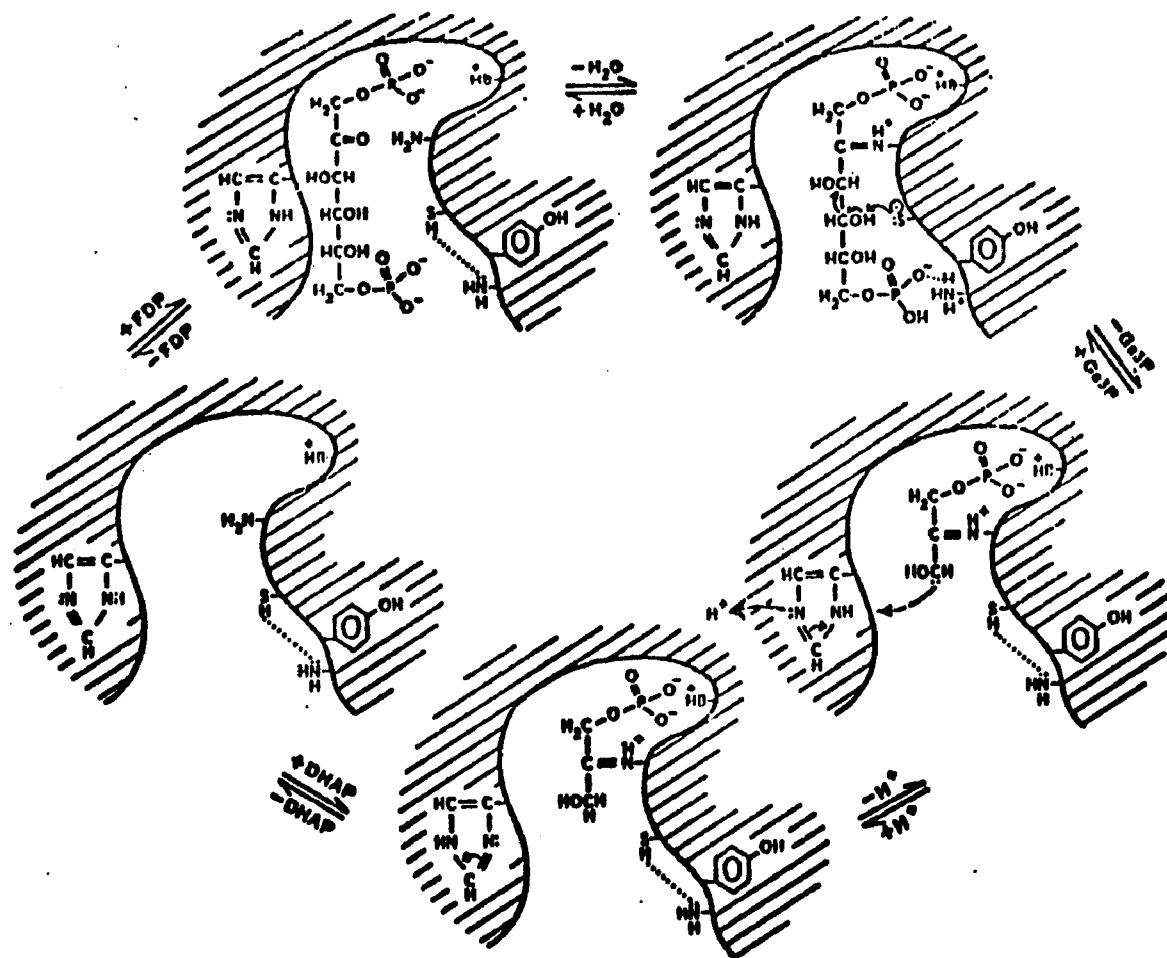
#### General Mechanistic Considerations

The mechanism by which muscle aldolase is believed to act on fructose 1,6-bisphosphate is shown in Figure 7.<sup>20</sup> Following formation of the Michaelis complex, a Schiff base is formed between the carbonyl group of the substrate and a lysine residue located at the active site of the enzyme. Lysine groups have also been demonstrated to be involved in binding of the phosphate groups of the substrate.<sup>21,22</sup> A sulfhydryl group then removes a proton from 4-hydroxyl of the substrate. The pair of electrons on the hydroxylate come in to form the aldehyde portion of G3P with concomitant C3-C4 bond breakage to give the carbanion of DHAP.<sup>23</sup> The carbanion is then protonated by a histidine.<sup>24</sup> The Schiff base between DHAP and the enzyme is hydro-

Figure 7. Mechanism of Muscle Aldolase <sup>20</sup>

Used by permission of Academic Press, New York,  
N.Y.

FIGURE 7



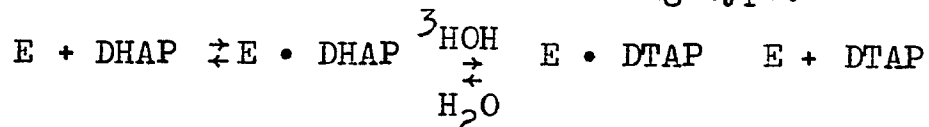
lyzed and the product dissociates.

### General Mechanistic Considerations - $K_M$ Values

The values found in the literature for the Michaelis constant ( $K_M$ ) determined for a particular type of aldolase may vary significantly.<sup>4,26,27</sup> This is probably due to the effects of various ions on aldolase as described previously.<sup>25,28</sup> Therefore, the values of these constants utilized in the experimental section which follows, were determined independently for the given set of conditions employed.

### General Mechanistic Considerations - Rate of $^3\text{HOH}$ Exchange into DHAP

Rose and Rieder<sup>29</sup> have demonstrated that tritium from  $^3\text{HOH}$  is exchanged onto the 3-position of DHAP by muscle aldolase. This exchange occurs in the absence of any other (aldehydic) substrate and, therefore, represents a reaction of the following type:



Further, it is found that the presence of FBP causes a significant decrease in the rate at which this exchange occurs in a region which is also involved in binding FBP. Finally, it was also found that the rate constant found by measuring exchange as a function of

time in the absence of any other substrate, is greater than the rate constant for the overall cleavage reaction of FBP.

### General Mechanistic Considerations - Competitive Inhibitors

In addition to being employed as analogues of the various anomeric forms, substrate analogues have been used as molecular probes of the active site of muscle aldolase by Hartman and Barker.<sup>30</sup> In this study mono- and bisphosphate derivatives of saccharides, diols, and polyols were employed as competitive inhibitors. The binding constants ( $K_i$ 's) were determined and an attempt was made to correlate tighter binding (smaller  $K_i$ ) with structural features of the molecules. From these studies, the authors concluded that maximal binding occurs when the competitive inhibitor has two phosphate moieties separated by ten to twelve angstroms. This distance was approximately the distance between the phosphates of fructose 1,6-bisphosphate. Further, the requirement of two phosphate groups for maximal binding was consistent with the fact that muscle exhibits a 50:1 preference for FBP as substrate over F1P as substrate. By way of comparison, the liver enzyme has been shown to utilize FBP and F1P equally well.<sup>20</sup> This has been attributed to a lack of a binding site for the 6-phosphate group of FBP at the active site of

the liver enzyme. Finally, the authors concluded that the presence of free hydroxyls was not an important factor in binding.

General Mechanistic Considerations - Inactivation  
Using 1-Chloro 2,4-dinitrobenzene

Chlorodinitrobenzene has been shown by Kowal, Cremona, and Horecker<sup>52</sup> to inactivate rabbit muscle aldolase. This reagent is specific for lysine groups and the active site of muscle aldolase had been shown previously by Horecker's group to contain lysine residues. It might, therefore, have been predicted that the inactivation of muscle aldolase involved the dinitrophenylation of the lysine group(s) present at the active site. This, however, was not the case. The reaction with muscle aldolase was much slower than that described for similar enzymes such as transaldolase. Furthermore, when chlorodinitrobenzene was utilized previously to inactivate other enzymes, the inactivation had been shown to involve only a small number of lysine residues (in some cases a single residue was dinitrophenylated). The number of chlorodinitrobenzene groups taken up by muscle aldolase was found to be  $> 10$  per mole of enzyme. The inactivation of the muscle enzyme was done under mildly basic conditions (pH  $\geq 9.0$ ). At pH 9.0, the inactivation was only 50% complete after 150 minutes of incubation at 25°C. When the pH was

raised to 9.6 or greater the inactivation was nearly complete in 60 minutes. When the enzyme from this last inactivation was hydrolyzed, no peak for the  $\epsilon$ -DNP-lysine was found in the amino acid analysis. On high voltage electrophoresis of the hydrolyzate, no  $\epsilon$ -DNP-lysine was observed but instead a spot was observed which migrated identically with S-DNP-cysteine. This inactivation was found to be greatly reduced by the presence of FBP, DHAP, and F1P, all of which are substrates. F6P, which is not a substrate, did not prevent the inactivation of the enzyme. Therefore, it was concluded that this cysteine group was located at the active site of muscle aldolase. The identity of cysteine as the group involved in the inactivation was confirmed by amperometric titration of the denatured enzyme following inactivation. Following this work by Horecker's group, the presence of cysteine at the active site of muscle aldolase was confirmed by a variety of techniques.<sup>31-35</sup> The role of the sulfhydryl group of cysteine in the cleavage of FBP is shown in Figure 7. This mechanism is proposed based on groups which are known to be present at the active site.<sup>20,36</sup> In the direction of FBP cleavage, following formation of the Michaelis complex and Schiff base formation, the cysteine group functions to remove a proton from the 4-hydroxyl of the substrate. The hydroxylate anion

intermediate collapses to form the aldehyde with the breakage of the C<sub>3</sub>-C<sub>4</sub> bond. The reaction sequence is then completed by protonation of the enamine form of DHAP by a histidine residue, breakdown of the Schiff base, and release of DHAP from the enzyme. One of the steps following cleavage of the C<sub>3</sub>-C<sub>4</sub> bond is believed to be rate determining for the muscle aldolase sequence.

#### General Mechanistic Considerations - Inactivation by Pyridoxal 5-phosphate

Aldolase A, from muscle was found to be reversibly inhibited by pyridoxal 5-phosphate (PLP). This inhibition was reversed on dilution. The presence of substrate or substrate analogues protected the enzyme from this inhibition. Further, FBP was found to reverse this inhibition.<sup>37</sup> On this basis, it was postulated that this inhibition is an active site phenomenon.

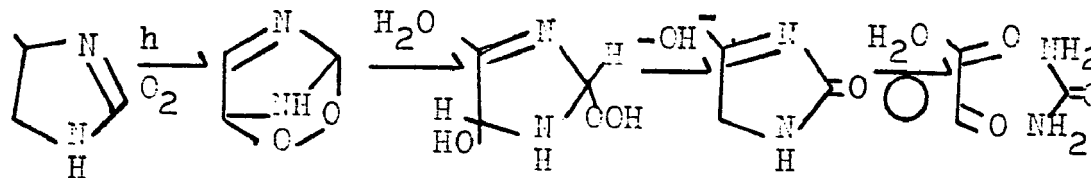
The sodium borohydride (NaBH<sub>4</sub>) reduction product of the PLP-aldolase A complex has been isolated and characterized. PLP was found to have reacted with a lysine at the active site via Schiff base formation. Following the NaBH<sub>4</sub> reduction of the PLP-aldolase complex, the enzyme is found to be catalytically inactive. However, it was observed that this reduction product can still form a Schiff's base with DHAP. Following the NaBH<sub>4</sub> reduction of the PLP-aldolase-DHAP complex and cyanogen bromide digestion, it was noted that PLP

is linked principally to a lysine in the amino terminal peptide, whereas, the DHAP was attached to a lysine in the active site fragment. The carbonyl to phosphate distance in PLP was approximately the same as the phosphate to phosphate distance in FBP. Therefore, it is believed that PLP binds first via its phosphate (at the position normally occupied by the 1-phosphate of FBP) and then forms a Schiff base with the lysine involved in the binding of the 6-phosphate of the substrate.<sup>20,37</sup>

Another interesting observation is that aldolase A (muscle) was vulnerable to photoinactivation in the presence of PLP and that aldolase B (liver) was not affected under identical conditions.<sup>24,38</sup> This photoinactivation was more rapid than the dark reaction (mentioned above) and required the presence of oxygen. The photoinactivation was not prevented by presence of substrate analogues.\*

\*The photoinactivated rabbit muscle aldolase has only four out of forty-four histidines destroyed (1 per subunit) and all other amino acids intact, but is 95% inactivated. It has the same  $K_m$  for FDP and F1P, and forms a Schiff base with DHAP (which has been isolated by  $\text{NaBH}_4$  reduction).<sup>24,38</sup> Although Ripa and Pontremoli<sup>66</sup> have shown that pyridoxal phosphate will specifically sensitize histidine in other proteins, other histidine sensitizers such as rose bengal destroy 22 out of the 44 histidines in rabbit muscle aldolase.<sup>24</sup> The precise nature of the photoreaction is not well understood since the oxidized histidines were never isolated and characterized. The rate of inactivation is proportional to sensitizer concentration, up to a maximum of four moles of pyridoxal phosphate per mole

of enzyme. The rate of inactivation is also dependent on the partial pressure of oxygen.<sup>58</sup> This oxygen dependence implies that pyridoxal, like rose bengal, acts by producing singlet oxygen.<sup>67</sup> Singlet oxygen forms an adduct with dienes, including heterocycles, which breaks down into oxidation products.<sup>67,68</sup> Speculatively, one possibility for the photoreaction might be:



The resulting urea would be incapable of acting as a proton sink necessary in the aldolase reaction.

## Rationale

The objectives of the present study are twofold. The first objective is to determine the anomeric specificity of liver aldolase and where possible to determine the mechanistic and biological results of the anomeric specificity. The second objective is to study the mechanism of action of this enzyme bearing in mind the differences between the properties of liver aldolase and muscle aldolase in spite of extensive sequence and structural homology.

One of the most promising techniques for studying the anomeric specificity is stopped flow kinetics. This is particularly true because of the particularly rapid rate of interconversion of  $\alpha$ -FDP and  $\beta$ -FDP. With the stopped flow instrument, it is possible to study the reaction of liver aldolase at times shorter than the half time for substrate interconversion. In addition, it may be possible to obtain information regarding the anomeric specificity of liver aldolase by way of a mixed muscle aldolase - liver aldolase stopped flow experiment. Schray et al.<sup>6</sup> have used mixed rapid kinetic experiments to determine the anomeric specificity of yeast aldolase and also to study the anomerase activity of this enzyme.

In the past it has often been advantageous to employ a computer simulation of complex enzyme systems.<sup>51</sup>

The present experiments with three substrate forms and in the case of the mixed muscle aldolase-liver experiment, two enzymes and up to six Michaelis complexes are ideally suited to computer simulation. The reaction kinetics will be simulated based on a given anomeric specificity and the results will be compared to the experimental data.

Another less direct approach to determining the anomeric specificity of liver aldolase is the use of substrate analogues as competitive inhibitors. Analogues of  $\alpha$ -,  $\beta$ -, and open FBP will be employed and the binding constant  $K_i$  of the analogue can be taken as a measure of the strength of the interaction between the corresponding substrate form and the enzyme.

Finally by slowly generating  $\beta$ -FBP by using phosphofructokinase and F6P and measuring the rate of the aldolase reaction with varying levels of aldolase present, it is possible to distinguish between  $\beta$ -FBP utilization and utilization of the open form following  $\beta$ - to open interconversion.<sup>18</sup>  $[5-^3\text{H}]$ F6P will be utilized as the substrate for PFK and the aldolase reaction will be coupled to triosephosphate isomerase (TI). TI will rapidly exchange the tritium out of the  $[2-^3\text{H}]$  G3P produced in the aldolase reaction. The counts per minute (cpm) found in  $^3\text{HOH}$  divided by the counts found in  $[5-^3\text{H}]$  FBP will then be a measure of the aldolase

reaction rate.

In order to achieve the second objective, it will be necessary to probe the active site of the enzyme on a molecular level. One fruitful approach to probing the active site is the use of active site directed inactivators. In the past, many reagents have been utilized to specifically inactivate a single type of amino acid group at the active site of aldolases such as: chlorodinitrobenzene (specific for lysine below pH 9.0 and specific for cysteine above pH 9.6),<sup>52,53</sup> phenylglyoxal (specific for arginine),<sup>54,55</sup> N-bromoacetyethanolamine phosphate (specific for histidine),<sup>56,57</sup> pyridoxal phosphate (specific for lysine),<sup>37</sup> and tetranitromethane (specific for sulfhydryls).<sup>33,34</sup> In the present study chlorodinitro benzene, pyridoxal phosphate, and 4-hydroxymercuribenzoate (specific for sulfhydryls) will be employed to probe the active site of liver aldolase.

Another commonly employed technique is to measure the rate of isotope exchange either into or out of a substrate. By so doing it will be possible to determine whether or not the steps in the reaction sequence involved in the exchange are rate determining to the overall reaction. In particular, by measuring the rate at which <sup>3</sup>H is exchanged from <sup>3</sup>H<sub>2</sub>O into <sup>3</sup>H-DHAP by liver aldolase, it will be possible to determine if the process of protonation of the DHAP carbanion is rate

determining.

Finally, an interesting approach to determining the number of phosphate binding loci at the active site of aldolase was developed by Hartman and Barker.<sup>30</sup> They studied the relative binding strength of a series of mono- and bisphosphate analogues of FBP. One of the differences between muscle aldolase and liver aldolase is supposedly a lack of a binding site for the six phosphate of FBP in the liver enzyme. To probe this possibility the relative binding strength of ribulose 1,5-bisphosphate, ribulose 5-phosphate and ribose 5-phosphate will be measured.

## Experimental Methods

### Liver Aldolase Preparation

Aldolase from rabbit liver was prepared by the procedure of Gracy et al.<sup>27</sup> and by the procedure of Chappel et al.<sup>50</sup> In the procedure of Gracy et al. 500 grams of frozen, mature, full fed, New Zealand White rabbit liver (obtained from Pel-Freeze Biologicals) was passed through a meat grinder. This material was then homogenized with 1 litre of 0.1M Tris (Cl), 2mM EDTA, at pH 7.5 in a Waring type blender for 1 minute. The pH was readjusted to pH 7.5 by addition of a small amount of 1M NaOH. The homogenate was then centrifuged for 1 hour @ 11,000xg. Following centrifugation the supernatant was decanted and ammonium sulfate added to 35% of saturation. The 35% solution was stirred for 30 minutes. Then the solution was centrifuged @ 11,000xg for 1 hour. Following centrifugation, a layer of cream colored material was observed floating on top of the supernatant. The supernatant was removed by suction filtration to avoid this floating material. Ammonium sulfate was then added to raise the level to 65% saturation. The 65% solution was stirred for 30 minutes and then was centrifuged @ 11,000xg for 30 minutes. After centrifugation, the supernatant was decanted and the precipitate was taken up in 170 ml of 10mM Tris (Cl), 1mM EDTA, pH 7.5. This solution was

then dialyzed three times against this same buffer to remove the sulfate. The volume of the dialyzate was 350 mls. This was loaded on a phosphocellulose column 80 x 2.4 cm which had been preequilibrated with 10mM Tris (Cl), 1mM EDTA at pH 7.4. The flow rate during loading was initially 0.7 ml/min and this had slowed to 0.2 ml/min by completion of the loading phase. The loaded column was washed with a litre of the same buffer. During the wash, the protein concentration of the wash eluant was monitored ( $A_{280}$ ) and the level dropped from  $> 30\text{mg/ml}$  to  $\leq 0.15\text{ mg/ml}$ . Continued washing beyond one litre did not substantially lower the protein concentration in the eluant below 0.15 mg/ml. The column was then eluted with a linear gradient formed between a reservoir which contained 10mM Tris (Cl), 1mM EDTA, pH 7.4 and a reservoir which contained 100mM Tris (Cl), 500mM NaCl, pH 7.4. The flow rate at the beginning of the gradient was  $\leq 0.5\text{ ml/min}$ . By the end of the gradient, the flow rate was  $\geq 1.0\text{ ml/min}$ . Fractions of 18 mls were collected. Most of the activity was found in fractions 22-38 inclusive. These fractions were combined and dialyzed overnight against saturated  $(\text{NH}_4)_2\text{SO}_4$  at pH 7.5. The enzyme which had been dialyzed was centrifuged for one half hour @ 11,000xg. The pellet was taken up in 7 mls of 10mM Tris (Cl), 1mM EDTA, pH 7.5. Following resuspension of the pellet, the solution was

dialyzed against three changes of the same buffer. The dialyzate was placed on a phosphocellulose column 2.4 x 60cm which had been preequilibrated with 50mM Tris (Cl), 1mM EDTA, pH 7.5. The column was then washed with 2000mls of 50mM Tris (Cl), 1mM EDTA, pH 7.5. Following washing the column was eluted with this same buffer containing 2.5mM FBP. The flow rate during this elution was approximately 1ml/min. Fractions of 12mls were collected and activity was found in fractions 15 to 24. These fractions were combined and dialyzed against saturated ammonium sulfate to give a precipitate. The enzyme was stored as the ammonium sulfate precipitate. The yields from this procedure were poor (See Table 2), the specific activity was mediocre, and the product was unstable on storage as the ammonium sulfate precipitate. Therefore another procedure was sought which would improve the quantity, quality, and stability of the enzyme produced. A procedure which promised to be useful in this connection was the procedure of Chappel et al.<sup>50</sup>

The procedure of Chappel et al. was used with only slight modification. In this procedure, 500 grams of frozen, mature, full fed, New Zealand White rabbit liver was passed through a meat grinder. This material was then homogenized by blending for one minute in a Waring

Table 2

Aldolase Purification by Procedure of Gracy et al.  
Starting with 500 gms of Frozen Rabbit Liver

<u>Step</u>	<u>Volume</u>	<u>Units/ml</u>	<u>Total Units</u>	<u>Protein mg/ml</u>	<u>Specific Activity units/mg</u>
Homogenate	1600 mls	1.76	2816	118	0.015
35-65% (NH <sub>4</sub> ) <sub>2</sub> SO <sub>4</sub>	1150	0.68	784	81	0.017
P-cell Column- Linear NaCl Gradient	195	0.54	105	—	—
P-cell Column FBP Elution	70	0.84	59	98	0.6

type blender with one litre of 50mM Tris (Cl), 5mM EDTA, 50%  $(\text{NH}_4)_2\text{SO}_4$  at pH 7.4. The homogenate was centrifuged @ 16,000xg for one hour at 4°C. The supernatant was then filtered through multiple layers of cheesecloth to remove the light material floating on the top of the solution. After filtration, sufficient ammonium sulfate was added to the filtrate to raise the concentration from 40% (concentration following the homogenization and centrifugation) to a concentration of 60%. This was the only step in the procedure at which it was possible to stop for two to three days without loss of activity. The 60% ammonium sulfate solution was centrifuged @ 16,000xg for 30 minutes at 4°C. The supernatant was decanted following centrifugation and the pellet was resuspended in a minimal volume (150-200 mls) of 10mM Tris (Cl), 2mM EDTA, pH 8.0. This solution was then dialyzed against three changes of this same buffer to remove the ammonium sulfate. The dialyzate was treated with 200 gms (dry weight) of diethylaminoethyl cellulose (DEAE) in a batchwise manner. The DEAE enzyme suspension was immediately filtered in a Buchner filter. Then the filtrate was adjusted to pH 7.4 by addition of 1M HCl.\*

\*Note: The original procedure specified adjusting the filtrate to pH 7.0. However, it was found that on adjusting to pH 7.0, protein precipitated from solution. This precipitated protein made loading the column in the succeeding step impossible.

The adjusted filtrate was then applied to a freshly poured column of phosphocellulose (2.5 x 60cm) which had been preequilibrated with 10mM Tris (Cl), 2mM EDTA, pH 7.4. The flow rate during loading was  $\leq 3$  ml/min. The loading step, as well as all subsequent washings and elutions, was accomplished using a closed system and a reservoir approximately six feet above the bottom of the column. During loading the eluant was checked for protein concentration and aldolase activity. While some protein did pass through the column during loading, little or no aldolase activity was found in this eluant. The column was then washed with one litre of 10mM Tris (Cl), 2mM EDTA, pH 7.4 and then was washed with one litre of this same buffer which contained 20mM KCl. During these washes, a great deal of protein was eluted but virtually no aldolase activity was eluted. During the second washing, protein concentration was found to decrease to a level of approximately 0.1 mg/ml after about 700 mls of buffer had passed through the column. The concentration then remained at about this level for the remainder of the wash. Following these washes, the column was eluted with 10mM Tris (Cl), 2mM EDTA, 20mM KCl, pH 7.4, and 0.2mM FBP, and 18 ml fractions were collected. Activity was found in the early fractions (fractions 2-7). The column was then eluted with 2.0mM FBP in 10mM Tris (Cl), 2mM EDTA, 20mM KCl at

pH 7.4. Fractions of 18 mls were collected. The authors of the procedure obtained 90 units of liver aldolase at a specific activity of 20.0 units/mg from the 0.2mM FBP elution step and 25 units of liver aldolase at a specific activity of 3.7 units/mg from the 2.0mM FBP elution step.

On repeating this procedure several times, typical results obtained were 100 units of liver aldolase at a specific activity of 1.16 units/mg from the 0.2mM FBP elution step. No detectable activity was obtained from the 2.0mM FBP elution. The fractions from the 0.2mM FBP elution were pooled and dialyzed against three changes of 50mM Tris (Cl) pH 7.4 to remove the substrate. This was followed by dialysis against 100%  $(\text{NH}_4)_2\text{SO}_4$ , 50mM Tris (Cl) at pH 7.4. This dialysis caused the protein to precipitate and the enzyme was stored in this form. The yields from this procedure were somewhat improved from those obtained using the procedure of Gracy et al. both in terms of total units and in terms of specific activity. (See Table 3 for details of purification.) However, the enzyme obtained proved also to be unstable on storage at 4°C as the ammonium sulfate precipitate. The activity dropped to one half its level on storage at 4°C as the precipitate for one month or less.

It was found that if fresh rabbit liver was

Table 3

Aldolase Purification by Procedure of Chappel et al. Starting with 500 gms of Frozen Rabbit Liver. Values listed are average values. Values in parentheses are best values obtained.

<u>Step</u>	<u>Volume</u>	<u>Units/ml</u>	<u>Total Units</u>	<u>Protein mg/ml</u>	<u>Specific Activity units/mg</u>
Homogenate	1420 mls	1.29 (1.8)	1832 (2700)	—	—
40% $(\text{NH}_4)_2\text{SO}_4$ Supernatant	793	0.37 (0.56)	293 (445)	—	—
40-60% $(\text{NH}_4)_2\text{SO}_4$ Precip-re-suspended	203	1.00 (1.29)	203 (214)	—	—
Dialyzate	387	0.76 (1.28)	293 (448)	—	—
DEAE filtrate	298	0.46 (0.88)	138 (353)	9.27	0.05 (0.10)
P-cell Column 0.2M FBP Elution	162	0.63 (0.96)	102 (150)	0.52	1.2

utilized instead of frozen rabbit liver, yields were higher and the enzyme obtained had vastly improved stability on storage. The rabbits were New Zealand White, California White, and mixed New Zealand-California. The average live weight was approximately 3 Kg and the average age was about four to five months. The rabbits were full fed until the time of slaughter. Within twenty minutes of slaughter, the livers were homogenized by blending 250 grams of liver with 500 ml of cold 50% ammonium sulfate, 50mM Tris (Cl), 5mM EDTA, at pH 7.4 for 1.5 minutes. A total of 500-800 grams of liver were utilized for each preparation of enzyme. The volumes in later steps were adjusted according to the amount of liver used. After homogenization, the solution was transported to Bethlehem packed in ice. All other steps in the procedure were as described above. The ratio of FBP:F6P activity was measured to be certain that the animals had reached maturity. In the embryo and in immature rabbits, the liver has been found to contain a muscle type aldolase. The enzyme has been shown to have an FBP:F6P activity ratio of approximately 50:1. Further, as the animal matures, it has been shown that this enzyme is replaced by the liver type aldolase (type B) which has a FBP:F6P ratio of 1:1.<sup>20</sup> A value of approximately 1:1 was found and therefore it was concluded that the rabbits were mature.

The yields of enzyme were higher and the specific activity was good. (See Table 4.) In addition, it was found that the enzyme was stable to storage at 4°C in the form of the 0.2mM FBP eluant from the phosphocellulose column. Furthermore, if this solution is concentrated 5-10 times by ultrafiltration, the enzyme is stable for periods of six months or longer.

Following the substrate elution, it was necessary to remove the FBP before attempting the stopped flow experiments. Dialysis was performed using Spectrapor 1 dialysis tubing (Mw cutoff 6000-8000) purchased from Fisher Scientific Inc. The aldolase solution was dialyzed against three changes of 50mM Tris (Cl), pH 7.4. The volume of the aldolase solution was 100-150 mls and the volume of each change of buffer was 10 litres. Dialysis was allowed to proceed for a minimum of three hours. The final change of buffer was allowed to dialyze for twelve hours. On attempting the stopped flow experiments, it was found that the enzyme solution still contained large amounts of substrate. At least two explanations of this problem were possible. The enzyme might have had an extremely tight binding constant or it was possible that the substrate was not dialyzed because of something external (e.g. the dialysis tubing, the buffer system, etc.). As will be shown later, the  $K_M$  for liver

Table 4

Aldolase Purification by Procedure of Chappel et al. Starting with 500-800 gms of Fresh Rabbit Liver. Values listed are average values. Values in parentheses are best values obtained.

<u>Step</u>	<u>Volume</u>	<u>Units/ml</u>	<u>Total Units</u>	<u>Protein mg/ml</u>	<u>Specific Activity units/mg</u>
Homogenate	1700	0.55	935	—	—
40% (NH <sub>4</sub> ) <sub>2</sub> SO <sub>4</sub> Supernatant	1133	0.79 (1.26)	895 (1130)	—	—
40-60% (NH <sub>4</sub> ) <sub>2</sub> SO <sub>4</sub> Precip-re-suspended	480	1.35 (2.4)	646 (785)	—	—
Dialyzate	635	0.68 (1.01)	431 (517)	68	0.01
DEAE Filtrate	1080	0.24 (0.80)	258 (370)	12	0.02
P-cell Column 0.2mM FBP Elution	160	0.78 (2.0)	125 (176)	1.08	0.72 (1.35)

aldolase was found to be approximately  $1 \times 10^{-6} M$ . ( $K_M = K_S$  for liver aldolase.) Even though this was a tight binding, the binding alone was not adequate to explain the large amounts of substrate present following dialysis. Therefore, it was decided to explore further the possible effects of the conditions of dialysis.

A solution of  $0.2mM$  FBP in  $10mM$  Tris (Cl),  $2mM$  EDTA,  $20mM$  KCl, at pH 7.0 was dialyzed versus  $1mM$  Tris (Cl), pH 7.5 at  $4^{\circ}C$ . The volume of the FBP solution was 150 mls and the volume of the dialysis buffer ( $1mM$  Tris (Cl), pH 7.5) was 10 litres. At various times, 0.1 ml aliquots were removed from the dialysis tubing and were assayed for FBP concentration. It was found that no significant dialysis had occurred at times between 0 and 2 hours. At longer times (between 3 and 6 hours) some slight dialysis had occurred. At 1 day, 83% of the initial concentration of FBP still remained inside the tubing. At 5 days approximately 65% FBP remained. A similar experiment was performed with dialysis tubing obtained from Thomas Scientific Inc. which had a similar cutoff. At times up to 3 hours, no significant dialysis had occurred. Therefore, the particular dialysis tubing employed was not the causal agent. In all cases the tubing was prepared for use according to the manufacturers instruc-

tions. Spectrapor 1 tubing was used in the following experiments.

A 0.2mM solution of FBP in distilled water was dialyzed against distilled water. This was also done at 4°C as were all successive dialysis experiments. At times up to six hours, no significant dialysis had occurred. At three days, 37% of the initial FBP remained. The pH of the distilled water was approximately pH 5.

A similar experiment was performed using F6P in 10mM Tris (Cl), 2mM EDTA, pH 7.4. After three hours of dialysis, approximately 85% of the F6P was found to remain in the dialysis tubing and after nineteen hours 30% of the original F6P remained. The assays of F6P were performed enzymatically with multiple determinations of the three hour and the nineteen hour points. Thus, F6P was found to dialyze at a rate greater than that for FBP. Long times were required for the dialysis system to reach equilibrium.

The same experiment was performed using ATP in 10mM Tris (Cl), 2mM EDTA, pH 7.4. After three hours, 92% of the ATP remained and at 7.5 hours, 83% of the ATP remained.

Glucose was then dialyzed under the above conditions. After three hours, only 18% of the glucose remained. It was also found that NaCl dialyzed under

the same conditions and had substantially reached equilibrium at three hours. Finally, on testing the dialyzate using barium nitrate following the 40-60%  $(\text{NH}_4)_2\text{SO}_4$  precipitation step in the procedure for purifying liver aldolase (as per above), it was found that the  $(\text{NH}_4)_2\text{SO}_4$  dialysis was nearly complete in three hours.

Based on the above experiments, it was concluded that dialysis of phosphate containing compounds through regenerated cellulose tubing required establishing that dialysis had occurred. In terms of the present preparative procedure, it was concluded that dialysis was not an efficient method for removing FBP from the final enzyme solution. Instead, the FBP was removed by adding a stoichiometric amount of NADH along with a small amount of  $\alpha$ -glycerophosphate dehydrogenase and triosephosphate isomerase. By this means the FBP was converted to  $\alpha$ -glycerol phosphate. The NAD produced and the  $\alpha$ -glycerol phosphate have been shown to have inhibitory effects on  $\alpha$ -glycerophosphate dehydrogenase at high concentrations. However, control runs under the conditions employed in the stopped flow experiments showed that increasing the levels of the coupling enzymes did not increase the velocity of the measured reaction. It was therefore concluded that this did not cause an interference.

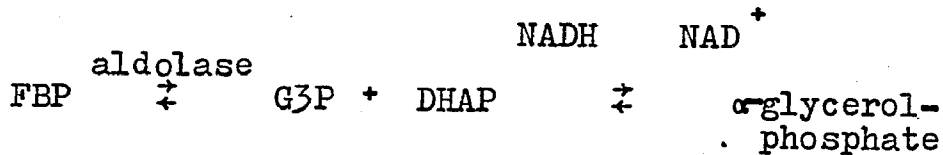
The liver aldolase solution was reduced in volume by ultrafiltration following removal of the FBP. This volume reduction typically resulted in a tenfold increase in protein concentration. The concentrated solution was then dialyzed against three changes of 50mM Tris (Cl), 5mM EDTA, pH 7.5 at 4°C. If it was desired to reduce the volume further following this dialysis, Sephadex G-25 was layered on the dialysis tubing.

#### Assay Procedure Utilized in Liver Aldolase Isolation and Purification

The assay procedure of Rutter, et al.,<sup>1</sup> was employed with slight modification. A typical assay mixture included:

310  $\lambda$  H<sub>2</sub>O  
20  $\lambda$  1M Triethanolamine (Cl) pH 7.5  
20  $\lambda$  0.166M FBP  
20  $\lambda$  100 unit/ml  $\alpha$ -glycerolphosphate dehydrogenase-triosephosphate isomerase  
10  $\lambda$  10mM NADH  
20  $\lambda$  aldolase solution

The change in absorbance at 340 nanometers was monitored using a Beckman model 25 UV-visible spectrophotometer and this was then converted to units/ml in the aldolase solution being assayed. The assay can be represented schematically as:



## TI

In this assay procedure, the final concentration of FBP is 8.3mM. It was found that under conditions of lower final concentration of FBP, 25  $\mu$ M for example, but still  $\gg K_M$ , the rate of the aldolase reaction was approximately 20% greater. This would appear to be a case of substrate inhibition at high concentration of FBP. Caution must therefore be exercised in reporting activities using this assay. Unless otherwise specified, the above listed conditions were employed in all instances where aldolase is measured in terms of units.

### Preparation of Hemoglobin for Use as Standard in Electrophoresis

As was noted previously by Chappel et al.,<sup>50</sup> hemoglobin was found to be one of the major protein contaminants in the procedure for isolating liver aldolase. It was therefore desirable to have a source of purified hemoglobin to use as a standard for gel electrophoresis. If the phosphocellulose column chromatography was effective, three bands of hemoglobin were observed following elution with 0.2mM FBP, 10mM Tris (Cl), 2mM EDTA, 20mM KCl, pH 7.4 solution. The hemoglobin

was then eluted by using a solution of 10mM Tris (Cl), pH 7.3, and 40mM KCl. Fractions of 20 mls were collected, and the first band of hemoglobin eluted in fractions 72-83. The leading band of the hemoglobin was used for electrophoresis, since this component was most likely to be a contaminant in the liver aldolase fractions.

#### Stopped Flow

The stopped flow experiments were performed using a Durrum model D 134 stopped flow instrument. (See Figure 2 for schematic.) Stopped flow runs were made with muscle aldolase, liver aldolase, and muscle plus liver aldolase. In the muscle aldolase experiment, the final concentrations were 12  $\mu$ M FBP, 20 units/ml muscle aldolase (23  $\mu$ M sites, from Sigma), 175 units/ml  $\alpha$ -glycerophosphate dehydrogenase, 4320 units/ml triosephosphate isomerase, 30  $\mu$ M NADH, 25mM Tris (Cl), 5mM EDTA. The pH was 7.5 and the volume of the reaction mixture was approximately 0.6 ml. In the liver aldolase experiment, the conditions were as in the muscle aldolase experiment except the following conditions: 4.5 units/ml liver aldolase (189  $\mu$ M sites), 50mM Tris (Cl), and 10mM EDTA. In the mixed liver plus muscle aldolase experiment, the final concentrations were 12  $\mu$ M FBP, 20 units/ml muscle aldolase (23  $\mu$ M sites), 2.25 units/ml liver aldolase (93  $\mu$ M

sites), 175 units/ml  $\alpha$ -glycerophosphate dehydrogenase, 4320 units/ml triosephosphate isomerase,  $30\mu$  M NADH, 50mM Tris (Cl), 10mM EDTA. The pH and reaction volume were as above.

#### Computer Simulation

The Chemical Reaction Analysis Modeling System (CRAMS) program, described previously by Benkovic and co-workers,<sup>32,33</sup> was utilized along with an IBM 370-168 computer to simulate the results of the stopped flow experiment assuming various anomeric specificities. In this program, time-reaction progress curves are generated for given initial concentration and given rate constants. The concentrations utilized for these simulations were those employed in the actual stopped flow experiments. Binding constants ( $K_M = K_S$ ) were determined independently under the conditions of the stopped flow experiments. (See Figures 8 and 9.) It has been reported previously by Mehler<sup>25</sup> and by Rose and O'Connell<sup>23</sup> that monovalent anions effect the strength of the binding interactions and hence the necessity of determining the value of  $K_M$  under the experimental conditions employed. The rate constants for the interconversions of the anomeric forms of FBP were those reported by Rose and co-workers.<sup>19</sup> The anomeric composition was assumed to be 4:1,  $\beta$ -:  $\alpha$ - with less than 2% of the open chain intermediate

Figure 8. Lineweaver-Burk Plot for Muscle Aldolase

Velocity was measured as  $\Delta A_{340}$ /minute in assay mixture which contained FBP at concentrations indicated, 63  $\mu\text{M}$  NADH, (except that the highest FBP concentration assay contained 125  $\mu\text{M}$  NADH), 5 unit/ml  $\alpha$ -glycerol-phosphate dehydrogenase/triosephosphate isomerase, 0.002 unit/ml muscle aldolase, 25mM Tris (Cl), 5mM EDTA, pH 7.5, in a total volume of 400  $\mu\text{l}$ .

FIGURE 8

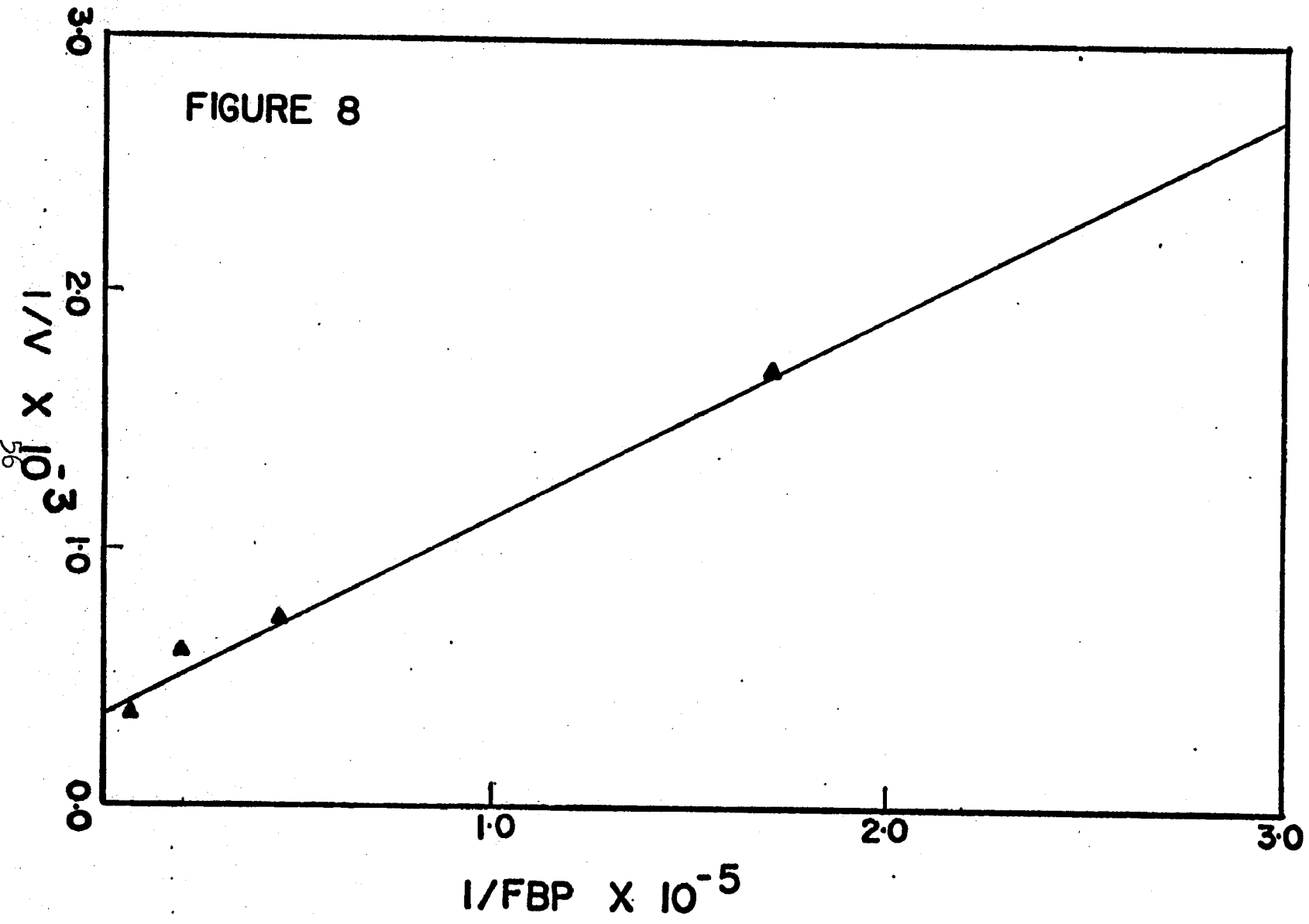
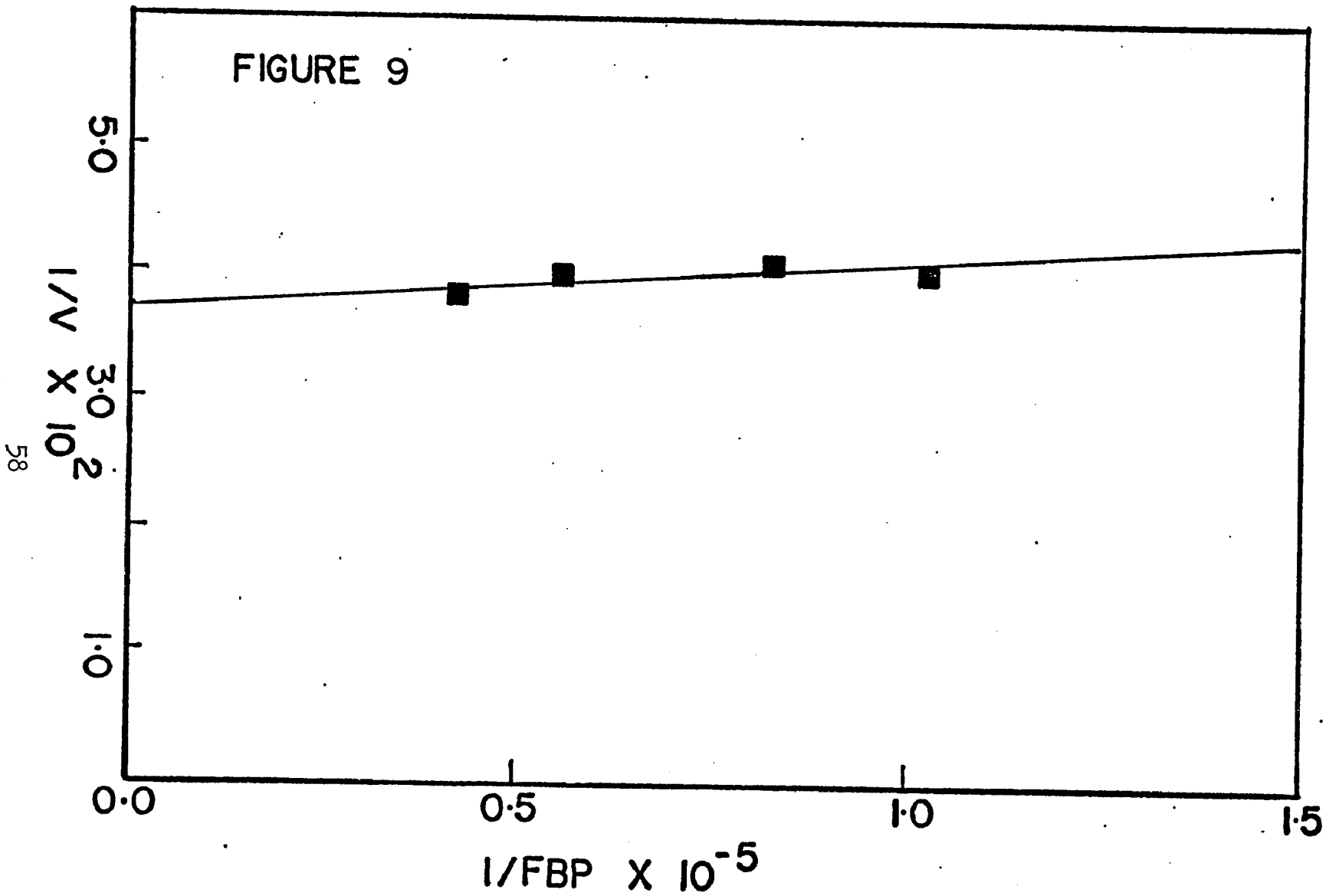


Figure 9. Lineweaver-Burk Plot for Liver Aldolase

Velocity was measured as  $\Delta A_{340}$ /minute in assay mixture which contained FBP at concentrations indicated, 125  $\mu$ M NADH, 5 unit/ml  $\alpha$ -glycerolphosphate dehydrogenase/triosephosphate isomerase, 0.005 unit/ml liver aldolase, 50mM Tris (Cl), 10mM EDTA, pH 7.5, in a total volume of 400  $\mu$ l.

FIGURE 9



present in solution as reported by Gray and Barker.<sup>58-60</sup> The overall reaction scheme utilized in the simulations is shown in Figure 10. In individual simulations, the system was simplified by utilizing only the appropriate portion of this overall reaction scheme. Utilizing the  $K_M$ 's determined independently, the "on" step rate was assumed to be diffusion limited and the "off" step rate was then determined from the  $K_M$ . The usual value for a diffusion controlled process of  $10^8 \text{ sec}^{-1}$  was determined based on molar concentrations.<sup>61</sup> All concentrations were expressed in the program as micromolar concentrations and therefore this number becomes  $10^2 \text{ sec}^{-1}$ .

The competitive binding simulation between the two Michaelis complexes (liver aldolase • FBP and muscle aldolase • FBP) in the absence of product forming steps was accomplished similarly utilizing the ICRS program of Shientel and Maghenase and a Mod Comp II computer. This is illustrated in Figure 11.

#### Inhibition Utilizing Substrate Analogues to Determine the Anomeric Specificity of Liver Aldolase

A number of inhibitors were employed in an effort to further elucidate the anomeric specificity of liver aldolase. These were variously analogues of the  $\alpha$ -anomer, the  $\beta$ -anomer or the open form of FBP. The assays were performed as described earlier except

**Figure 10. Reaction Scheme Used in Computer Simulations**

**FIGURE 10**

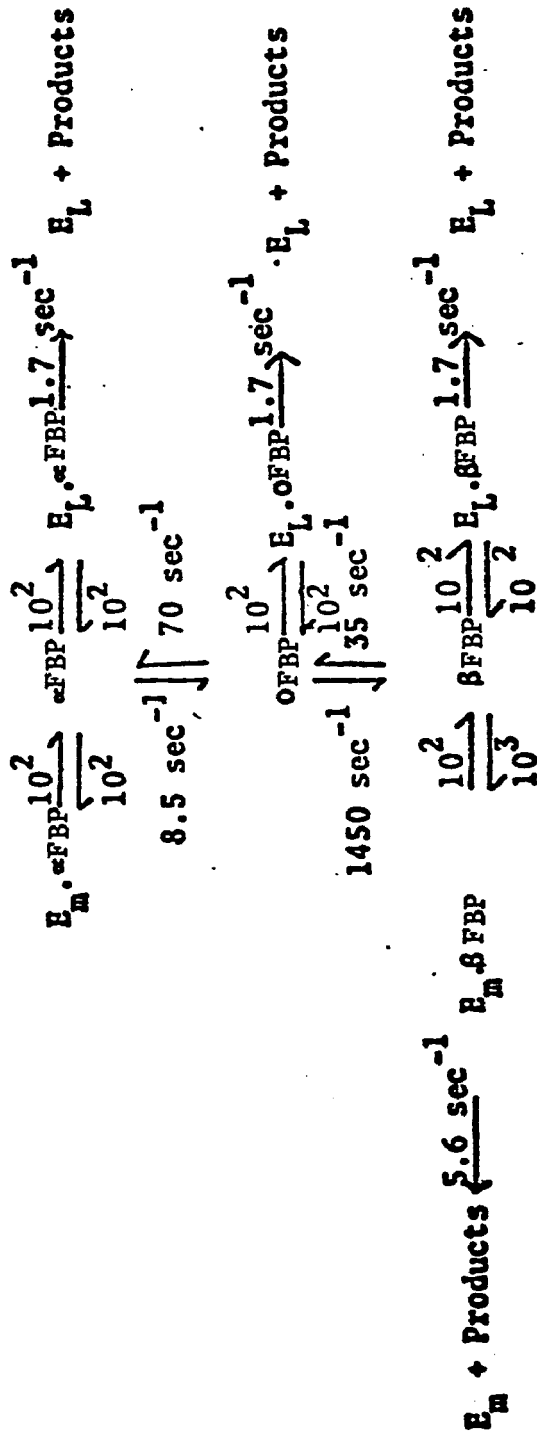
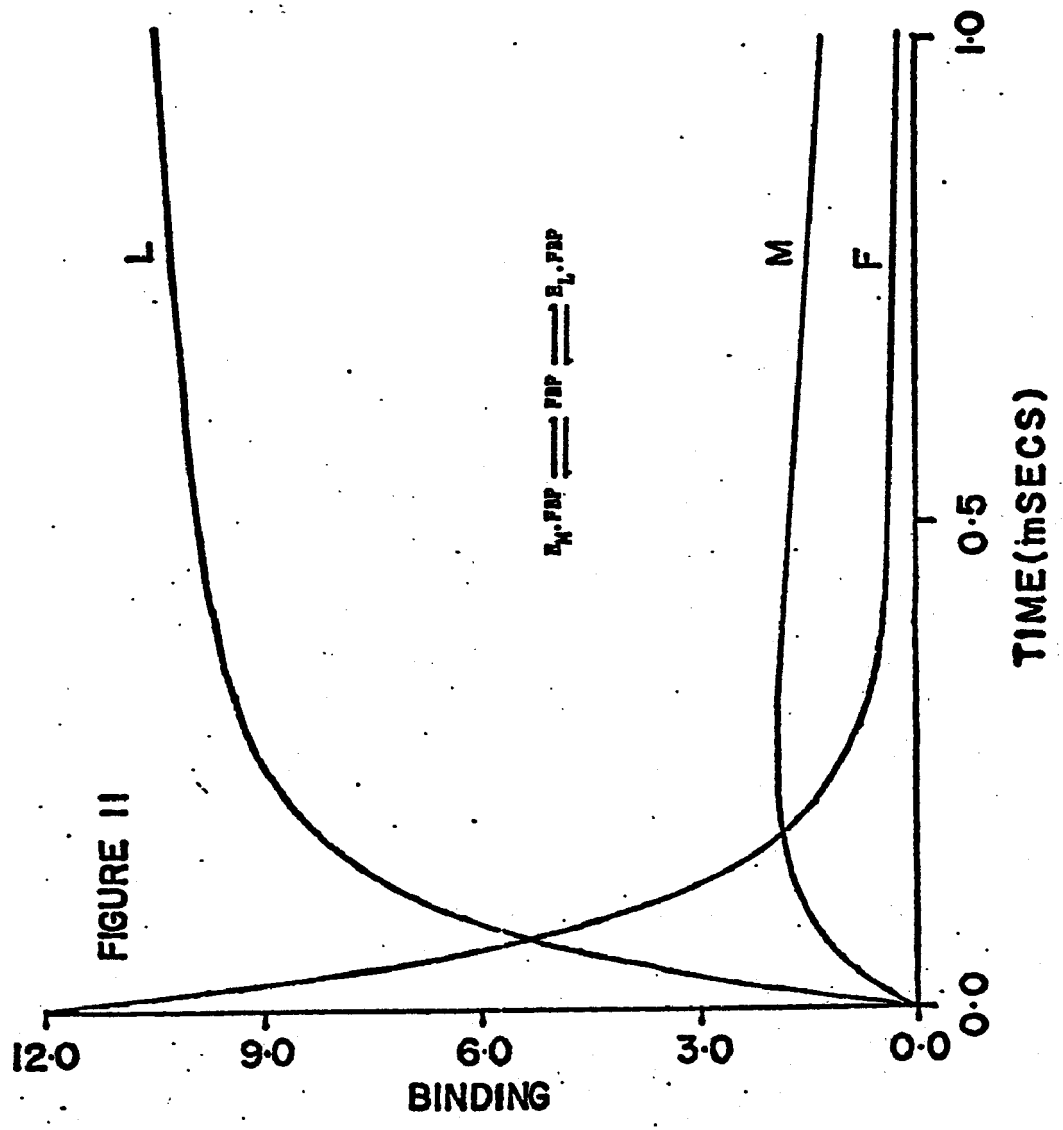


Figure 11. Simulation of Competitive Formation of  
the Michaelis Complexes

Simulated for  $93.4 \mu\text{M}$  liver aldolase sites,  
 $23.4 \mu\text{M}$  muscle aldolase sites,  $12.0 \mu\text{M}$  FBP,  $K_M(\text{liver}) =$   
 $1 \times 10^{-6}\text{M}$ ,  $K_M(\text{muscle}) = 1 \times 10^{-5}\text{M}$ , with on steps  
assumed to be diffusion limited.  $F = (\text{FBP})$ ,  $M =$   
 $(\text{muscle aldolase} \cdot \text{FBP})$ , and  $L = (\text{liver aldolase} \cdot \text{FBP})$



that Tris (Cl) buffer was used instead of TEA (Cl). The data was then plotted using a double reciprocal (Lineweaver-Burk) plot and the binding constants were determined from these plots. Glucitol 1,6-bisphosphate,  $\alpha$ -2,5-Anhydroglucitol 1,6-bisphosphate,  $\beta$ -2,5-Anhydromannitol 1,6-bisphosphate, and  $\alpha$ -,  $\beta$ -methylfructofuranoside 1,6-bisphosphate employed in these studies were the generous gift of Dr. Stephen J. Benkovic, Pennsylvania State University. All other inhibitors were purchased from Sigma Chemical Company and used without further purification.

#### Preparation of [5-<sup>3</sup>H]F6P

[5-<sup>3</sup>H]F6P was prepared starting from [5-<sup>3</sup>H]glucose obtained from Amersham Inc. This material was phosphorylated with yeast hexokinase, and isomerized with PGI, all of which were obtained from Sigma Chemical Company. The final reaction mixture had a volume of 1.25 ml, which contained (final concentrations) 40mM TEA (Cl), pH 8.0, 2mM ATP, 4mM MgCl<sub>2</sub>, 0.86 unit/ml hexokinase, 0.4 unit/ml PGI, 83 nanomoles [5-<sup>3</sup>H]glucose, and 83 nanomoles unlabeled glucose. The reaction mixture was allowed to equilibrate for 10 minutes and then was quenched by addition of 100  $\lambda$  of 30% HClO<sub>4</sub>. Following this addition of HClO<sub>4</sub>, the quenched mixture was allowed to incubate for 2 hours to insure the complete destruction of the PGI activity. The mixture

was then neutralized to pH paper neutrality by addition of 200  $\lambda$  of 3M KOH. After neutralization, 20  $\lambda$  G6PDH (2000 unit/ml) and 10  $\lambda$  of 0.02M TPN were added to remove the G6P which had been formed. This mixture was allowed to equilibrate for 10 minutes. Then it was applied to a freshly poured and washed Dowex-2 (Cl) column which was 0.5 x 3 cm. After loading, the column was washed with 15 mls of 25mM Tris (Cl), pH 7.5. The column was then eluted with 5mM HCl and approximately 0.7 ml fractions were collected. The activity of the samples was determined by counting of 50  $\lambda$  of the sample in 400  $\lambda$  H<sub>2</sub>O + 5 mls of 2,5-diphenyloxazole: 1,4 bis [2-(5-phenyloxazole)] benzene cocktail. A Hewlett Packard model 3330 Tri-Carb scintillation counter was employed. Based upon the cpm in the fractions, a total of 27 nanomoles of [5-<sup>3</sup>H]F6P were obtained in fractions 12-14. All of the above steps were carried out at 25°C. Fractions 12-14 from the 5mM elution step were then stored frozen until they were used for the PFK: aldolase experiment. This storage period was less than one week.

Measurement of the Rate of Liver Aldolase Reaction under Conditions of Slow Production of  $\beta$ -FBP by PFK

The rate of liver aldolase at high enzyme to substrate concentrations was measured using FBP generated slowly from [5-<sup>3</sup>H]F6P and muscle phosphofructo-

kinase (PFK) according to the procedure of Rose and O'Connell.<sup>18</sup> At  $t = 0$  the reaction was initiated by injecting the enzymes into the solution containing the labeled F6P with vortexing. The reaction was terminated at  $t = 2.5$  sec. by addition of concentrated HCl which contained unlabeled FBP. The final concentration of HCl was  $0.6M$  and the final concentration of FBP was  $0.5mM$ . All of the above steps were done at  $0^{\circ}C$ . It was necessary to make two additions of  $0.25$  mg of pepsin. Each addition was followed by an incubation of one hour at  $0^{\circ}C$ . This was necessary because PFK and aldolase have been shown to regain activity on neutralization. Neutralization was accomplished by addition of  $300 \lambda$  of  $2M$  TEA to give a final  $pH = 7.4$ . After neutralization the solution was diluted to a final volume of  $5$  mls and applied to a freshly poured and washed Dowex-2 (Cl) column  $0.5 \times 2.5$  cm. The column was then washed with  $20$  mls of  $25mM$  Tris (Cl),  $pH 7.5$ . Elution with  $5mM$  HCl yielded  $20$  fractions of  $1$  ml each. Subsequent to this, the column was eluted with  $100mM$  HCl and  $20$  fractions of  $1$  ml each were collected from this elution as well. The samples were counted in  $5$  mls of 2,5-diphenyloxazole: 1,4-bis-[2-(5-phenyloxazole)]benzene cocktail plus  $400 \lambda$  of water and  $100 \lambda$  of sample. The fractions were assayed for FBP and the amount of FBP recovered was

used to adjust the number of cpm to 100% FBP recovery.

#### Preparation of $\beta$ - $^3\text{H}$ DHAP

Dihydroxyacetone phosphate, cyclohexylamine salt, dimethyl ketal  $\cdot \text{H}_2\text{O}$  was purchased as a lyophilized solid from Sigma Chemical Company. Dihydroxyacetone phosphate was prepared by dissolving 25mg of the solid in 2 mls of distilled water, and this mixture was then vortexed with 0.5 gm of Dowex 50 ( $\text{H}^+$ ) resin. The solution was then filtered and the filtrate kept at  $40^\circ\text{C}$  for 4 hours to completely hydrolyze the ketal. The solution of DHAP was then stored frozen at  $\text{pH} = 1$ . Under these conditions of storage, the solutions were stable for a week or more. However, DHAP was prepared as close to the time it was used as possible. On calculating the theoretical amount of DHAP which should have been produced from the ketal, it was found that hydrolysis was nearly quantitative.

To prepare  $\beta$ - $^3\text{H}$  DHAP, one millilitre of the DHAP solution (14.2mM DHAP) was adjusted to  $\text{pH} 7.4 - 7.6$  by addition of 30  $\lambda$  2M TEA. After neutralization, 4 units of muscle aldolase were added to the solution. This solution was taken up in a syringe and then added to 1 ml of 0.1 Ci/ml  $^3\text{HCH}$  in a sealed vial. At the end of 1.5 hours the reaction was quenched by adding 2 mls of 20mM  $\text{Cu}(\text{OAc})_2$ . The quenched reaction mixture was applied to a freshly washed and poured Dowex-2 (Cl)

column which was 1.1 x 4 cm. The column was washed with 30 mls distilled H<sub>2</sub>O and then eluted with 50mM HCl. Twenty fractions of 1 ml were collected. The labeled DHAP was found between fractions 11 and 19. The specific activity was approximately 1  $\mu$  Ci/ $\mu$  Mole. The low specific activity of the DHAP was the result of the fact that the <sup>3</sup>HOH was of low specific activity, 1.8  $\mu$  Ci/ $\mu$  Mole. The total radioactivity of the water was 0.1 Ci/ml. In the exchange experiment which follows, it would have been desirable to measure the rate of exchange both out of DHAP and into DHAP. However, the low specific activity would have necessitated the handling of enormous total amounts of radioactivity as <sup>3</sup>HOH in order to obtain [<sup>3</sup>-<sup>3</sup>H] DHAP of sufficient specific activity to measure the rate of exchange out of DHAP.

Measurement of the Rate of Exchange of <sup>3</sup>H into DHAP Catalyzed by Liver Aldolase

A stock solution of unlabeled DHAP was prepared as above. The concentration of DHAP was found to be 26.1mM. A 2.0 ml portion of this solution was neutralized by addition of 60  $\lambda$  of 2M TEA and mixed with 1.0 ml of liver aldolase which was 1.1 units/ml (specific activity = 0.66 units/mg) and 0.6 ml of distilled water. At t = 0, 400  $\lambda$  of 100mCi/ml <sup>3</sup>HOH was added to initiate the exchange reaction. The

reaction mixture was immediately divided into four equivalent 1.0 ml portions. The final concentrations in the reaction mixture were 13.1mM DHAP, 0.27 units/ml liver aldolase, and 10mCi/ml  $^3\text{HOH}$ . At  $t = 2, 4, 10,$  and 90 minutes, one of the portions was quenched by addition of 1.0 ml of 20mM  $\text{Cu}(\text{OAc})_2$ . The quenched samples were centrifuged to remove denatured protein and then applied to a freshly washed and poured Dowex-2 (Cl) column. Care was taken in preparing the Dowex-2 (Cl) columns to be sure that the pH of the column prior to loading was 7.4. Each column was then washed with 100 mls of 20mM TEA pH 7.5. Following the washing, the columns were eluted with 50mM HCl and fifteen fractions of 1.5 ml were collected. Counting was accomplished using 5 mls of the cocktail described above plus 400  $\lambda$   $\text{H}_2\text{O}$ , and 100  $\lambda$  of the sample. The fractions were also assayed spectrophotometrically for DHAP. The exchange is shown schematically in Figure 12.

#### Inactivation of Muscle Aldolase by 1-chloro 2,6-dinitrobenzene

At  $t = 0$ , 10  $\lambda$  of 250mM 1-chloro 2,6-dinitrobenzene was added to a 2 ml solution which contained 2.0 units/ml muscle aldolase in 10mM  $\text{HCO}_3^- - \text{NaCO}_3$  buffer at pH 9.6. At various times, 20  $\lambda$  of the reaction mixture was removed and assayed for aldolase activity. The same

Figure 12. Polyacrylamide Gel Electrophoresis Patterns by Procedure of Ornstein and Davis.

Tracking stain is represented by anodic end in figure. Patterns shown are for a.) 50  $\mu$ l of 0.57 unit/ml liver aldolase (spec. activity = 0.5 unit/mg) in 25% sucrose, b.) 50  $\mu$ l of 50 unit/ml  $\alpha$ -glycerolphosphate dehydrogenase/triosephosphate isomerase in 25% sucrose, c.) 50  $\mu$ l of 40-60% ammonium sulfate supernatant in 25% sucrose.

FIGURE 12

71



experiment was repeated with a volume in the reaction mixture of 1.0 ml. This gave a final concentration of 1-chloro 2,6-dinitrobenzene of 2.5mM. The above inactivations were performed at 25°C. A control portion of enzyme at the same concentration, in the same buffer, and at 25°C showed no decrease in activity during the time of the experiment.

Inactivation of Muscle Aldolase and Liver Aldolase by 1-chloro 2,4-dinitrobenzene

Similar experiments were performed using 1-chloro 2,4-dinitrobenzene and both muscle and liver aldolase. In the experiment involving muscle aldolase, 2 mls of a 1.0 unit/ml muscle aldolase solution buffered with 10mM  $\text{Na}_2\text{CO}_3:\text{HCO}_3^-$ , pH 9.6 was mixed with 10 $\lambda$  of 0.5M 1-chloro 2,4-dinitrobenzene (in ETOH). Periodically aliquots of 20  $\lambda$  were removed and assayed for aldolase activity. The inactivation was performed at 25°C. A control under identical conditions but without 1-chloro 2,4-dinitrobenzene was also run. (10  $\lambda$  of ETOH was added at t = 0.)

The inactivation of liver aldolase was initiated by adding 10 $\lambda$  of 0.5M 1-chloro 2,4-dinitrobenzene to a solution of 0.435 unit/ml liver aldolase in 20mM  $\text{Na}_2\text{CO}_3:\text{HCO}_3^-$ , at pH 9.8 with a total volume of 1 ml. The specific activity of the aldolase was 0.73 units/mg. A control was run under the conditions of the experiment

and the temperature was 25°C. The experiment was repeated with 0.2mM FBP + DHAP + G3P equilibrium mixture present in the reaction mixture.

Inactivation of Liver Aldolase by 4-hydroxymercuribenzoate (disodium salt)

In this inactivation study, a 1 ml solution of 0.74 unit/ml liver aldolase in 20mM H<sub>2</sub>CO<sub>3</sub>:NaCl buffer, pH 7.4 was inactivated by adding 10  $\lambda$  of 100mM 4-hydroxymercuribenzoate (obtained from Aldrich) at time zero and periodically removing aliquots of this solution for assay. Note that the buffer system employed was at the limit of its buffering range. This was done in an effort to maintain conditions similar to the previous inactivations. The experiment was done at room temperature, with the appropriate controls, and both in the presence and absence of substrate.

Inactivation of Muscle Aldolase and Liver Aldolase by Pyridoxal 5-phosphate (PLP)

A 1.0 ml solution of 1.40 unit/ml muscle aldolase, 20mM TEA (Cl) pH 7.5 and PLP final concentrations of 10  $\mu$ M, 20  $\mu$ M, and 25  $\mu$ M were employed to study this inactivation. The inactivation was initiated by addition of the PLP. The reactions were at 25°C and the appropriate controls were also run. Aliquots of 20  $\lambda$  were again withdrawn at various times and assayed for activity. The inactivation mixture was

kept in the dark by wrapping the reaction vessel with aluminum foil. This was to prevent the photoinactivation of muscle aldolase as reported previously by Horecker's group.<sup>38</sup> The inactivation was also studied under higher levels of PLP (up to 5.0mM) but inactivation was so rapid that these measurements were more difficult. The same experiment was performed with liver aldolase. The specific activity of the liver aldolase was 0.5 units/mg. In the case of the liver enzyme it was necessary to go to 200  $\mu$  M PLP final concentration to effect inactivation. In both the liver aldolase and muscle aldolase inactivation studies, it was noted that when aliquots were removed and assayed, there was a gradual increase in the activity at longer times of the assays. This was probably a reversal of the inactivation on dilution as reported earlier by Horecker's group. The activity of the particular assay was taken from the first 1.5 minutes of the assay.<sup>37</sup> In both the muscle and liver aldolase experiments, controls were run under the same conditions except no PLP was added.

#### Polyacrylamide Gel Electrophoresis of Liver Aldolase

Polyacrylamide gel electrophoresis was performed on a solution of liver aldolase from a fresh rabbit liver preparation using the procedure of Ornstein and Davis as modified by Clarke.<sup>62,63</sup> The gels were

loaded as shown in Table 5. Gels 7, 8, and 9 were sliced every 2 mm from the bottom to the top. The remaining tubes were stained with a mixture of 1.25 gms Coomasie brilliant blue, 454 mls of 50% methanol and 46 mls of glacial acetic acid as described by Weber and Osborn.<sup>64</sup> The gels were then destained with a mixture of 375 mls H<sub>2</sub>O, 50 mls methanol, and 75 mls of glacial acetic acid. On staining it was found that both the hemoglobin from the 40-60% ammonium sulfate supernatant gels and the aldolase had migrated to the cathode. The staining for the 40-60% ammonium sulfate supernatant gels and for the triosephosphate isomerase/ $\alpha$ -glycerolphosphate dehydrogenase gels are shown in Figure 12. An attempt was made to isolate the activity of  $\alpha$ -glycerolphosphate dehydrogenase and triosephosphate isomerase from gel 8, but this attempt was unsuccessful. It was apparent that what was needed was a procedure which employed the opposite polarity.

A procedure which employs the opposite polarity is the method of Reisfeld et al.<sup>65</sup> The gels were loaded as shown in Table 6. All samples were run with a 0.001% methyl green standard which vanished. The electrophoresis was allowed to proceed at 6 mamps/tube and 150 volts. The buffer employed was  $\beta$ -alanine: acetic acid at pH 4.3. Gels 1, 2, 6, and 10 were stained as above. The remaining gels were sliced into

Table 5

## Loading of Polyacrylamide Electrophoresis Gels - Procedure of Ornstein and Davis

<u>Gel</u>	<u>Loaded</u>	
1	20 $\lambda$	0.6 unit/ml liver aldolase, 25% sucrose
2	20 $\lambda$	100 unit/ml glycerophosphate dehydrogenase/triosephosphate isomerase, 25% sucrose
3	20 $\lambda$	40-60% $(\text{NH}_4)_2\text{SO}_4$ supernatant, 25% sucrose
4	50 $\lambda$	0.6 unit/ml liver aldolase, 25% sucrose
5	50 $\lambda$	100 unit/ml glycerophosphate dehydrogenase/triosephosphate isomerase, 25% sucrose
6	50 $\lambda$	40-60% $(\text{NH}_4)_2\text{SO}_4$ supernatant, 25% sucrose
7	100 $\lambda$	0.6 unit/ml liver aldolase, 25% sucrose
8	100 $\lambda$	100 unit/ml glycerophosphate dehydrogenase/triosephosphate isomerase, 25% sucrose
9	100 $\lambda$	40-60% $(\text{NH}_4)_2\text{SO}_4$ supernatant, 25% sucrose
10	10 $\lambda$	0.6 unit/ml liver aldolase, 25% sucrose
11	10 $\lambda$	100 unit/ml glycerophosphate dehydrogenase/triosephosphate isomerase, 25% sucrose
12	10 $\lambda$	40-60% $(\text{NH}_4)_2\text{SO}_4$ supernatant, 25% sucrose

Table 6

Loading of Polyacrylamide Electrophoresis Gels - Procedure of Reisfeld et al.

<u>Gel</u>	<u>Loaded</u>	
1	50 $\lambda$	Hemoglobin standard in 25% sucrose
2	50 $\lambda$	1.0 unit/ml liver aldolase in 25% sucrose (0.5 units/mg aldolase)
3	100 $\lambda$	1.0 unit/ml liver aldolase in 25% sucrose (0.5 units/mg aldolase)
4	100 $\lambda$	1.0 unit/ml liver aldolase in 25% sucrose (0.5 units/mg aldolase)
5	100 $\lambda$	1.0 unit/ml liver aldolase in 25% sucrose (0.5 units/mg aldolase)
6	100 $\lambda$	1.0 unit/ml liver aldolase in 25% sucrose (0.5 units/mg aldolase)
7	150 $\lambda$	1.0 unit/ml liver aldolase in 25% sucrose (0.5 units/mg aldolase)
8	150 $\lambda$	1.0 unit/ml liver aldolase in 25% sucrose (0.5 units/mg aldolase)
9	150 $\lambda$	1.0 unit/ml liver aldolase in 25% sucrose (0.5 units/mg aldolase)
10	150 $\lambda$	1.0 unit/ml liver aldolase in 25% sucrose (0.5 units/mg aldolase)
11	150 $\lambda$	1.0 unit/ml liver aldolase in 25% sucrose (0.5 units/mg aldolase)
12	150 $\lambda$	1.0 unit/ml liver aldolase in 25% sucrose (0.5 units/mg aldolase)

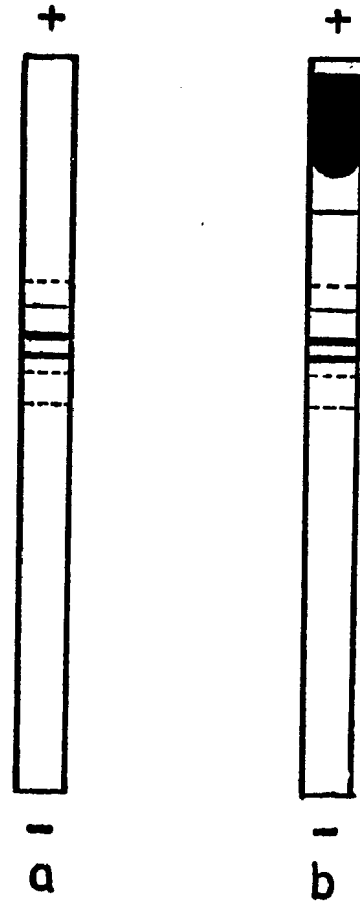
4 mm slices. Each slice was covered with 0.5 ml of 20mM Tris (Cl), 4mM EDTA, pH 7.5 and allowed to diffuse at 4°C overnight. The slices from gels 7, 11, and 12 were combined. These had a total of 450λ of 1.0 unit/ml liver aldolase loaded onto them at the outset of electrophoresis. On assaying the diffusate from these combined gel slices, a trace of activity seemed to be localized in slices 4-6 but even this was minimal. The gel patterns from the stained gels are shown in Figure 13. It was interesting to note that following electrophoresis the unstained gels were 60-70 mm in length. Following the staining and destaining procedure it was found that this length had increased to approximately 90 mm.

Based on the electrophoresis patterns observed, several experimental conclusions were reached. First, hemoglobin was the constituent that made up the series of bands which had migrated furthest towards the cathode. The smeared heavy band which had migrated very slowly from the anode was liver aldolase, and the small sharp remaining band was fructose 1,6-bisphosphate (FBPase). FBPase activity was found in trace amounts in the aldolase preparation by spectrophotometric assay. FBPase was no doubt eluted from the phosphocellulose column by the 0.2mM FBP. However, it was found that under the conditions of the stopped

Figure 13. Polyacrylamide Gel Electrophoresis Patterns by Procedure of Reisfeld et al.

Patterns shown are for a.) 50  $\mu$ l of hemoglobin prepared as in text in 25% sucrose, b.) 100  $\mu$ l of 0.5 unit/ml liver aldolase (spec. activity  $\approx$  0.5 unit/mg) in 25% sucrose. Gels were run for 1.5 hours @ 150 volts x 6 ma/tube.

FIGURE 13



flow experiment (ie. 10mM EDTA) there was no measurable  
FBPase activity. The last observation to be made  
from the electrophoresis experiments was that liver  
aldolase activity is lost under the condition of the  
Reisfeld procedure. This was most likely the result  
of the low pH of the buffer employed.

## Results

### Stopped Flow Kinetics

#### Muscle Aldolase

The oscilloscope trace from a typical muscle aldolase stopped flow experiment is shown in Figure 14A. The conditions and final concentrations under which the experiment was performed are: 12  $\mu\text{M}$  FBP, 20 units/ml muscle aldolase (23.4  $\mu\text{M}$  sites), 175 units/ml  $\alpha$ -glycerolphosphate dehydrogenase, 4320 units/ml triosephosphate isomerase, 30  $\mu\text{M}$  NADH, 25mM Tris (Cl), 5mM EDTA, pH 7.5. The straight line crossing the lower portion of the photograph is the infinite time point which was taken several minutes after the initiation of the reaction. Note also that the offset for the infinite time point is 0.3 O.D. units and the offset for the reaction was 0.4 O.D. units. The first line above the border corresponds to the offset value.

The first-order replot from this data is shown in Figure 15. The curve consists of a rapid initial phase followed by a slower second phase. Extrapolation of the second phase to time zero showed that the first phase accounted for 70-74% of the total substrate and the second phase 26-30%. The pseudo first-order rate constant for the first phase is  $4.7 \text{ sec}^{-1}$  and the constant for the second phase is  $0.69 \text{ sec}^{-1}$ .

Figure 14. Stopped Flow Oscilloscope Traces

A.) 20 unit/ml ( $23.4 \mu\text{M}$  sites) muscle aldolase, 175 unit/ml  $\alpha$ -glycerolphosphate dehydrogenase/triosephosphate isomerase,  $30 \mu\text{M}$  NADH,  $12 \mu\text{M}$  FBP,  $25\text{mM}$  Tris (Cl),  $5\text{mM}$  EDTA, at pH 7.5. Slit width was 1 mm, vertical offset of 0.4 O.D., vertical scale of 0.05 O.D./division, horizontal scale of 0.1 sec/division. For the infinite time trace the vertical offset was 0.3 O.D.

B.) 4.5 unit/ml ( $187 \mu\text{M}$  sites) liver aldolase, 175 unit/ml  $\alpha$ -glycerolphosphate dehydrogenase/triosephosphate isomerase,  $30 \mu\text{M}$  NADH,  $12 \mu\text{M}$  FBP,  $50\text{mM}$  Tris (Cl),  $10\text{mM}$  EDTA, at pH 7.5. Slit width was 1 mm, vertical offset was 0.3 O.D., vertical scale of 0.05 O.D./division, horizontal scale of 0.2 sec./division.

C.) 2.25 unit/ml ( $93 \mu\text{M}$  sites) liver aldolase, 20 unit/ml ( $23.4 \mu\text{M}$  sites) muscle aldolase, 175 unit/ml  $\alpha$ -glycerolphosphate dehydrogenase/triosephosphate isomerase,  $30 \mu\text{M}$  NADH,  $12 \mu\text{M}$  FBP,  $50\text{mM}$  Tris (Cl),  $10\text{mM}$  EDTA, at pH 7.5. Slit width was 1 mm, vertical offset was 0.4 O.D., vertical scale of 0.05 O.D./division.

Note: Vertical offset value is one grid division from bottom of grid. All runs were at  $31^\circ\text{C}$ .

**FIGURE**

**14**

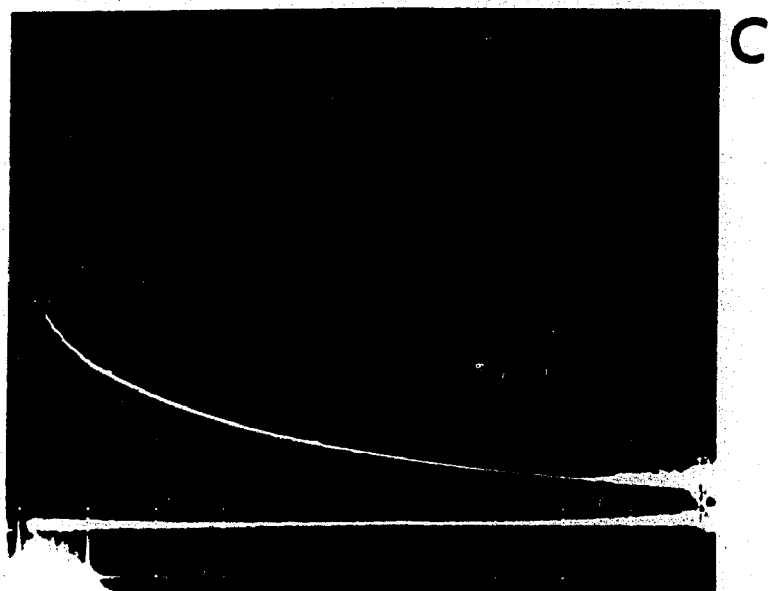
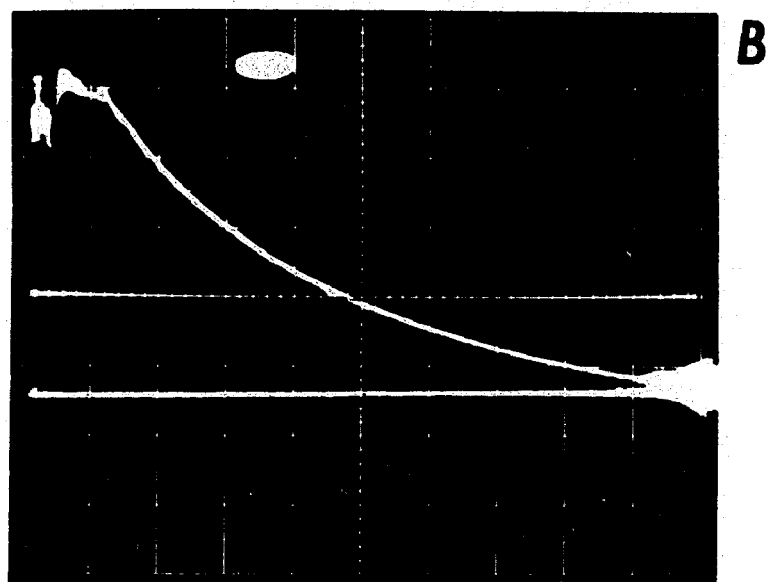
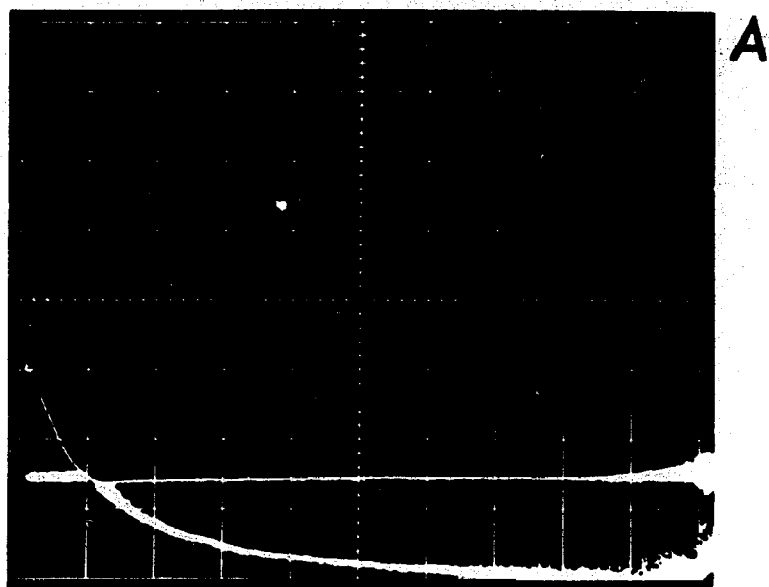
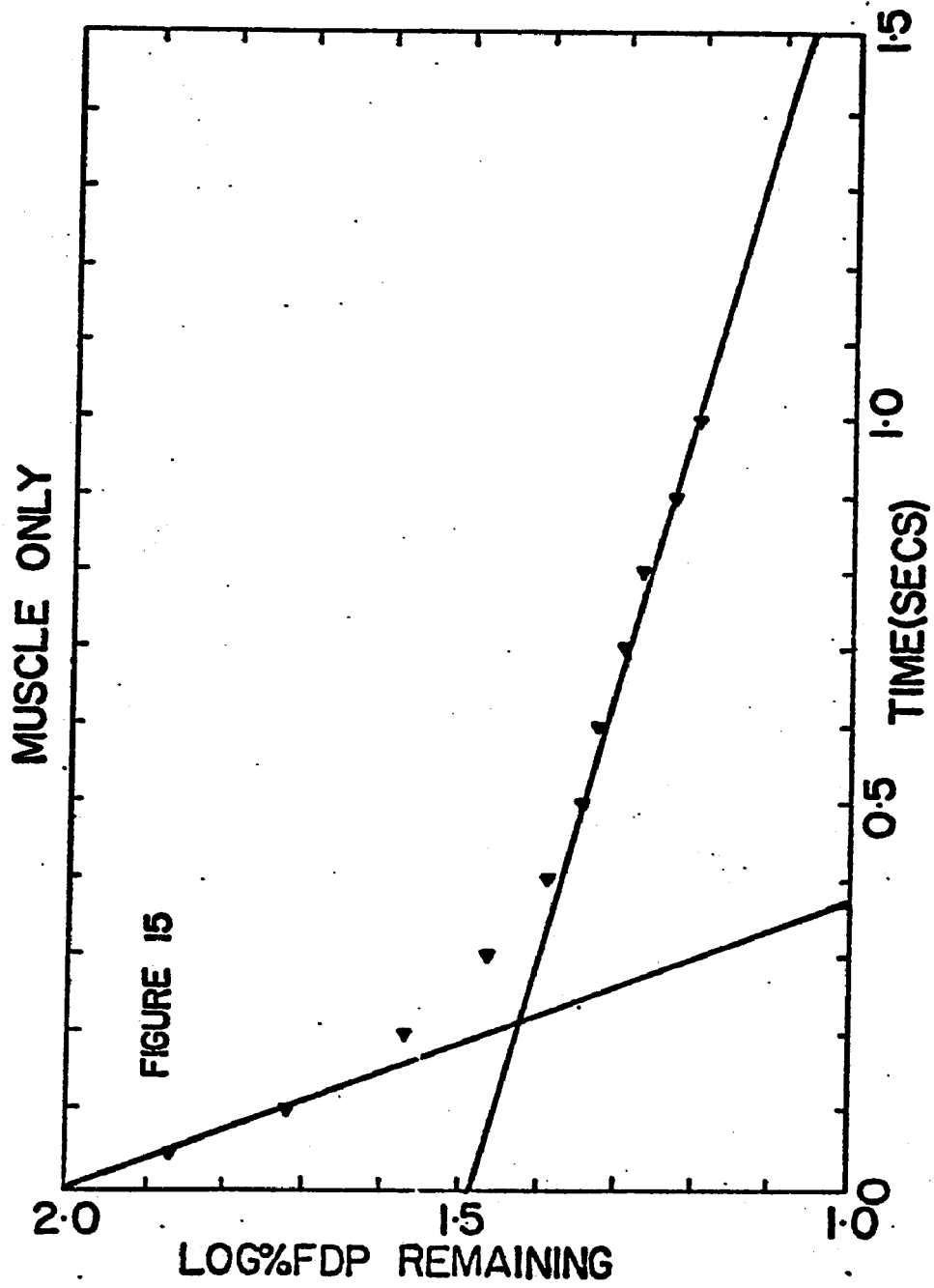


Figure 15. First-order Replot for Muscle Aldolase  
Stopped Flow Experiment (Oscilloscope trace Figure 14A)



### Liver Aldolase

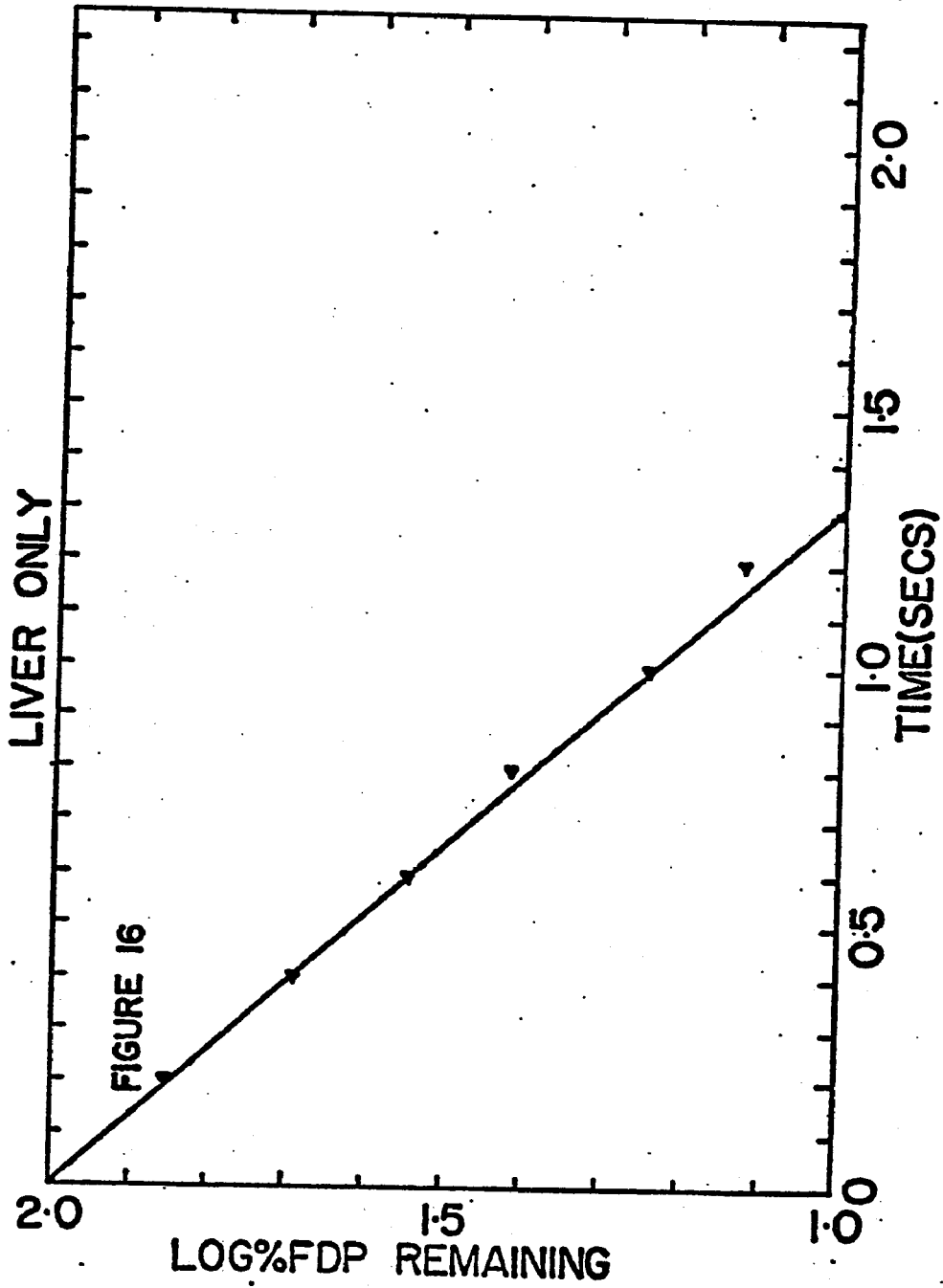
The oscilloscope trace from a typical liver aldolase experiment is shown in Figure 14B. The final concentrations in this experiment were:  $12 \mu\text{M}$  FBP, 4.5 units/ml liver aldolase ( $187 \mu\text{M}$  sites), 175 units/ml  $\alpha$ -glycerolphosphate dehydrogenase, 4320 units/ml triosephosphate isomerase,  $30 \mu\text{M}$  NADH,  $50\text{mM}$  Tris (Cl),  $10\text{mM}$  EDTA, at pH 7.5. In this photograph, the offset is the same for the infinite time point as during the reaction trace.

The first-order replot for this data is shown in Figure 16. It is readily apparent that this replot curve is not biphasic like the muscle enzyme but rather is a straight line. The rate constant for this reaction is  $1.7 \text{ sec}^{-1}$ .

### Muscle Aldolase Plus Liver Aldolase

In Figure 14C is shown the oscilloscope trace from a typical stopped flow experiment with both muscle and liver aldolase present. The final concentrations in this experiment were:  $12 \mu\text{M}$  FBP,  $23.4 \mu\text{M}$  sites muscle aldolase,  $93.4 \mu\text{M}$  sites liver aldolase, 175 units/ml  $\alpha$ -glycerolphosphate dehydrogenase, 4320 units/ml triosephosphate isomerase,  $30 \mu\text{M}$  NADH,  $50\text{mM}$  Tris (Cl),  $10\text{mM}$  EDTA, pH 7.5. Again, the vertical offset is the same for the infinite time point as it was for the reaction trace.

Figure 16. First-order Replot for Liver Aldolase  
Stopped Flow Experiment (Oscilloscope trace Figure 14B)



In Figure 17 is shown the first-order replot for the mixed muscle plus liver aldolase stopped flow experiment. The curve is again biphasic with a rapid initial phase followed by a slower second phase. Extrapolation of the second phase to time zero showed that each phase accounted for 50% of the overall reaction. The pseudo first-order rate constant for the first phase is  $2.5 \text{ sec}^{-1}$  and for the second phase  $0.69 \text{ sec}^{-1}$ .

### Computer Simulations

#### Liver Aldolase Only

The results of computer simulation of  $\alpha$ -anomer utilization by liver aldolase are shown in Figure 18 as a plot of  $\log \% \text{FBP}$  remaining versus time. This is plotted from data obtained by using the CRAMS program described earlier. The curve consists of a long lag period (approximately 400 msec) followed by a first-order utilization of the FBP.

A similar plot for the simulation of liver aldolase utilization of exclusively the open form of FBP is shown in Figure 19. This plot has a shorter lag period (approximately 80 msec) followed by a straight line utilization of FBP.

Lastly, in Figure 20 is shown the plot for the simulation of liver aldolase utilization of only the  $\beta$ -anomer of FBP. This utilization plot is first-order

Figure 17. First-order Replot for Mixed Aldolase  
Stopped Flow Experiment (Oscilloscope trace Figure 14C)

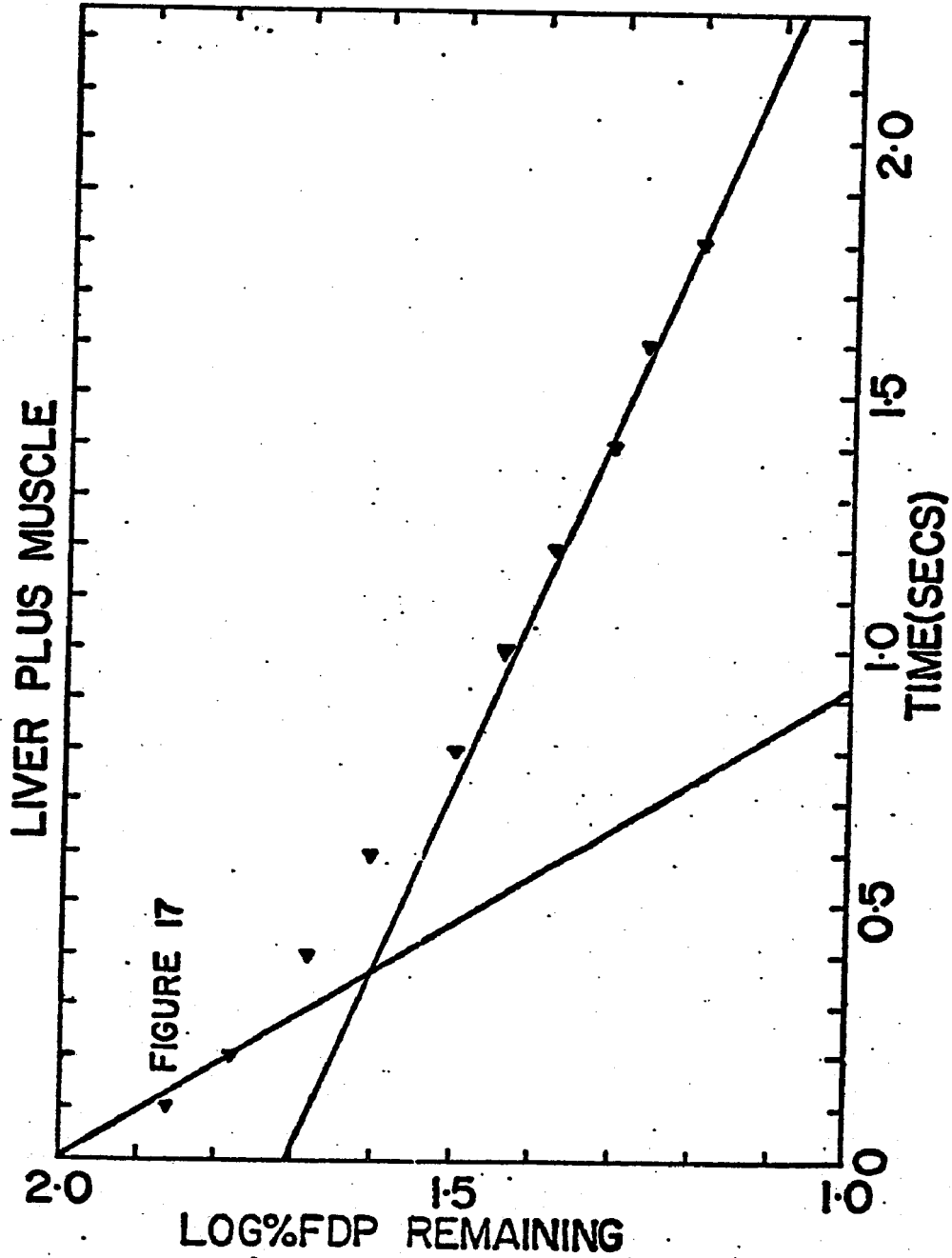


Figure 18. Simulation of Utilization of  $\alpha$ -FBP by Liver Aldolase

Simulation by Chemical Reaction Analysis Modeling System for  $93.4 \mu\text{M}$  liver aldolase sites and  $12 \mu\text{M}$  FBP. Values of the rate constants for binding steps were derived from  $K_M$  values determined independently under the conditions of the stopped flow experiments. The value of  $k_{\text{cat}}$  was the experimental value from the stopped flow. The rate constants for anomerization of  $\beta$ -FBP to  $\alpha$ -FBP were those of Midelfort et al.<sup>19</sup>

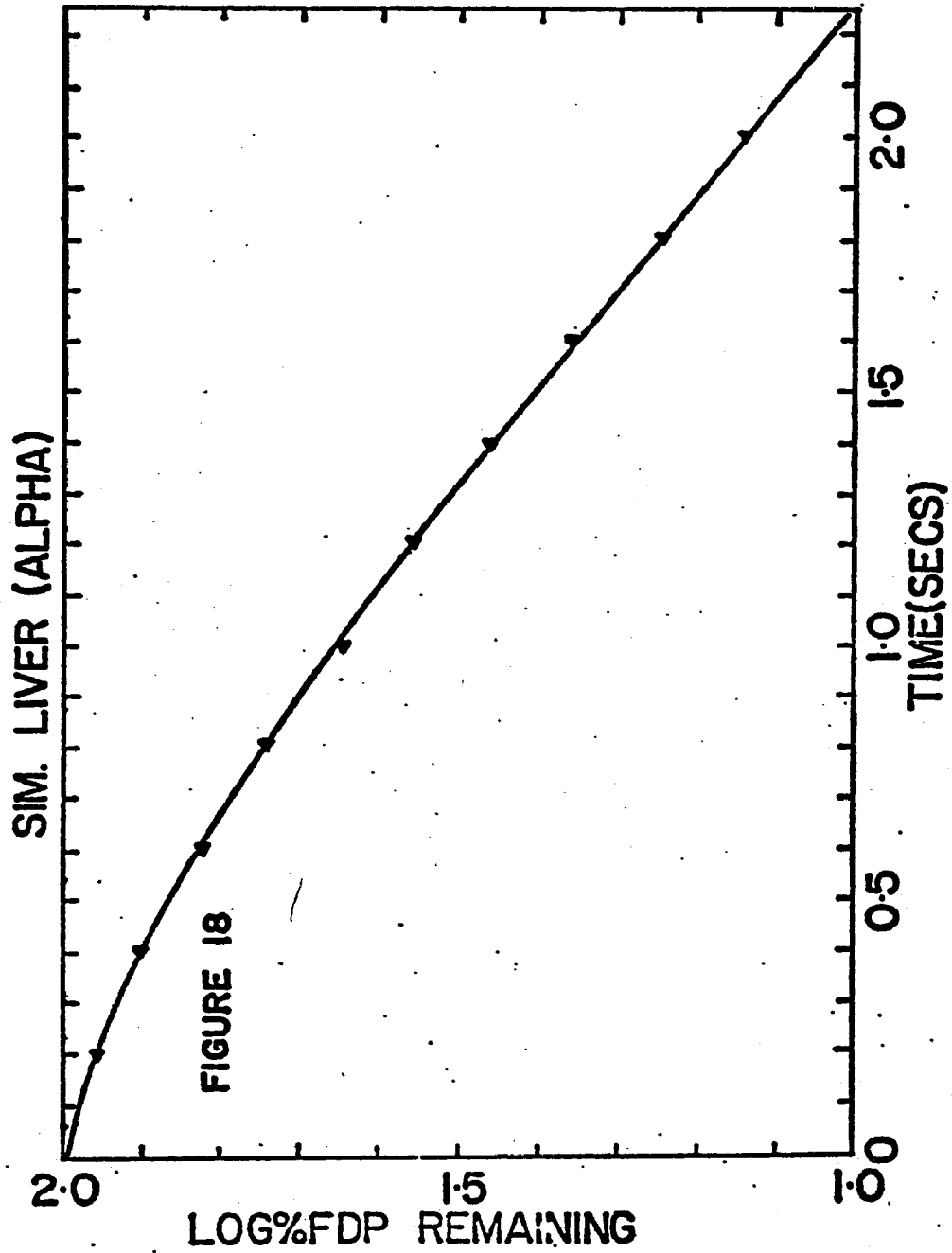


Figure 19. Simulation of Utilization of Open FBP by  
Liver Aldolase

Simulation by Chemical Reaction Analysis Modeling  
System for  $93.4 \mu \text{M}$  liver aldolase sites and  $12 \mu \text{M}$  FBP.  
Values of the rate constants for binding steps were  
derived from  $K_M$  values determined independently under  
the conditions of the stopped flow experiments. The  
value of  $k_{\text{cat}}$  was the experimental value from the  
stopped flow. The rate constants for ring opening  
were those of Midelfort et al.<sup>19</sup>

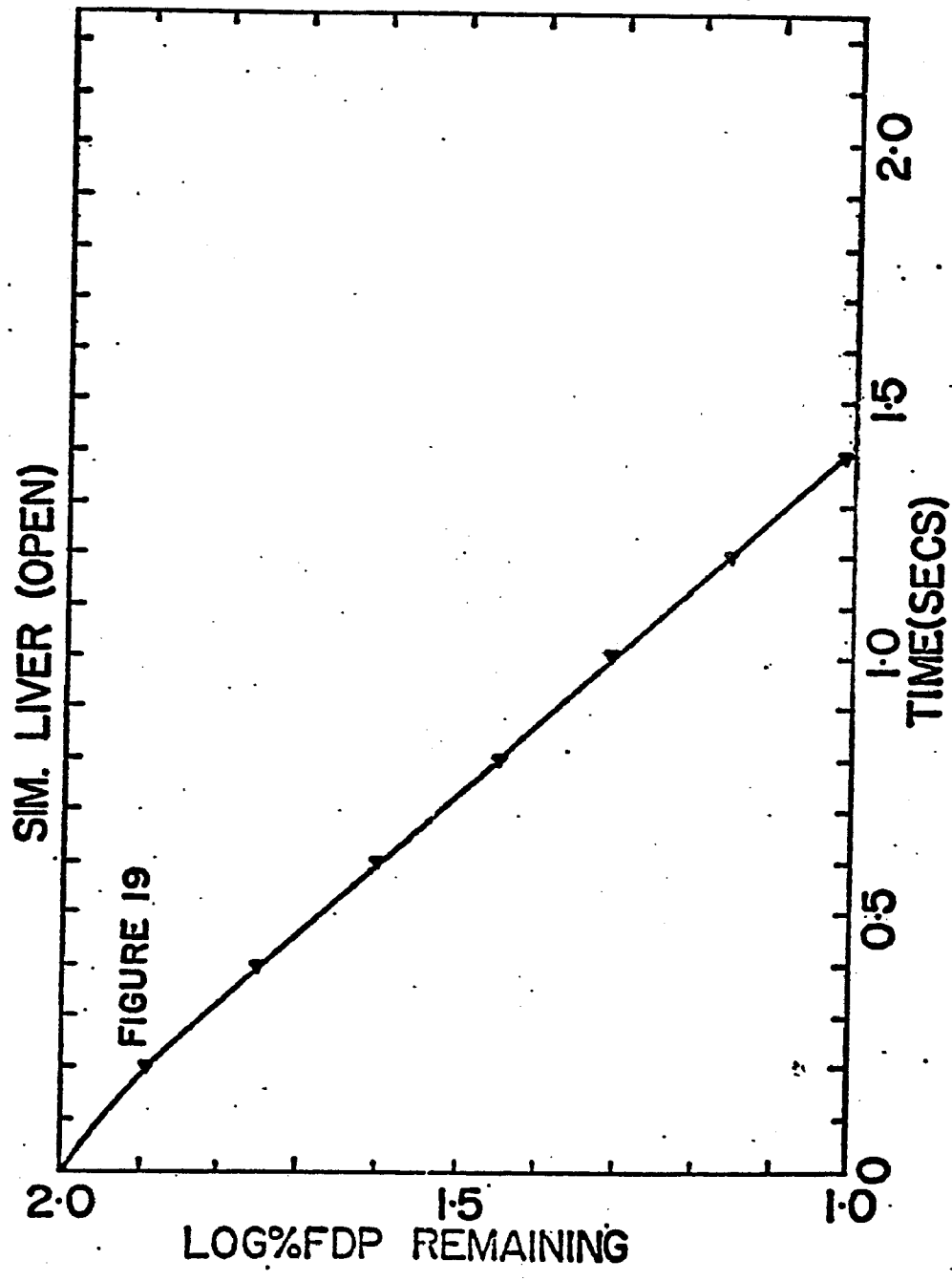
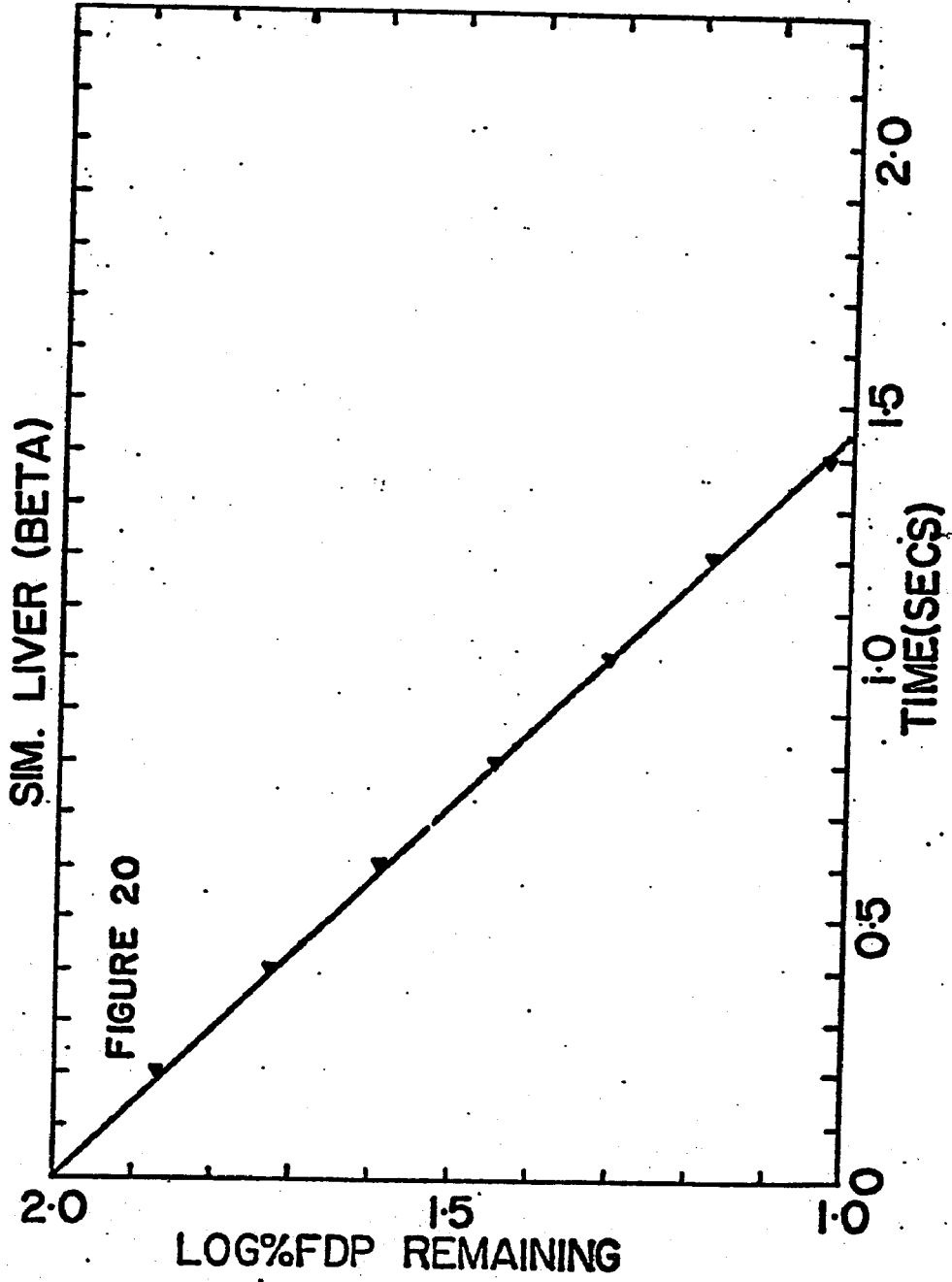


Figure 20. Simulation of Utilization of  $\beta$ -FBP by  
Liver Aldolase

Simulation by Chemical Reaction Analysis Modeling System for  $93.4 \mu\text{M}$  liver aldolase sites and  $12 \mu\text{M}$  FBP. Values of the rate constants for binding steps were derived from  $K_M$  values determined independently under the conditions of the stopped flow experiments. The value of  $k_{\text{cat}}$  was the experimental value from the stopped flow. The rate constants for anomerization of  $\alpha$ -FBP to  $\beta$ -FBP were those of Midelfort et al.<sup>19</sup>



for greater than three half lives of FBP consumption.

#### Muscle Aldolase Plus Liver Aldolase

The simulated first-order plot for the mixture of muscle plus liver aldolase under the same conditions as the stopped flow experiment is shown in Figure 21. In this simulation the muscle enzyme utilizes  $\beta$ -FBP and binds  $\alpha$ -FBP very tightly. Utilization of both the  $\alpha$ - and  $\beta$ -FBP by the liver enzyme is simulated. The plot is linear for greater than three half lives of FBP utilization.

Figure 22 is the simulated first-order plot with the muscle aldolase utilizing  $\beta$ -FBP and binding the  $\alpha$ -anomer of FBP very tightly and with utilization of only the  $\alpha$ -anomer of FBP by the liver enzyme. This simulation gives a nearly linear plot for three half-lives of FBP utilization.

If the simulation is performed assuming utilization of only the  $\beta$ -anomer of FBP by the liver enzyme and utilization as above by the muscle enzyme, the progress curve obtained is that shown in Figure 23. Note that this curve is biphasic.

The results of a similar simulation assuming liver aldolase uses only the open form of FBP is shown in Figure 24. This curve is also biphasic in nature.

Figure 21. Simulation of Mixed Liver Aldolase Plus Muscle Aldolase Experiment with Liver Aldolase Utilization of  $\alpha$ - and  $\beta$ - FBP

Simulation by Chemical Reaction Analysis  
Modeling System for  $93.4 \mu\text{M}$  liver aldolase sites,  $23.4 \mu\text{M}$  muscle aldolase sites, and  $12 \mu\text{M}$  FBP. Values of the rate constants for the binding steps were derived from  $K_M$  values determined independently under the conditions of the mixed stopped flow experiment except for the binding of  $\alpha$ -FBP by muscle aldolase. This value was determined experimentally as described below. The values of  $k_{\text{cat}}$  employed were those determined in the stopped flow experiments. The rate constants for the interconversion of the various forms of FBP were those of Midelfort et al.<sup>19</sup>

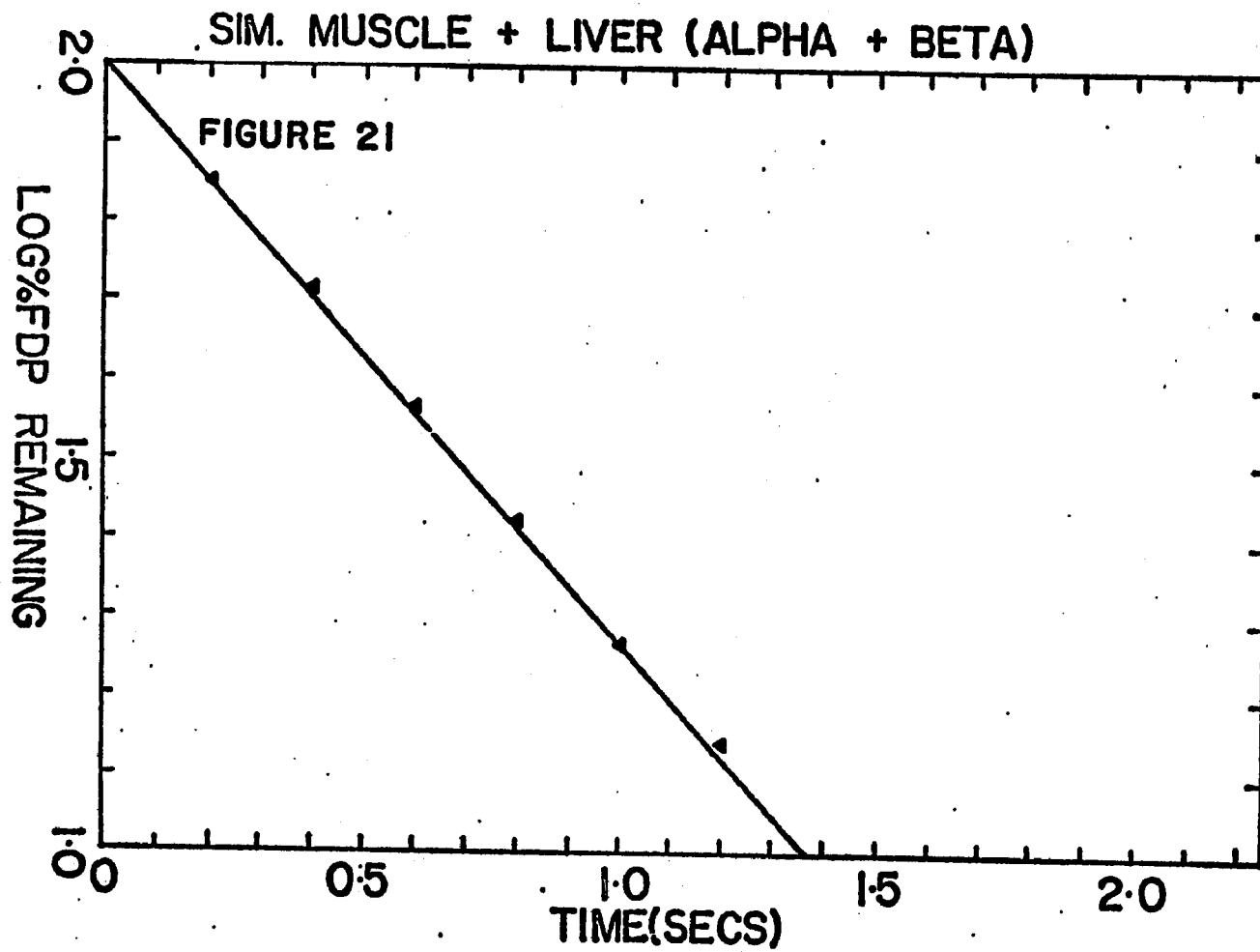


Figure 22. Simulation of Mixed Liver Aldolase Plus Muscle Aldolase Experiment with Liver Aldolase Utilization of  $\alpha$ -FBP

Simulation by Chemical Reaction Analysis Modeling System for  $93.4 \mu\text{M}$  liver aldolase sites,  $23.4 \mu\text{M}$  muscle aldolase sites, and  $12 \mu\text{M}$  FBP. Values of the rate constants for the binding steps were derived from  $K_M$  values determined independently under the conditions of the mixed stopped flow experiment except for the binding of  $\alpha$ -FBP by muscle aldolase. This value was determined experimentally as described below. The values of  $k_{\text{cat}}$  employed were those determined in the stopped flow experiments. The rate constants for the interconversion of the various forms of FBP were those of Midelfort et al.<sup>19</sup>

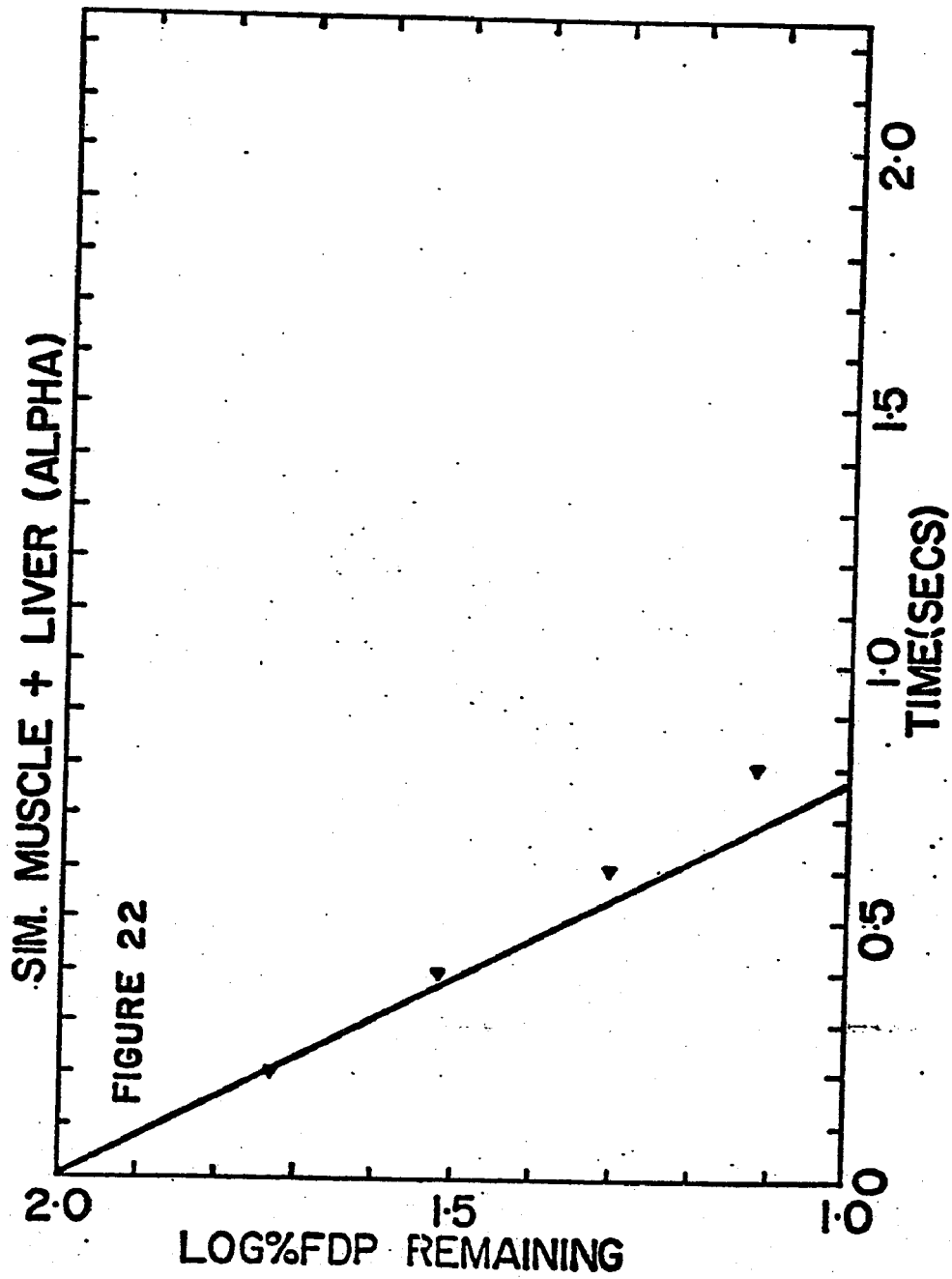


Figure 23. Simulation of Mixed Liver Aldolase Plus Muscle Aldolase Experiment with Liver Aldolase Utilization of  $\beta$ -FBP

Simulation by Chemical Reaction Analysis Modeling System for  $93.4 \mu\text{M}$  liver aldolase sites,  $23.4 \mu\text{M}$  muscle aldolase sites, and  $12 \mu\text{M}$  FBP. Values of the rate constants for the binding steps were derived from  $K_M$  values determined independently under the conditions of the mixed stopped flow experiment except for the binding of  $\alpha$ -FBP by muscle aldolase. This value was determined experimentally as described below. The values of  $k_{\text{cat}}$  employed were those determined in the stopped flow experiments. The rate constants for the interconversion of the various forms of FBP were those of Midelfort et al.<sup>19</sup>

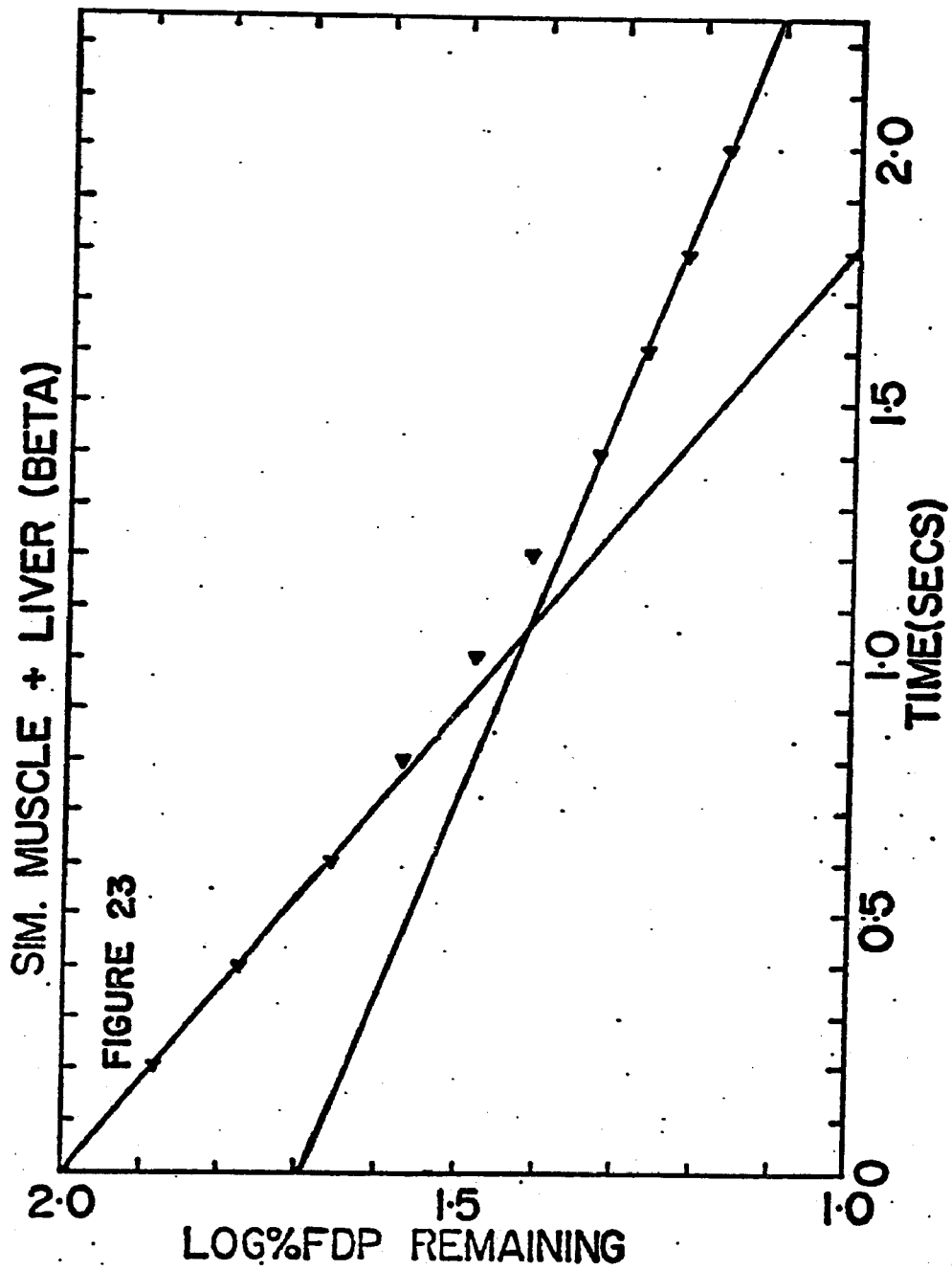
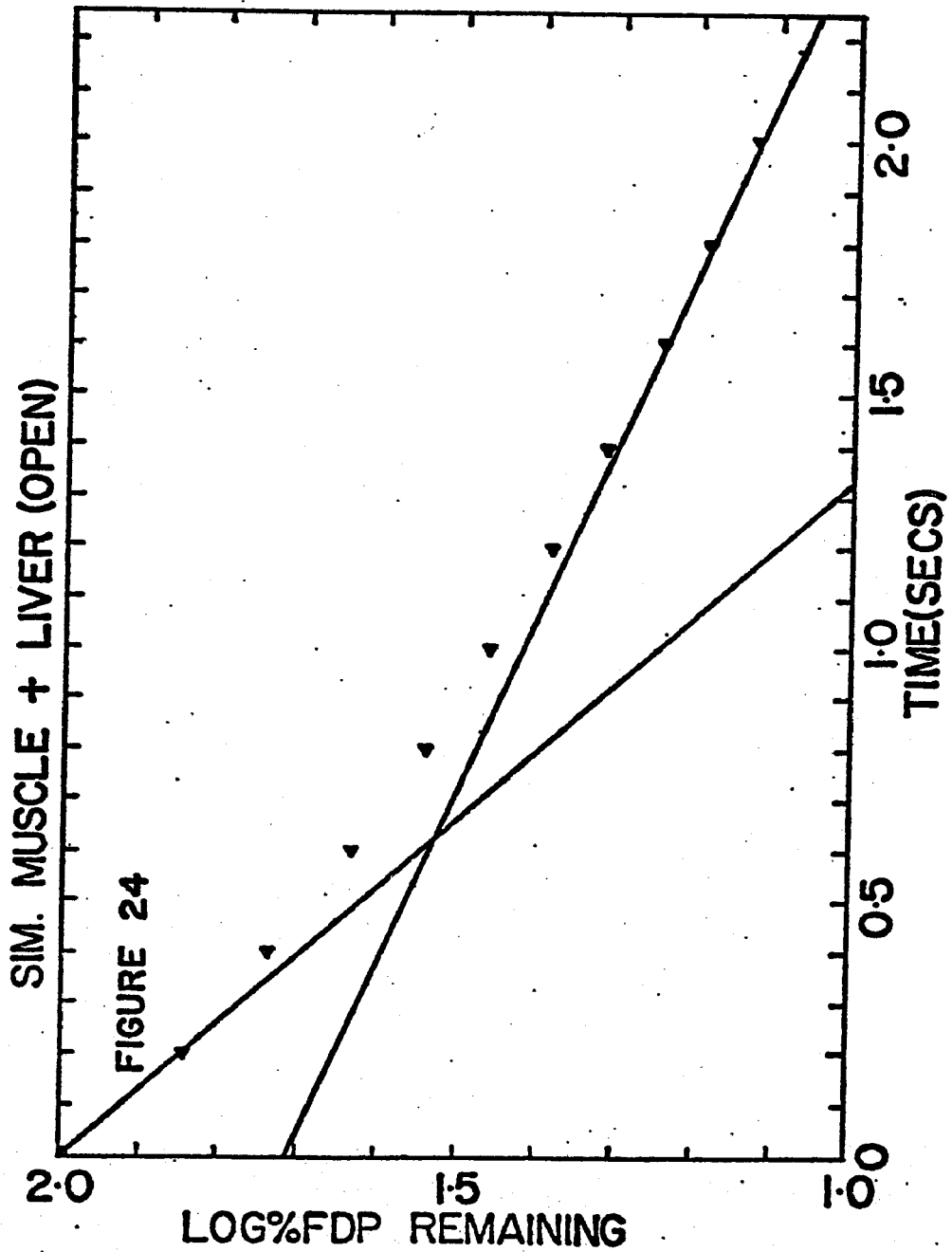


Figure 24. Simulation of Mixed Liver Aldolase Plus Muscle Aldolase Experiment with Liver Aldolase Utilization of Open FBP

Simulation by Chemical Reaction Analysis Modeling System for  $93.4 \mu\text{M}$  liver aldolase sites,  $23.4 \mu\text{M}$  muscle aldolase sites, and  $12 \mu\text{M}$  FBP. Values of the rate constants for the binding steps were derived from  $K_M$  values determined independently under the conditions of the mixed stopped flow experiment except for the binding of  $\alpha$ -FBP by muscle aldolase. This value was determined experimentally as described below. The values of  $k_{\text{cat}}$  employed were those determined in the stopped flow experiments. The rate constants for the interconversion of the various forms of FBP were those of Midelfort et al.<sup>19</sup>



## Inhibition Studies - Substrate Analogues

### $\alpha$ , $\beta$ -methyl fructofuranoside

The Lineweaver - Burk plot for the competitive inhibition of liver aldolase by a 1:1 mixture of  $\alpha$  -methyl fructofuranoside 1,6-bisphosphate and  $\beta$  -methyl fructofuranoside 1,6-bisphosphate is seen in Figure 25. The ratio of 1:1,  $\alpha$  :  $\beta$  , is the result of the conditions of synthesis. The  $K_i$  for this mixture is  $4.6 \times 10^{-5} \underline{M}$ .

In Figure 26 is shown the inhibition of muscle aldolase by this same 1:1 mixture of  $\alpha$ -and  $\beta$  -methyl fructofuranoside 1,6-bisphosphate. The  $K_i$  for this inhibition is  $2.7 \times 10^{-6} \underline{M}$

### $\alpha$ -2,5 - anhydroglucitol 1,6-bisphosphate

The results of a study employing  $\alpha$  -2,5 -anhydroglucitol 1,6-bisphosphate are shown in Figure 27. The inhibition pattern appears to be either noncompetitive or mixed. Treating the lines as noncompetitive leads to a value for  $K_i = 1.2 \times 10^{-3} \underline{M}$ .

### Glucitol 1,6-bisphosphate

The open chain FBP analogue glucitol 1,6-bisphosphate has a competitive inhibition pattern at all but the lowest FBP concentration where the inhibition is greater than expected for competitive inhibition. The  $K_i$  value for the linear portion of the plot is  $4.3 \times 10^{-6} \underline{M}$ . This plot is shown in Figure 28.

Figure 25. Competitive Inhibition of Liver Aldolase  
by  $\alpha$ - and  $\beta$ - Methylfructofuranoside 1,6-bisphosphate  
(MFFBP)

Final concentrations were 50mM Tris (Cl), 10mM  
EDTA, pH 7.5, FBP as shown, 125  $\mu$ M NADH, and  
500  $\mu$ M MFFBP ● , 200  $\mu$ M MFFBP ◐ , 100  $\mu$ M  
MFFBP ■ , uninhibited ▲ .

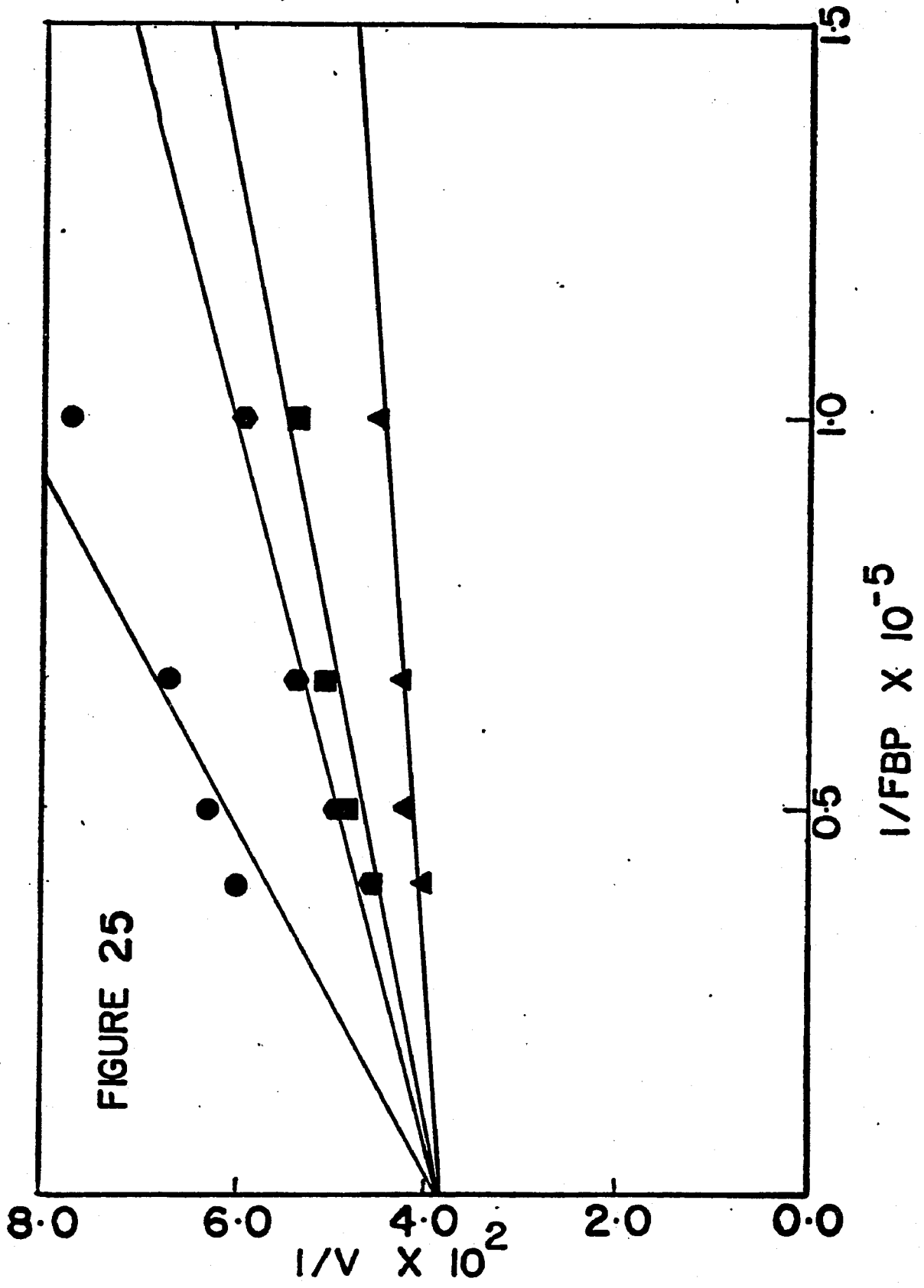


FIGURE 25

Figure 26. Competitive Inhibition of Muscle Aldolase  
by  $\alpha$ - and  $\beta$ - Methylfructofuranoside 1,6-bisphosphate  
(MFFBP)

Final concentrations were 25mM Tris (Cl), 5mM  
EDTA, pH 7.5, FBP as shown, 125  $\mu$ M NADH, and 5  $\mu$ M  
MFFBP ● , 2.5  $\mu$ M MFFBP ● , uninhibited ▲ .

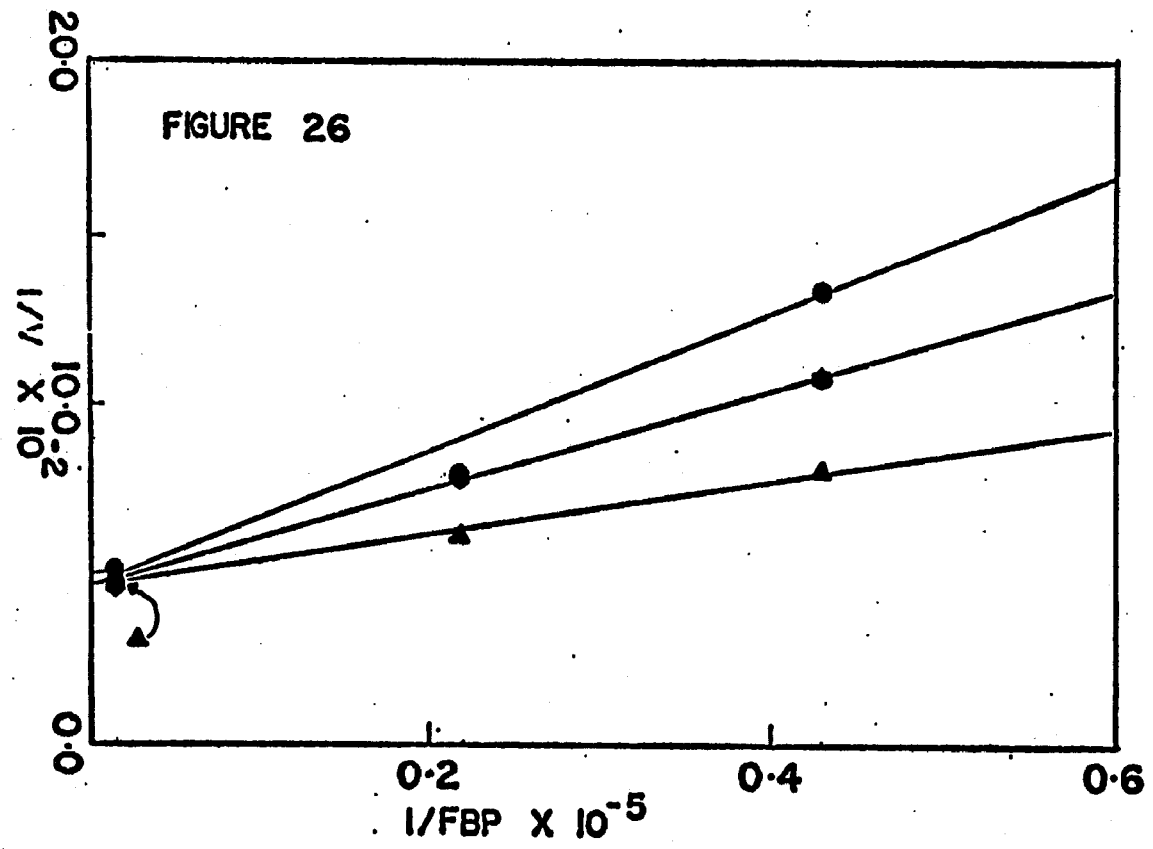


Figure 27. Inhibition of Liver Aldolase by  $\alpha$ -2,5-Anhydroglucitol 1,6-bisphosphate ( $\alpha$ -AGBP)

Final concentrations were 25mM Tris (Cl), 5mM EDTA, pH 7.5, FBP as indicated, 250  $\mu$ M NADH, and 420  $\mu$ M  $\alpha$ -AGBP  $\circ$  , 168  $\mu$ M  $\alpha$ -AGBP  $\bullet$  , 84  $\mu$ M  $\alpha$ -AGBP  $\blacksquare$  , uninhibited  $\blacktriangle$  .

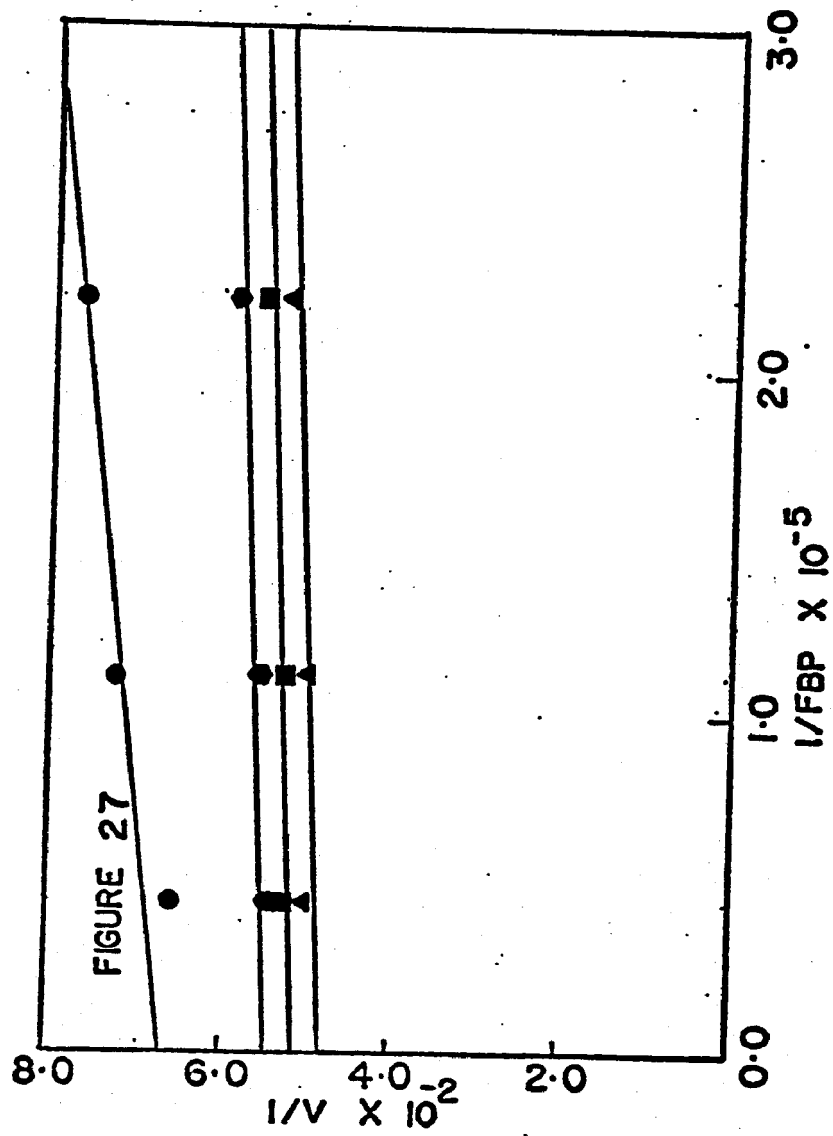
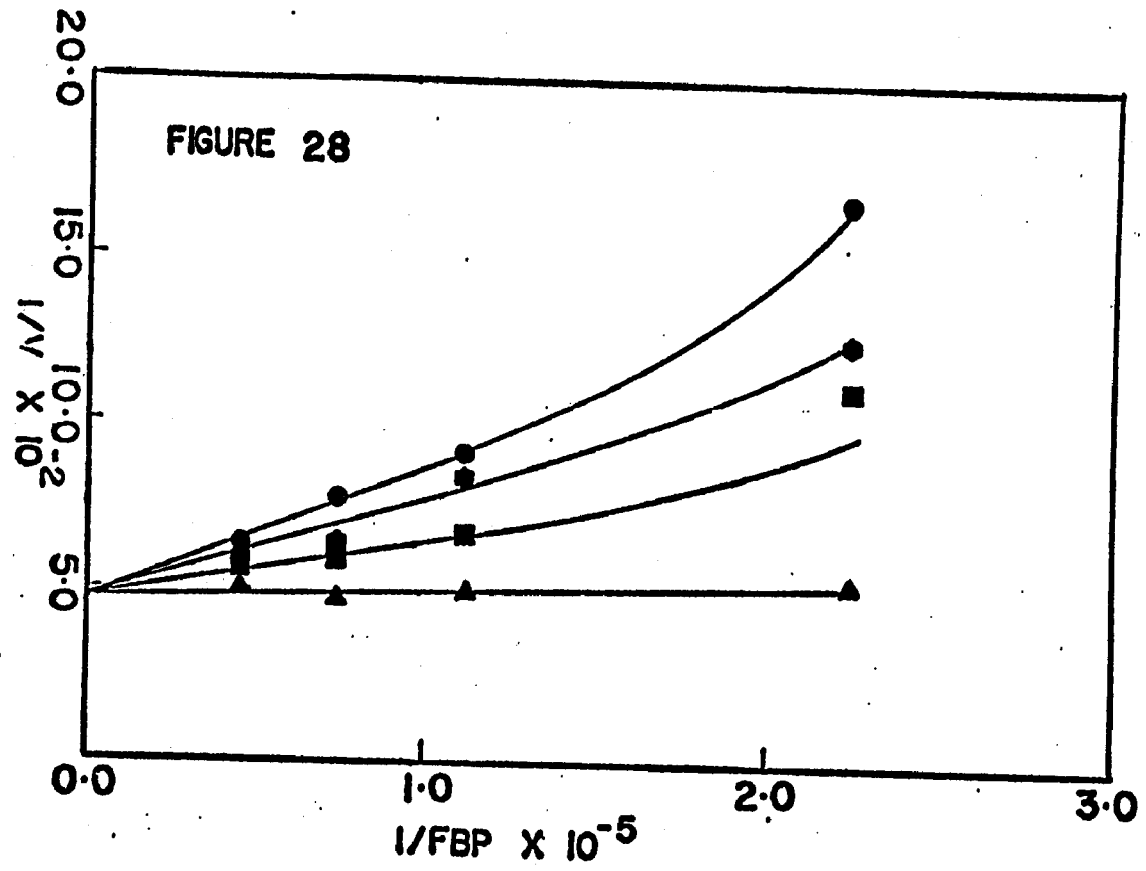


Figure 28. Competitive Inhibition of Liver Aldolase  
by Glucitol 1,6-bisphosphate

Final concentrations were 25mM Tris (Cl), 5mM  
EDTA, pH 7.5, FBP as indicated, 125  $\mu$ M NADH, and  
60  $\mu$ M glucitol 1,6-bisphosphate ● , 40  $\mu$ M glucitol  
1,6-bisphosphate ● , 20  $\mu$ M glucitol 1,6-bisphos-  
phate ■ , uninhibited ▲ .



### Ribulose 1,5-bisphosphate

Ribulose 1,5-bisphosphate inhibition of liver aldolase is shown in Figure 29. The inhibition is competitive with a  $K_i = 2.7 \times 10^{-6} \text{M}$ .

### Ribulose 5-phosphate

The inhibition of liver aldolase by ribulose 5-phosphate is presented in Figure 30. The inhibition pattern is either mixed or uncompetitive.

### Ribose 5-phosphate

In Figure 31 the competitive inhibition pattern obtained for the inhibition of liver aldolase by ribose 5-phosphate is shown. The value found for the inhibition constant is  $K_i = 1.18 \times 10^{-3} \text{M}$ .

### Measurement of the Rate of Liver Aldolase When $\beta$ -FBP Is Slowly Generated by PFK

The Dowex-2 (Cl) elution patterns for the measurement of the rate of aldolase when  $\beta$ -FBP is slowly generated by PFK is shown in Figure 32 and Figure 33. The product counts are found in the wash fractions as  $^3\text{HOH}$ . Fractions 1-20 contain unreacted  $[5\text{-}^3\text{H}]\text{F6P}$ , unlabeled DHAP and unlabeled G3P. Fractions 1-20 are from the  $5\text{mM}$  HCl elution of the Dowex-2 (Cl). As can be seen, much of the  $[5\text{-}^3\text{H}]\text{F6P}$  has not reacted to form  $\beta$ -FBP in the 2.5 sec the reactions were allowed to proceed. Fractions 21-40 are from the  $100\text{mM}$  HCl elution of the Dowex-2 (Cl) column and

Figure 29. Competitive Inhibition of Liver Aldolase  
by Ribulose 1,5-bisphosphate (RuBP)

Final concentrations were 25mM Tris (Cl), 5mM  
EDTA, pH 7.5, FBP as indicated, 125  $\mu$ M NADH, and  
50  $\mu$ M RuBP ● , 25  $\mu$ M RuBP ■ , uninhibited ▲ .

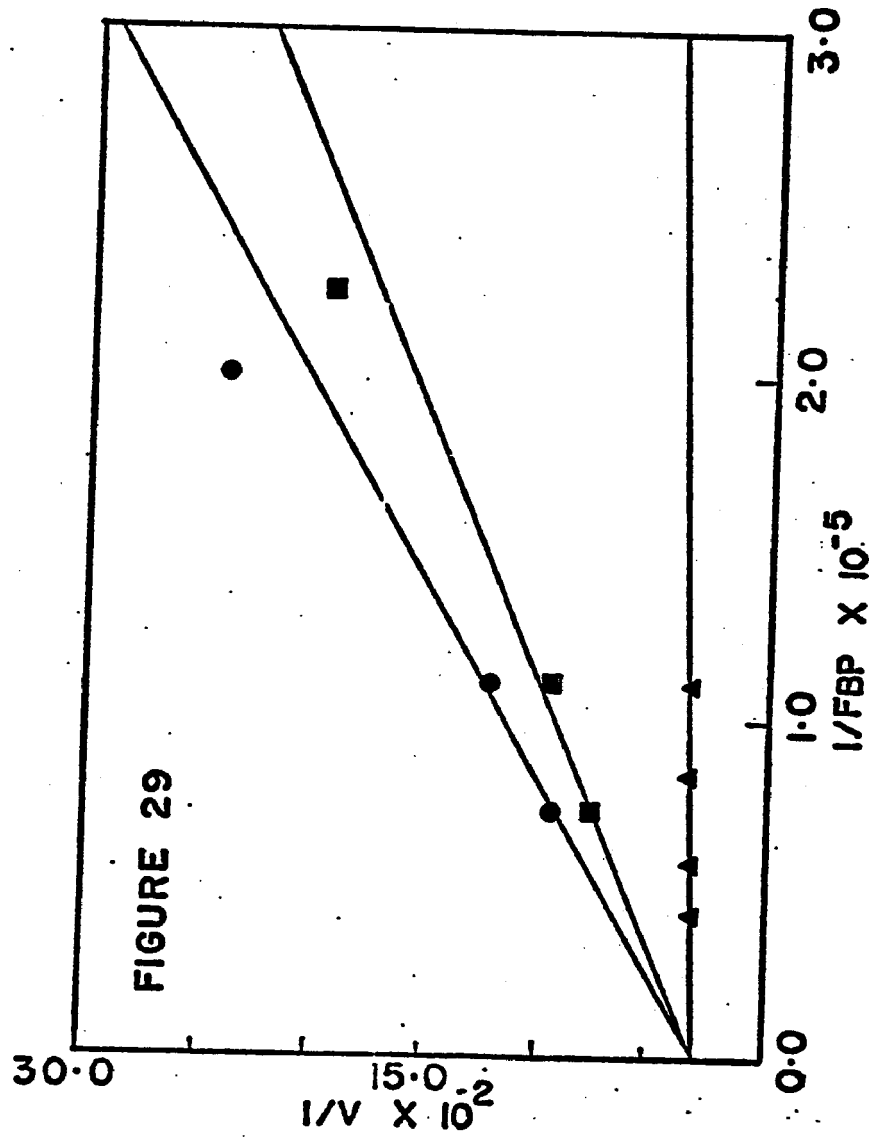


Figure 30. Inhibition of Liver Aldolase by Ribulose 5-phosphate (Ru5P)

Final concentrations were 25mM Tris (Cl), 5mM EDTA, pH 7.5, FBP as indicated, 125  $\mu$ M NADH, and 500  $\mu$ M Ru5P ● , 250  $\mu$ M Ru5P ● , 100  $\mu$ M Ru5P ■ , uninhibited ▲ .

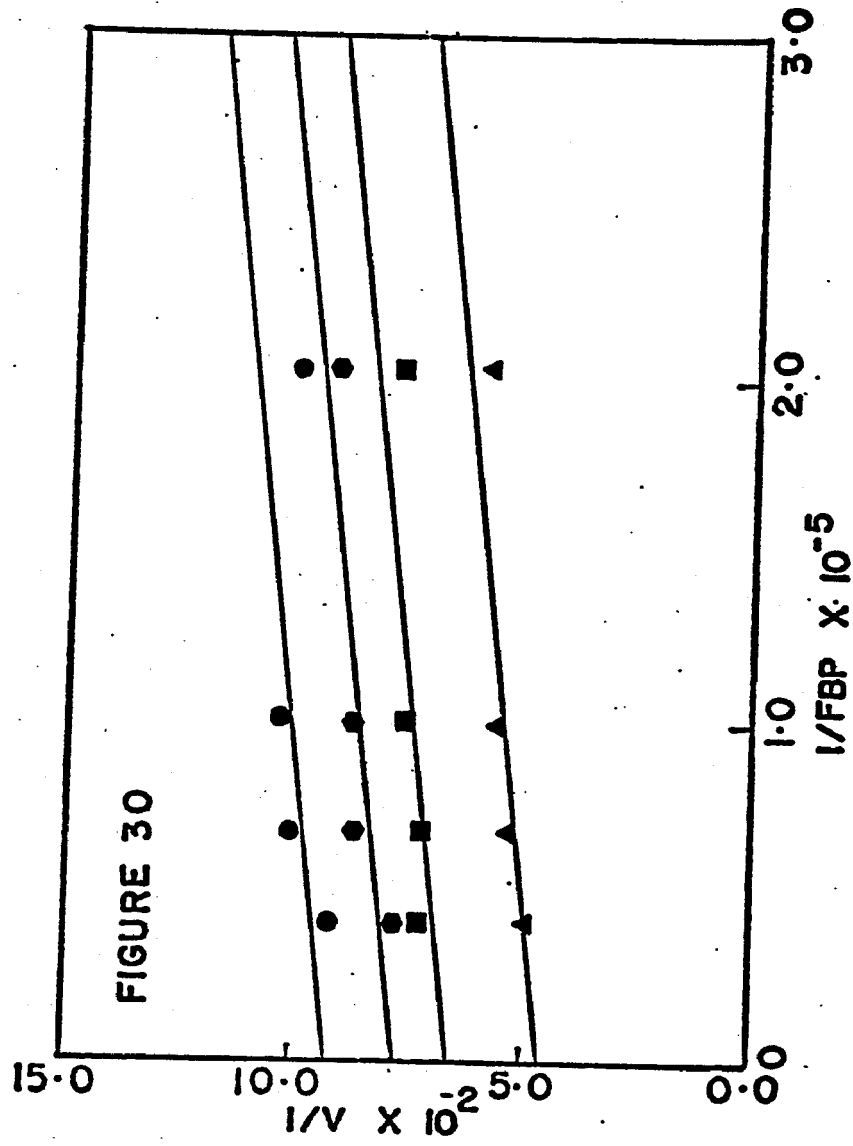


Figure 31. Competitive Inhibition of Liver Aldolase  
by Ribose 5-phosphate (R5P)

Final concentrations were 50mM Tris (Cl), 10mM  
EDTA, pH 7.5, FBP as indicated, 125  $\mu$ M NADH, and  
2.5mM R5P ● , 1.25mM R5P ● , uninhibited ▲ .

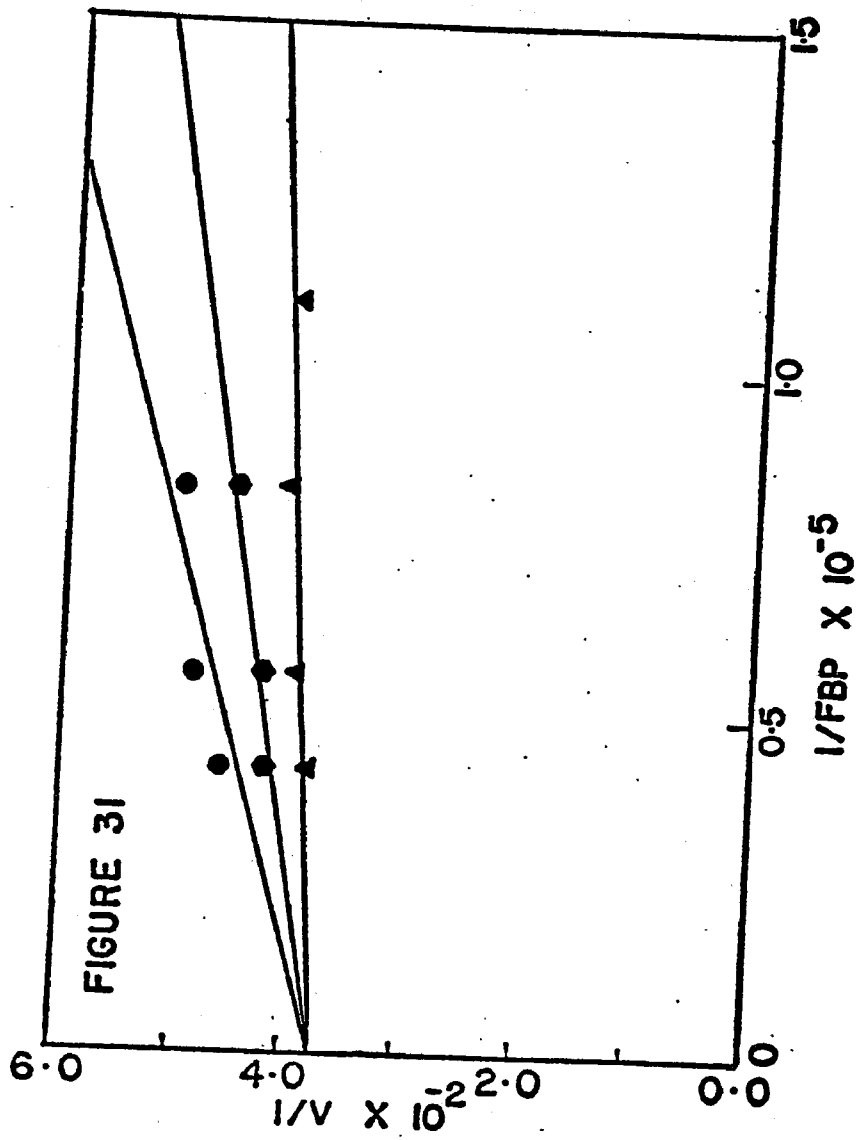


Figure 32. Dowex-2 (Cl) Elution Pattern from Measurement of Liver Aldolase Rate with  $\beta$ -FBP Generated by PFK - 9 Nanoequivalents of Aldolase Sites

Fractions of 1 ml were collected. Fractions 1-20 were from 5mM HCl elution and fractions 21-40 were from 100mM HCl elution. 100  $\lambda$  of each fraction was used for scintillation as described in the text. The volume of the wash fraction was 25 mls.

FIGURE 32

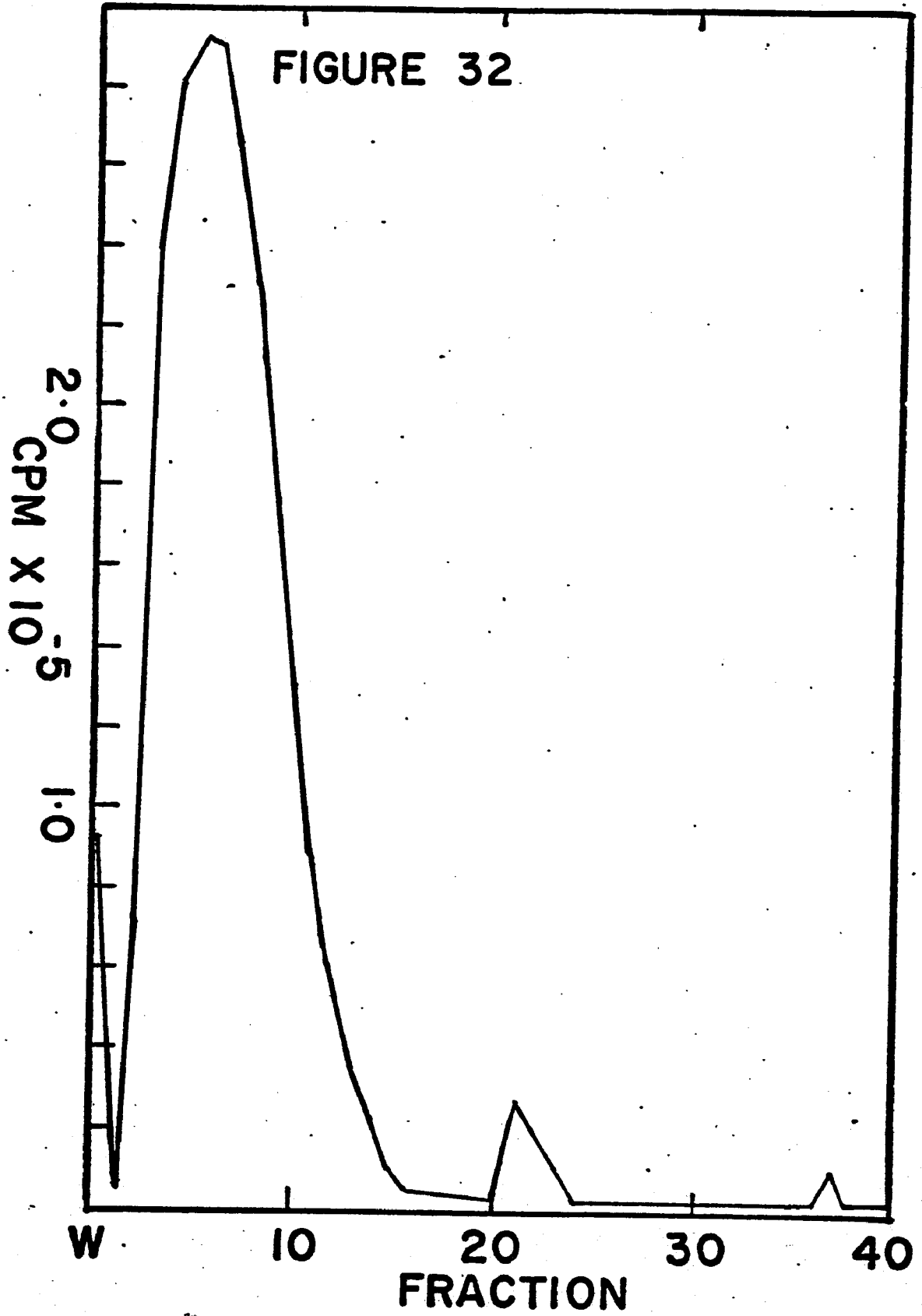
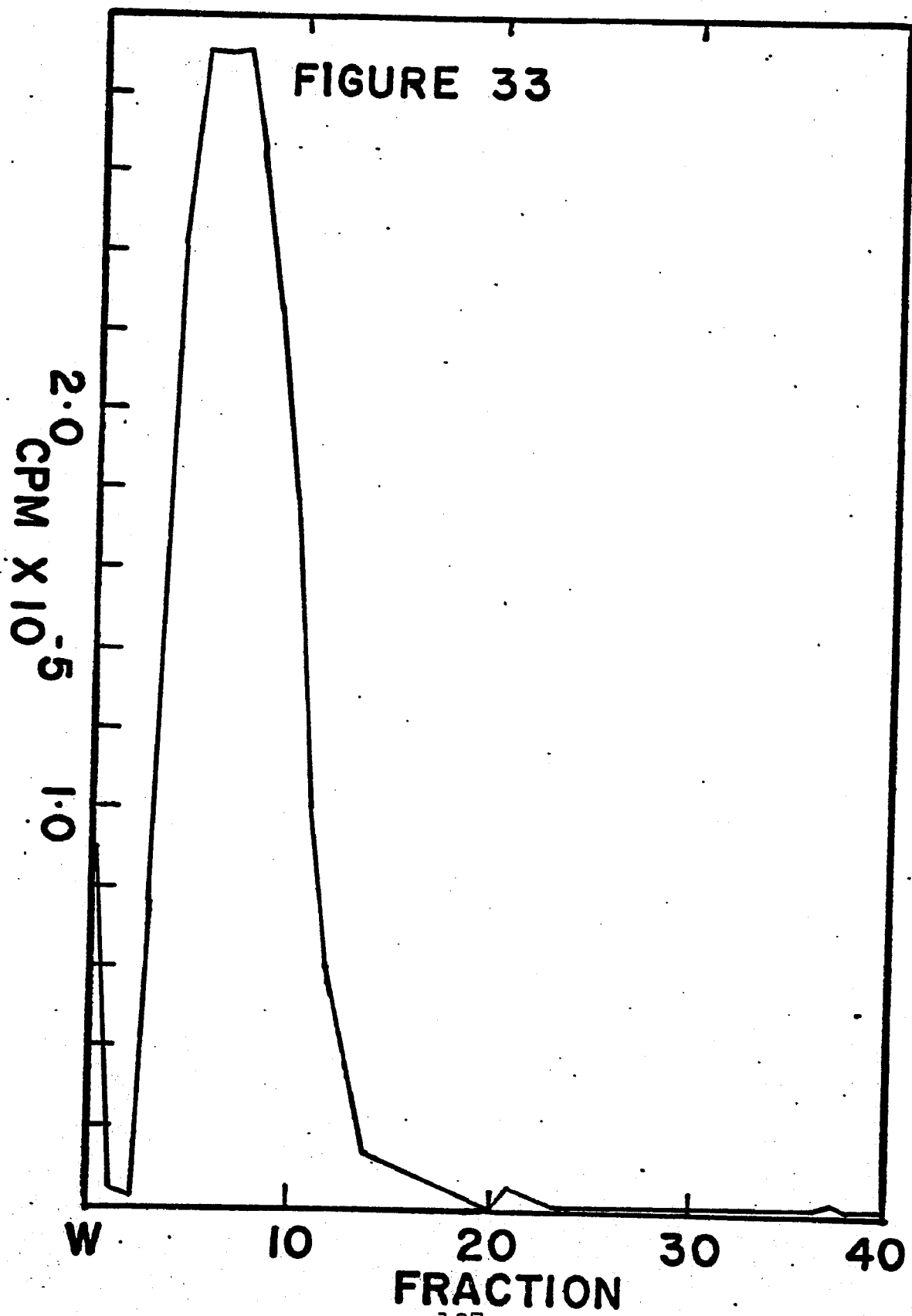


Figure 33. Dowex-2 (Cl) Elution Pattern from Measurement of Liver Aldolase Rate with  $\beta$ -FBP Generated by PFK - 56 Nanoequivalents of Aldolase Sites

Fractions of 1 ml were collected. Fractions 1-20 were from 5mM HCl elution and fractions 21-40 were from 100mM HCl elution. 100  $\lambda$  of each fraction was used for scintillation as described in the text. The volume of the wash fraction was 25 mls.



contain [5-<sup>3</sup>H]FBP and unlabeled FBP added along with the concentrated HCl quench. The theoretical amount of FBP should be  $\frac{50 \lambda}{1000 \lambda} \times \frac{10 \mu\text{Moles}}{\text{ml}} = 0.5\text{mM}$  FBP total. On assaying for FBP in fractions 21-23, it is found that 0.26 mole of FBP was recovered in the 9 nano-equivalent liver aldolase run. This corresponds to 52% recovery. The recovery rate in the 56 nanoequivalent liver aldolase run is found to be 42%. The counts per minute for FBP shown in Table 7 are corrected to 100% recovery. As can also be seen in Table 7, the rate of the liver aldolase reaction which is given by the proportionality:

$$\frac{d\text{FBP}}{dt} \propto \frac{\text{cpm } ^3\text{HOH}}{\text{cpm FBP} \times \text{time}}$$

increases on going from 9 nanoequivalents of liver aldolase to 56 nanoequivalents of liver aldolase.

#### Rate of <sup>3</sup>H Exchange into DHAP by Liver Aldolase

The Dowex-2 (Cl) elution patterns using 50mM HCl are shown in Figures 34-37. As mentioned previously, in this experiment the rate of exchange from <sup>3</sup>HOH into DHAP is being measured. This is in order to determine whether or not one of the steps involved in protonating DHAP is rate limiting to the overall liver aldolase reaction. The reaction progress curve and the first-order replot are shown in Figure 38 and Figure 39 respectively. From these plots a rate

Table 7

Measurement of the Rate of Liver Aldolase  
When  $\beta$  - FBP is Slowly Generated by PFK

<u>Equivalents of Aldolase Sites</u>	<u>cpm <math>^3\text{HOH}</math></u>	<u>cpm <math>5\text{-}^3\text{H FBP}</math></u>	<u>cpm <math>^3\text{HOH}</math> cpm FBP x time</u>
9	$2.33 \times 10^7$	$1.06 \times 10^6$	7.33
56	$2.19 \times 10^7$	$1.96 \times 10^5$	44.8

Figure 34. Dowex-2 (Cl) Elution Pattern Using 50mM  
HCl from  $^3\text{H}$  Exchange into DHAP by Liver Aldolase -  
2 Minutes of Exchange

Fractions of 1.5 ml were collected. 100  $\lambda$  of  
each fraction was used for scintillation as described  
in the text.

- - - DHAP

— cpm

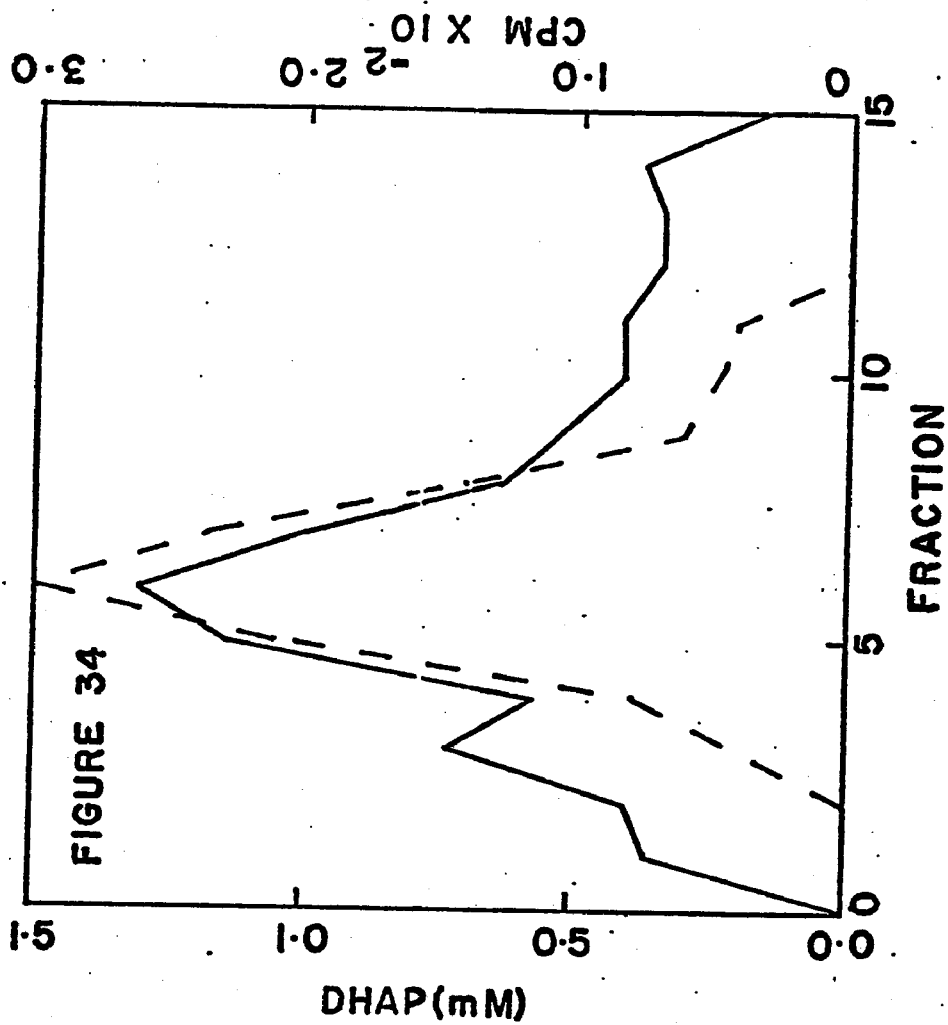


FIGURE 34

Figure 35. Dowex-2 (Cl) Elution Pattern Using 50mM  
HCl from  $^3\text{H}$  Exchange into DHAP by Liver Aldolase -  
4 Minutes of Exchange

Fractions of 1.5 ml were collected. 100  $\lambda$  of  
each fraction was used for scintillation as described  
in the text.

-- -- DHAP

—— cpm

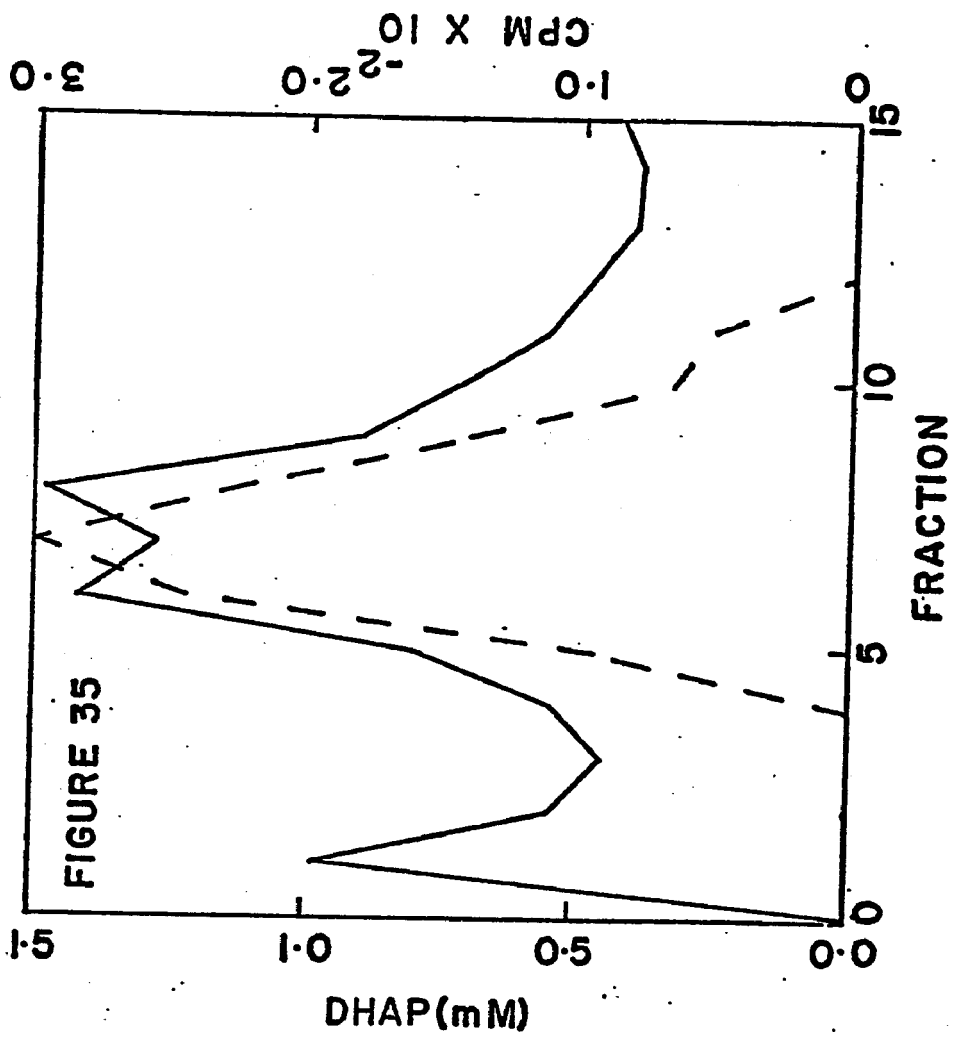


Figure 36. Dowex-2 (Cl) Elution Pattern Using 50mM  
HCl from  $^3\text{H}$  Exchange into DHAP by Liver Aldolase -  
10 Minutes of Exchange

Fractions of 1.5 ml were collected. 100  $\lambda$  of  
each fraction was used for scintillation as described  
in this text.

- - - DHAP

—— cpm

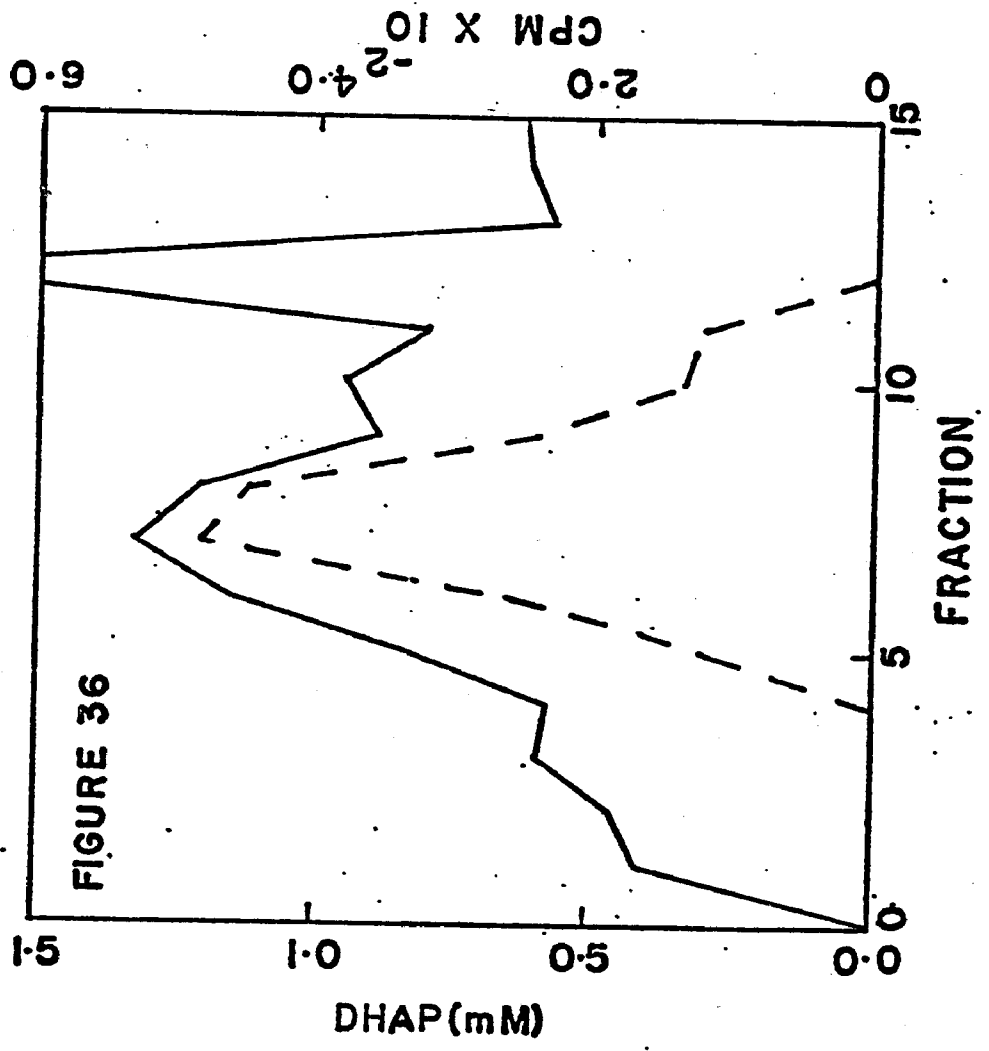


Figure 37. Dowex-2 (Cl) Elution Pattern Using 50mM  
HCl from  $^3\text{H}$  Exchange into DHAP by Liver Aldolase -  
90 Minutes of Exchange

Fractions of 1.5 ml were collected. 100  $\lambda$  of  
each fraction was used for scintillation as described  
in the text.

- - - DHAP

—— cpm

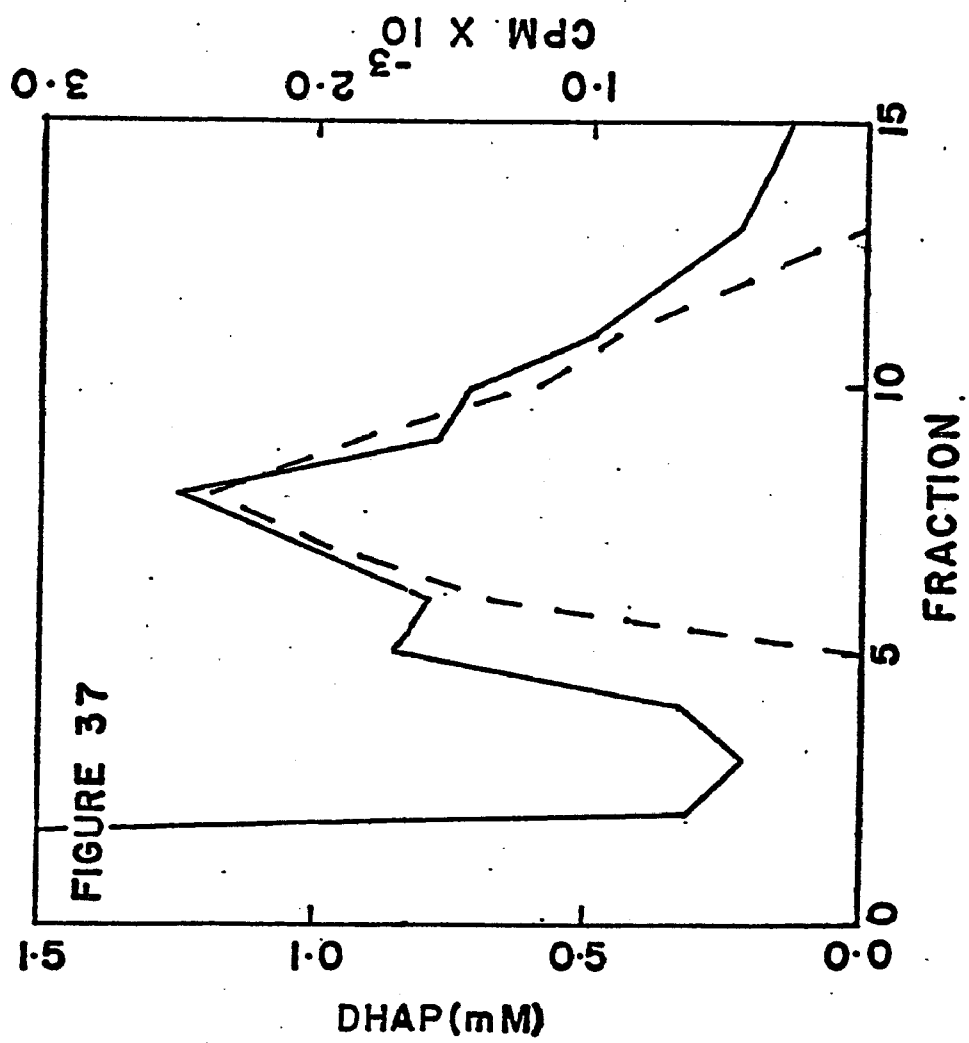


Figure 38. Progress Curve for  $^3\text{H}$  Exchange into DHAP  
by Liver Aldolase

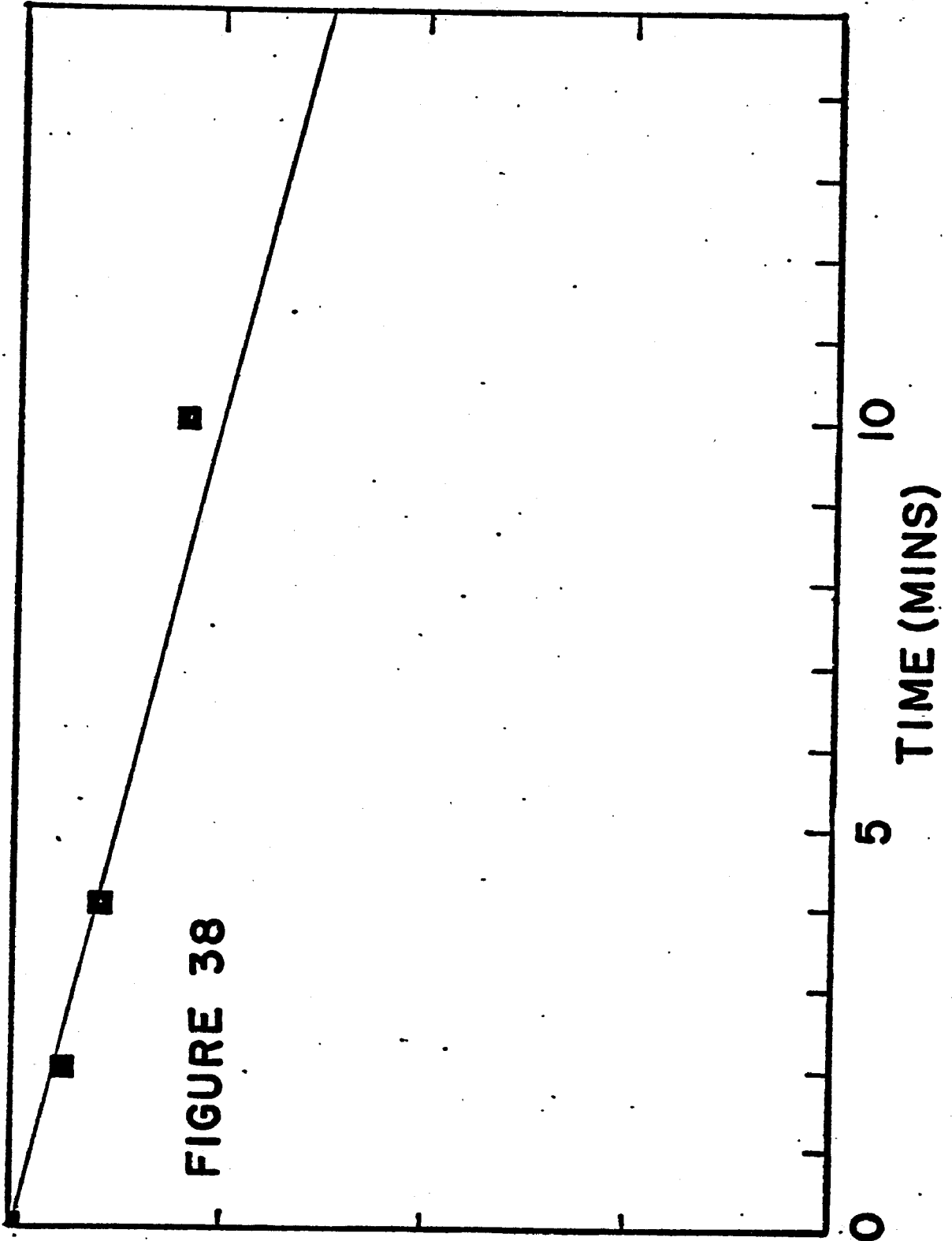
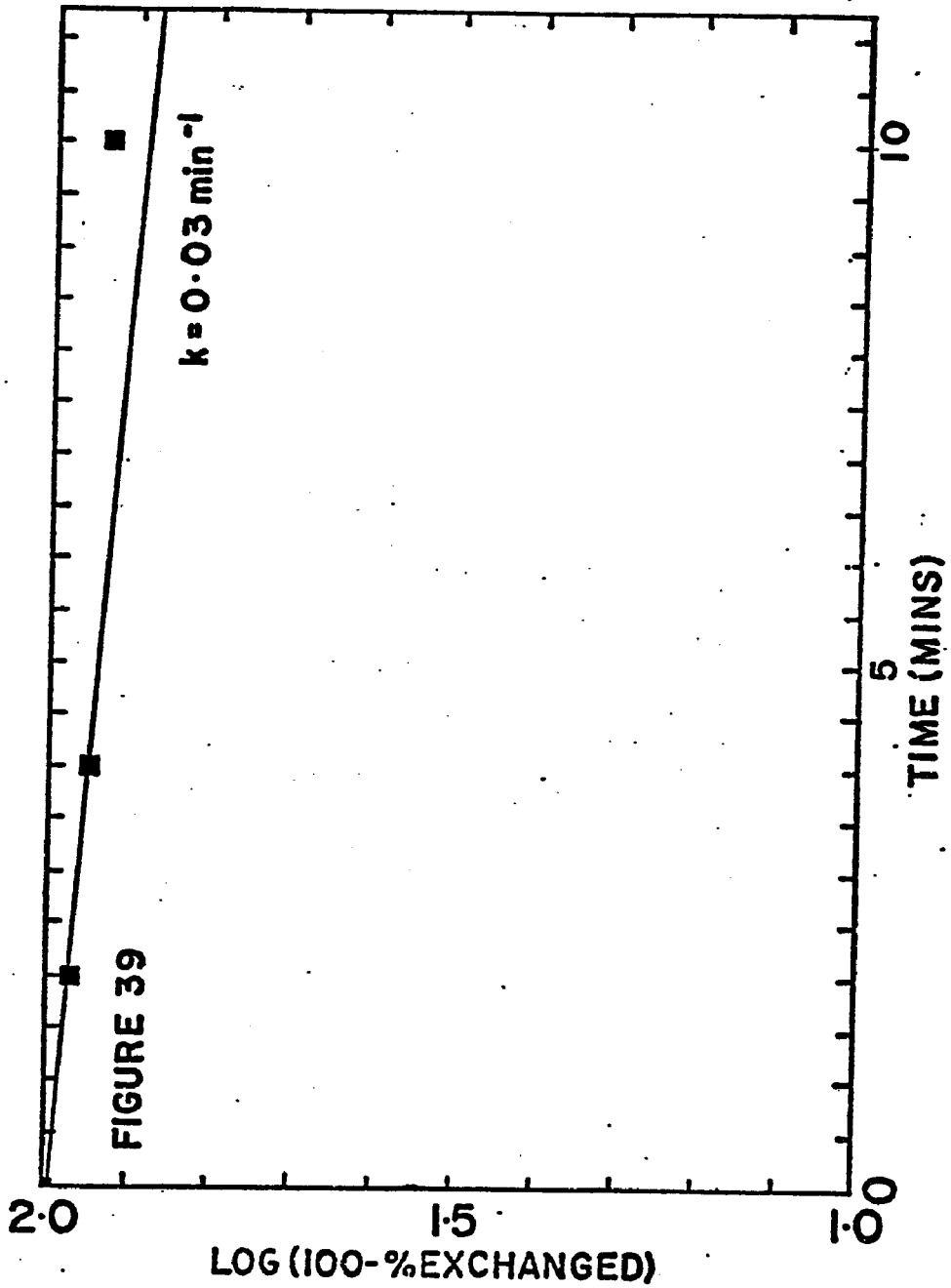


FIGURE 38

100-% EXCHANGED

Figure 39. First-order Replot for  $^3\text{H}$  Exchange into  
DHAP by Liver Aldolase



constant of  $k' = 0.028 \text{ min}^{-1}$  and an overall rate of 1.41  $\mu$  Moles of exchange per minute, are found.

Inactivation of Muscle Aldolase by 1-chloro 2,6-dinitrobenzene and by 1-chloro 2,4-dinitrobenzene

The inactivation of muscle aldolase by 1-chloro 2,6-dinitrobenzene at pH 9.6 is shown in Figure 40. The inactivation is 53% complete at 90 minutes and goes to about 85% inactivation at 210 minutes. The results of a similar inactivation of muscle aldolase by 1-chloro 2,4-dinitrobenzene is shown in Figure 41. In this case the inactivation is 50% complete in 15 minutes and is 93% complete in 60 minutes.

Inactivation of Liver Aldolase by 1-chloro 2,4-dinitrobenzene

Liver aldolase is also inactivated by 1-chloro 2,4-dinitrobenzene. This inactivation is shown in Figure 42. The inactivation is 50% complete in 10 minutes and reaches 97% completion in 50 minutes. In the presence of 100  $\mu$  M FBP, 100  $\mu$  M DHAP, and 100  $\mu$  M G3P in an equilibrium mixture, the inactivation is 22% complete at 10 minutes and is only 64% complete at 50 minutes.

Inactivation of Liver Aldolase by 4-hydroxymercuribenzoate

The sulfhydryl specific reagent 4-hydroxymercuribenzoate is shown to inactivate liver aldolase in

Figure 40. Inactivation of Muscle Aldolase by 1-Cl  
2,6-dinitrobenzene

● Aldolase activity remaining plotted as  
per cent inactivation

▲ Control

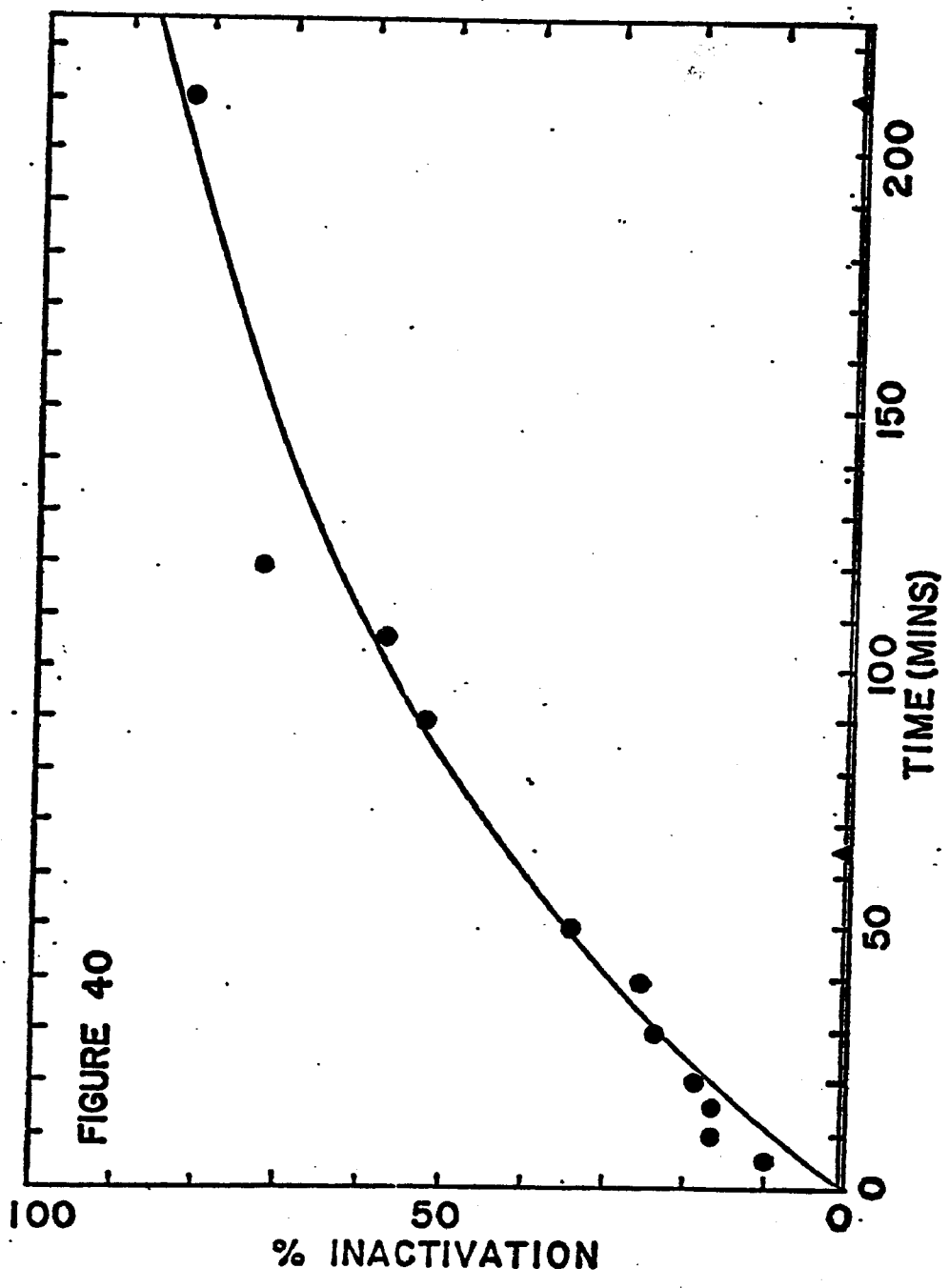


Figure 41. Inactivation of Muscle Aldolase by 1-Cl  
2,4-dinitrobenzene

● Aldolase activity remaining plotted as  
per cent inactivation

▲ Control

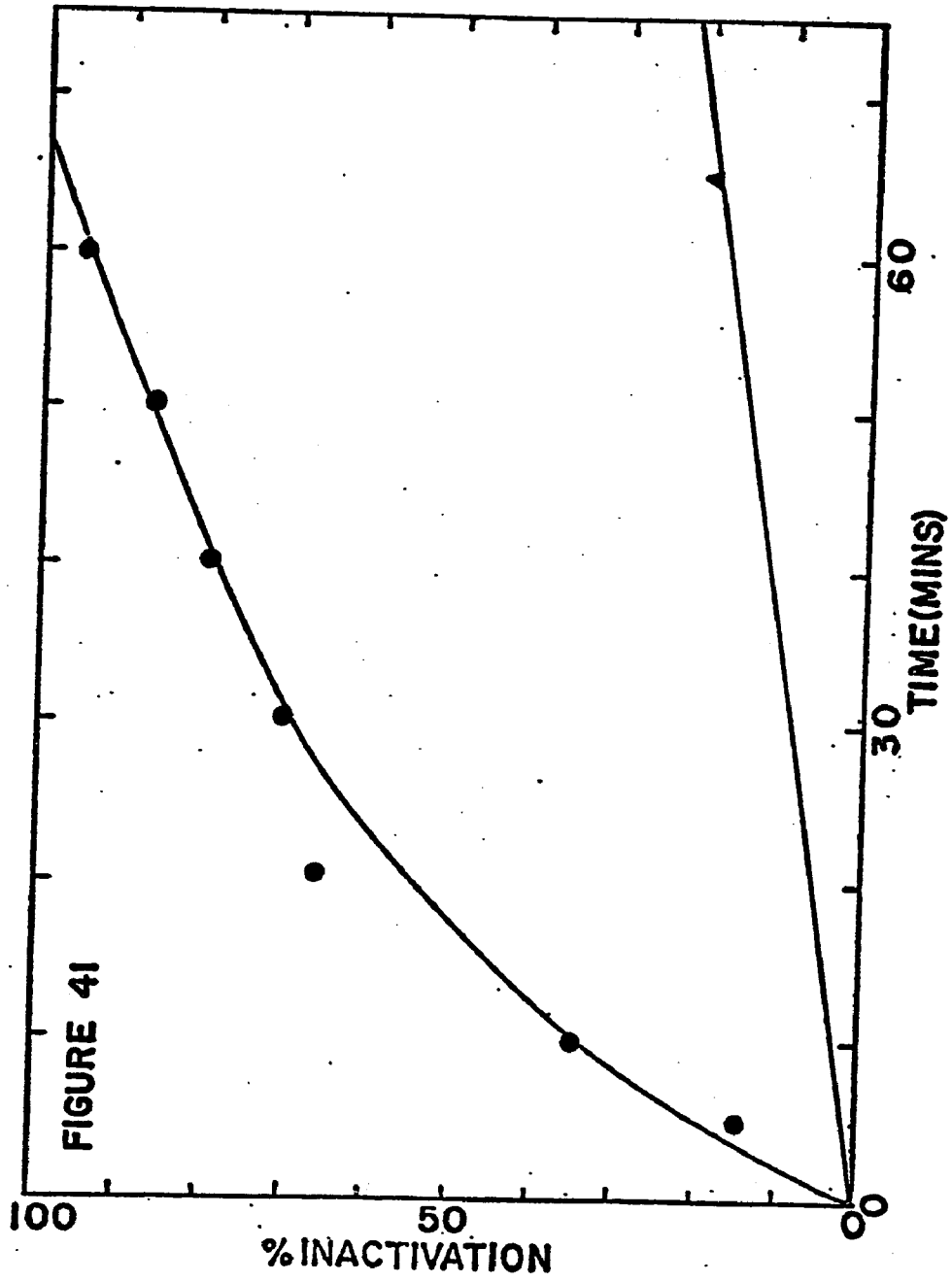


Figure 42. Inactivation of Liver Aldolase by 1-Cl  
2,4-dinitrobenzene

● Aldolase activity remaining plotted as per  
cent inactivation without substrate present

■ Aldolase activity remaining plotted as per  
cent inactivation with substrate present

● Control without substrate

▲ Control with substrate

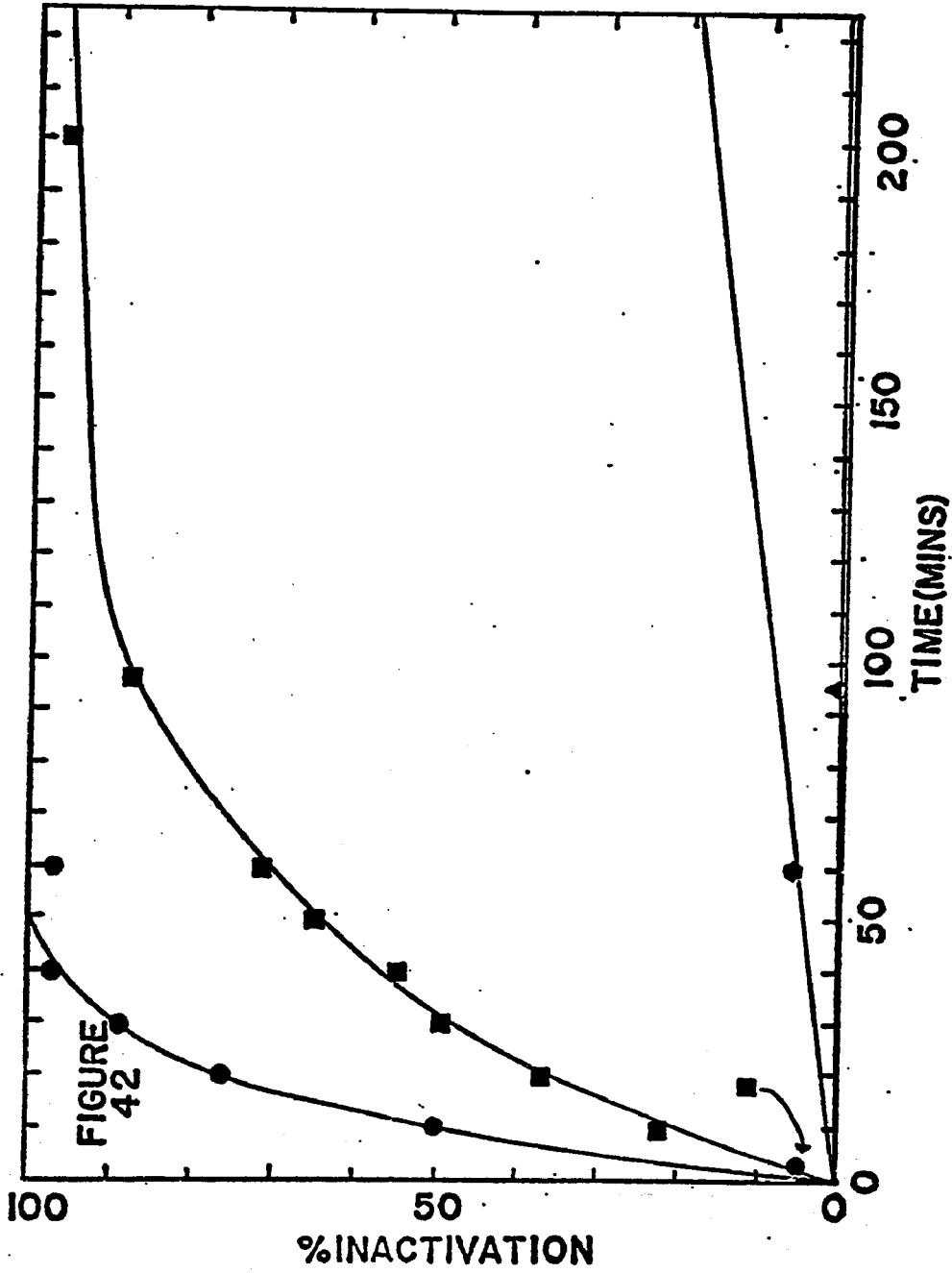


Figure 43. The inactivation is 90% complete at about 150 minutes, with 50% inactivation at about 25 minutes. In the presence of an equilibrium mixture of 100  $\mu\text{M}$  FBP, 100  $\mu\text{M}$  DHAP, and 100  $\mu\text{M}$  G3P, the inhibition is 75% complete at 150 minutes and 50% inactivation is reached at about 55 minutes.

Inactivation of Muscle Aldolase by Pyridoxal 5-phosphate (PLP)

In Figure 44 is shown the inactivation of muscle aldolase by 10  $\mu\text{M}$  PLP. The inactivation is 50% complete by 3 minutes and in 20 minutes is more than 85% complete. The inactivation first-order replot is shown for 10  $\mu\text{M}$ , 20  $\mu\text{M}$ , and 25  $\mu\text{M}$  PLP in Figure 45. All of the replot curves are nonlinear. The levels of PLP are such that the inactivation should be pseudo first-order. A nonintegrated first-order replot of the data in Figure 44 is presented in Figure 46. The resultant line is curved. The nonintegrated second-order replot of the data from Figure 44 is shown in Figure 47. This plot is also clearly nonlinear. In Figure 44, the data is plotted using the nonzero level of activity at which the inactivation appears to terminate as the infinite time value. In Figure 48 is the first-order replot obtained for the 10  $\mu\text{M}$  PLP inactivation utilizing zero activity as the infinite time value. This plot also is clearly

Figure 43. Inactivation of Liver Aldolase by 4-hydroxymercuribenzoate

● Aldolase activity remaining plotted as per cent inactivation without substrate present

■ Aldolase activity remaining plotted as per cent inactivation with substrate present

▲ Control with and without substrate

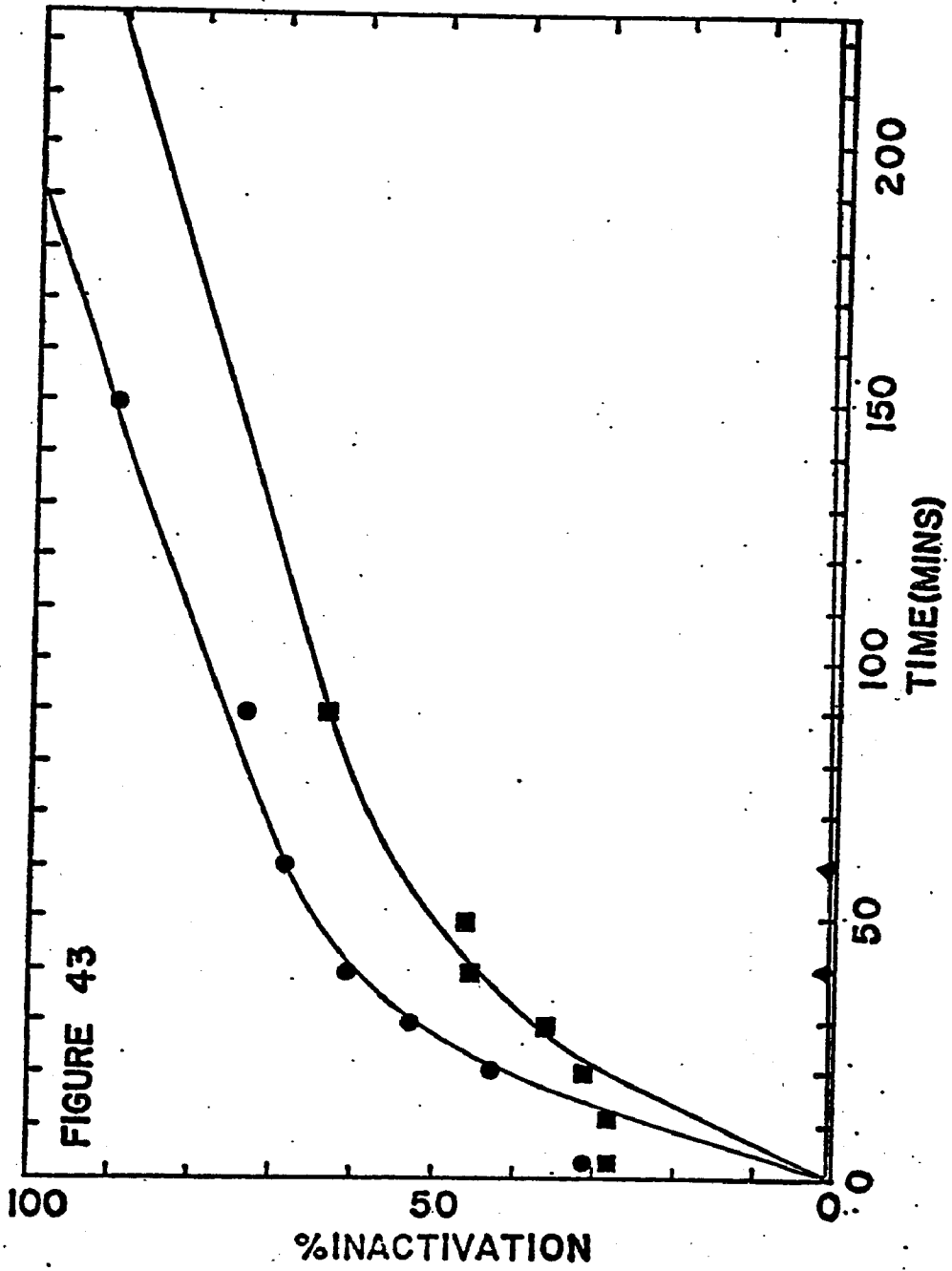


Figure 44. Inactivation of Liver Aldolase by Pyridoxal 5-phosphate

- Aldolase activity remaining
- ▲ Control. Both control and aldolase activities remained at or near the levels shown for times of up to 90 minutes.

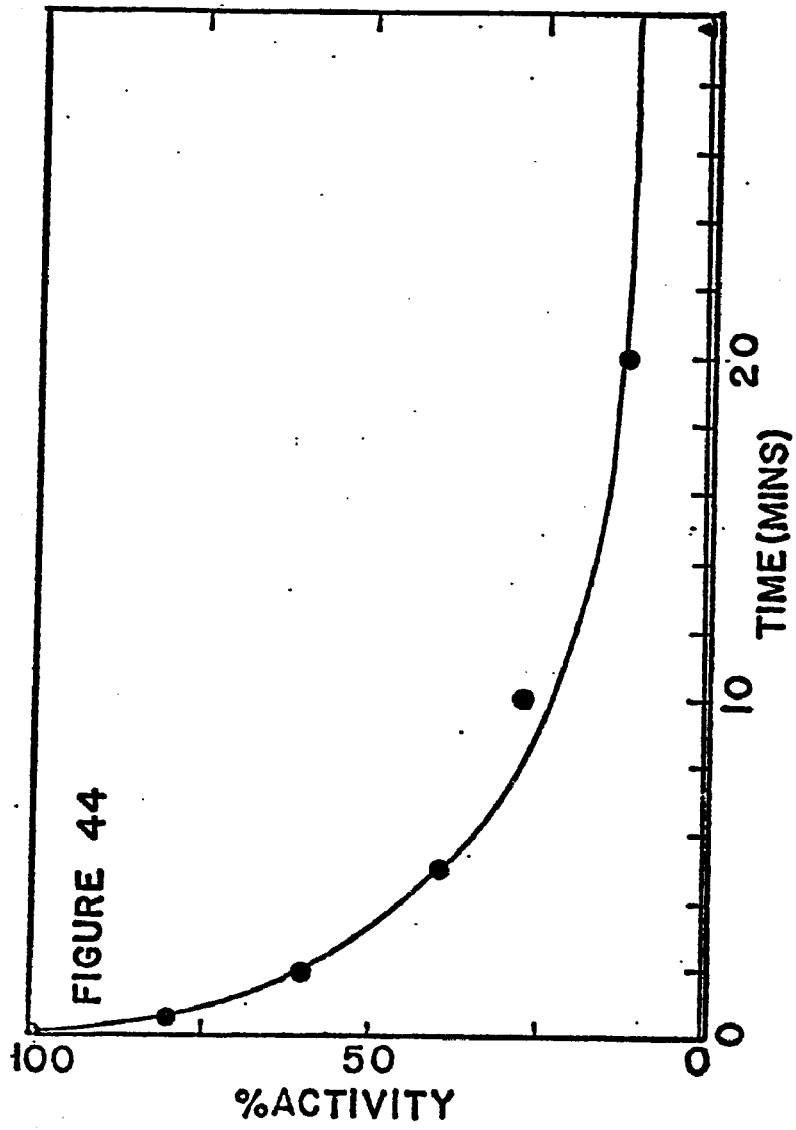


Figure 45. Log % Activity Remaining vs. Time for  
PLP Inactivation of Muscle Aldolase (10  $\mu$ M, 20  $\mu$ M,  
25  $\mu$ M PLP)

- ▲ 10  $\mu$ M PLP
- 20  $\mu$ M PLP
- 25  $\mu$ M PLP

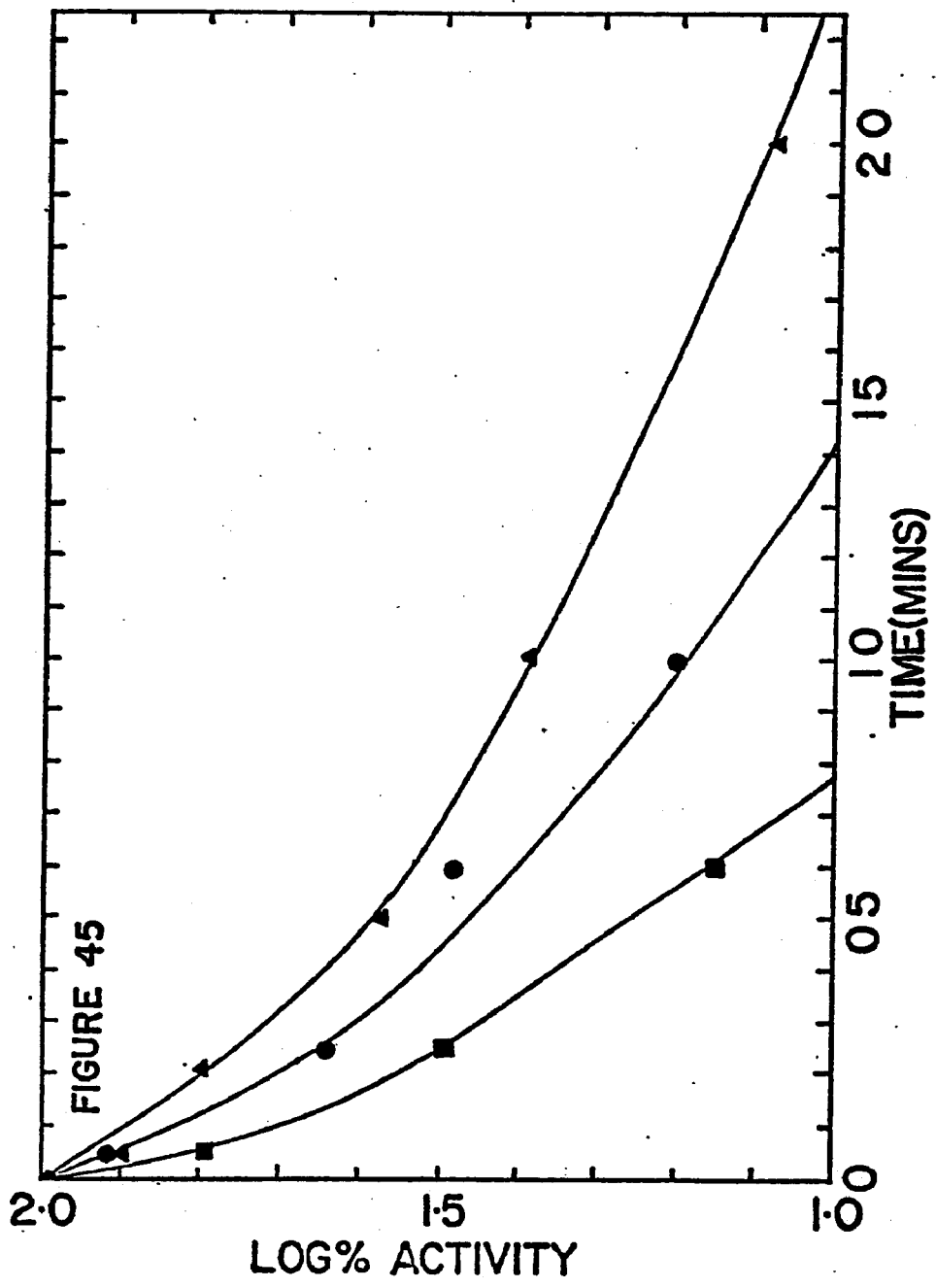


Figure 46. Nonintegrated First-order Replot for  
Inactivation of Muscle Aldolase by 10  $\mu$ M PLP

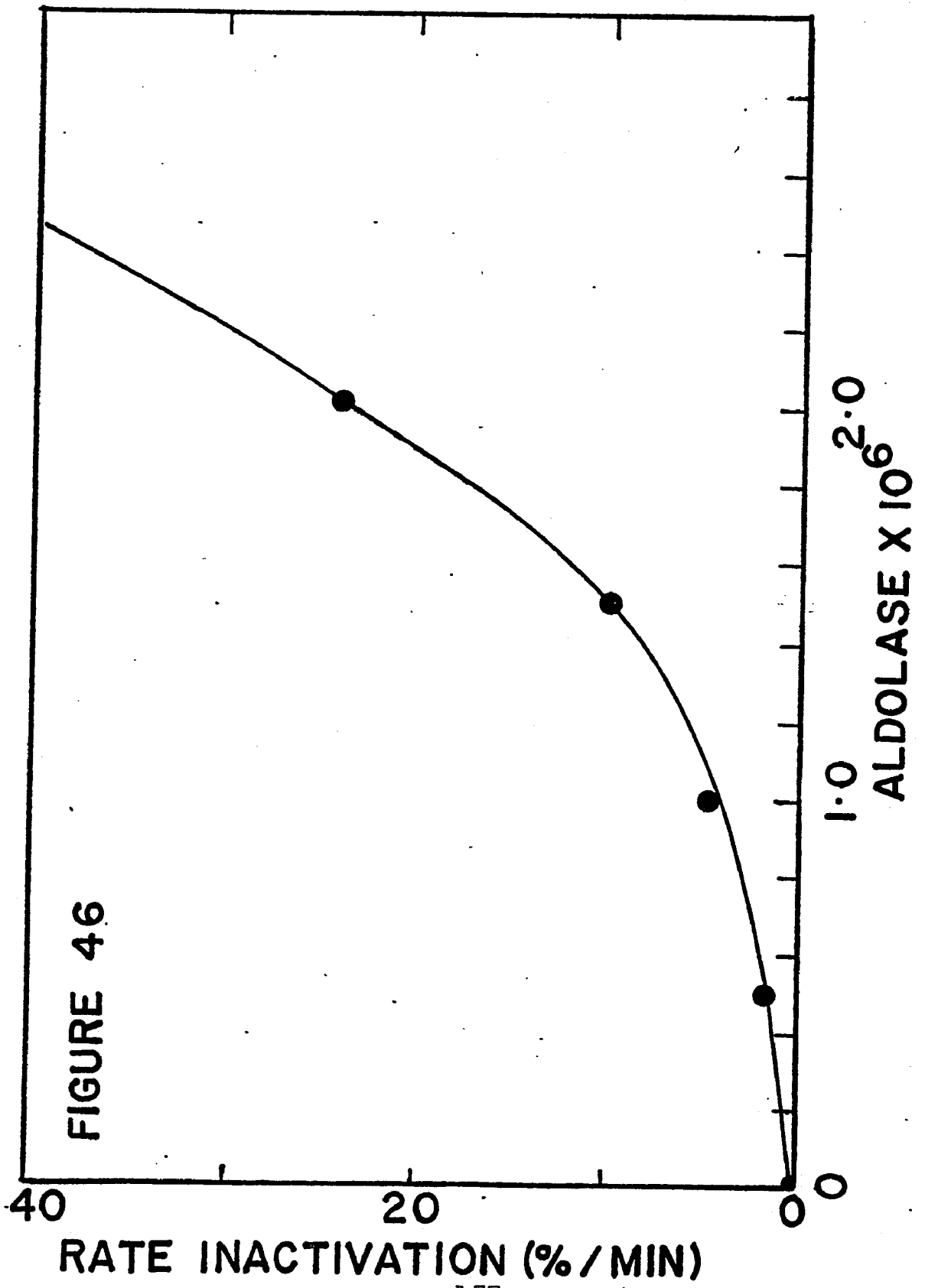


FIGURE 46

Figure 47. Nonintegrated Second-order Replot for  
Inactivation of Muscle Aldolase by 10  $\mu$ M PLP

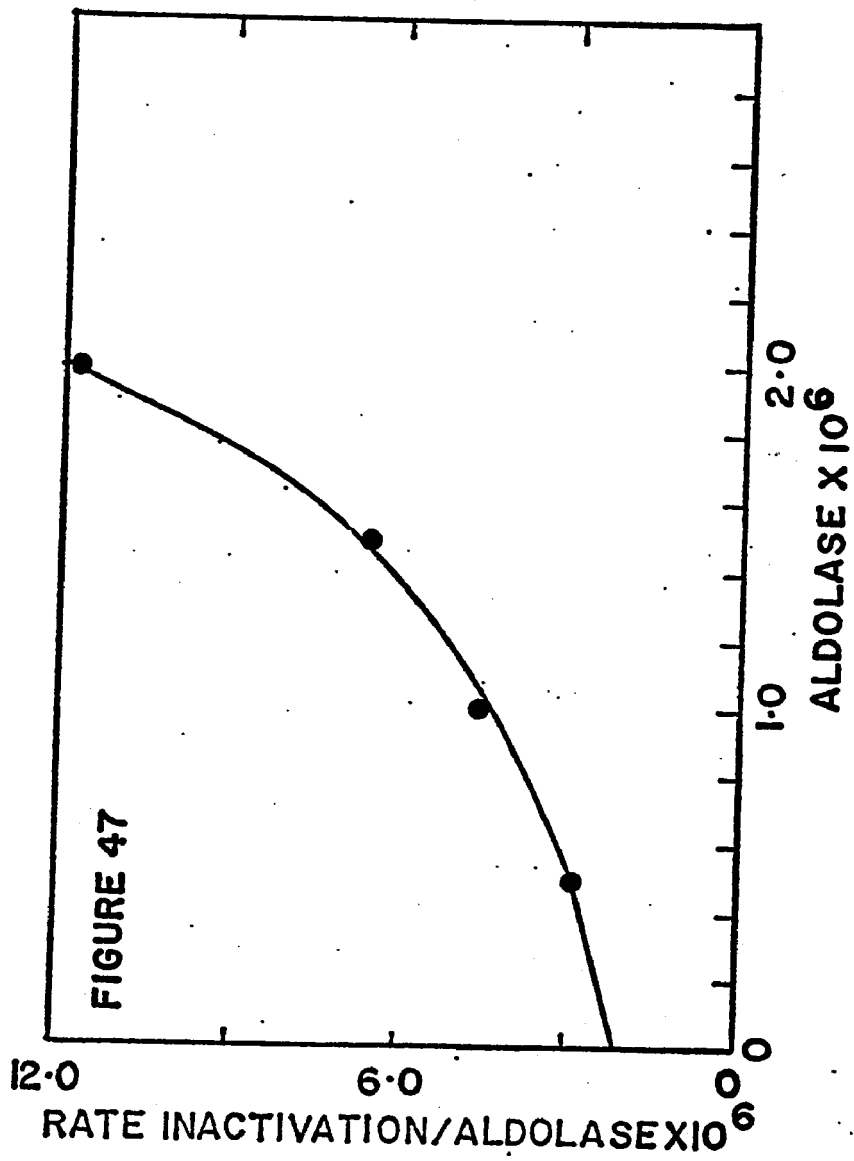
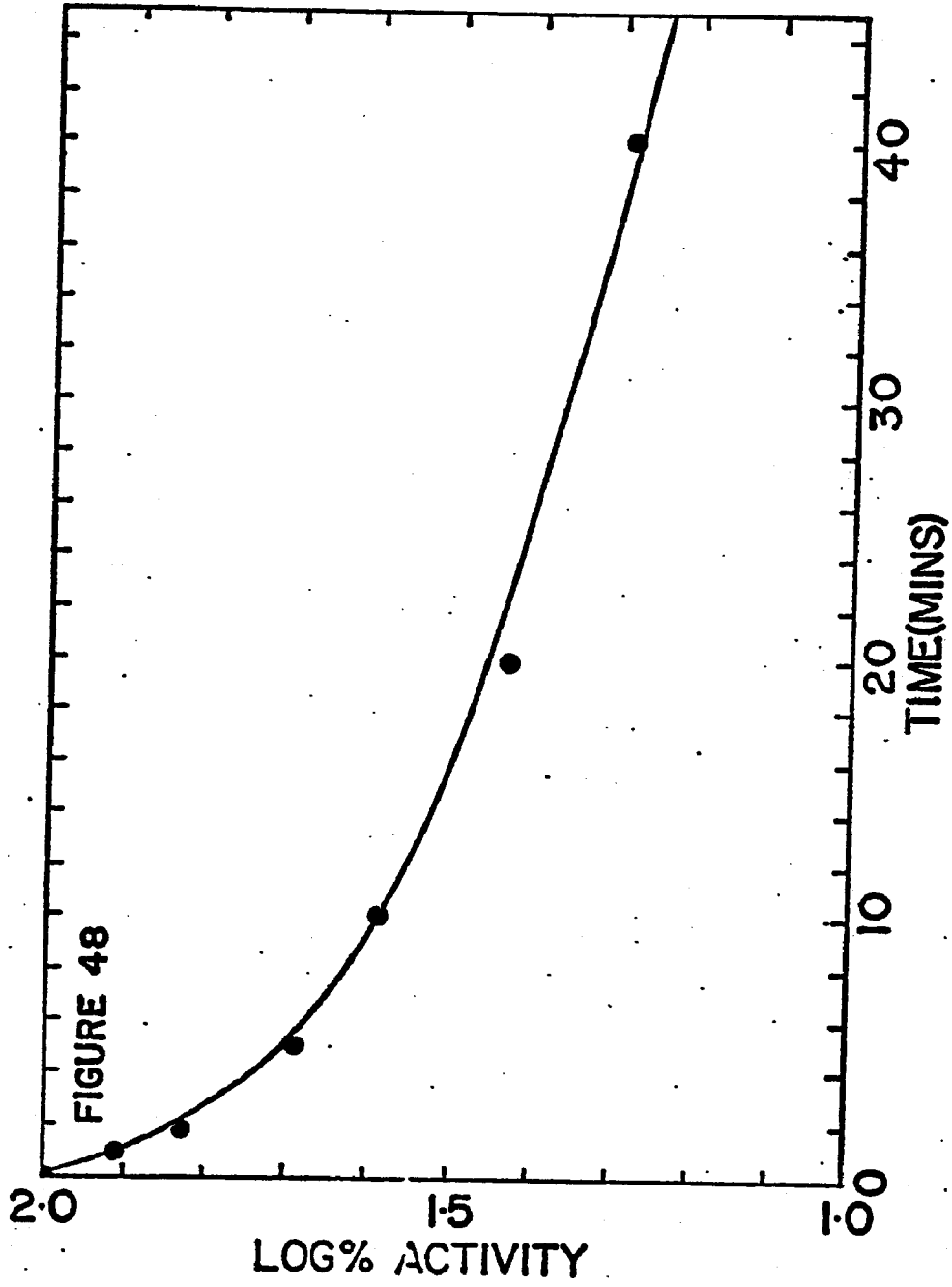


Figure 48. Log % Activity Remaining vs. Time for  
10  $\mu$ M PLP Inactivation of Muscle Aldolase with  
Zero Activity as Infinite Time Value



nonlinear.

Inactivation of Liver Aldolase by Pyridoxal 5-phosphate (PLP)

The results of the study of the inactivation of liver aldolase by 200  $\mu$ M PLP are shown in Figure 49. The activity drops to 60% in 5 to 10 minutes. At 40 minutes, the activity is still about 57%. The first-order replot (integrated form) is shown in Figure 50. This inactivation clearly also is not first-order.

Figure 49. Inactivation of Liver Aldolase by  
200  $\mu$ M Pyridoxal 5-phosphate

- Aldolase activity remaining
- ▲ Control

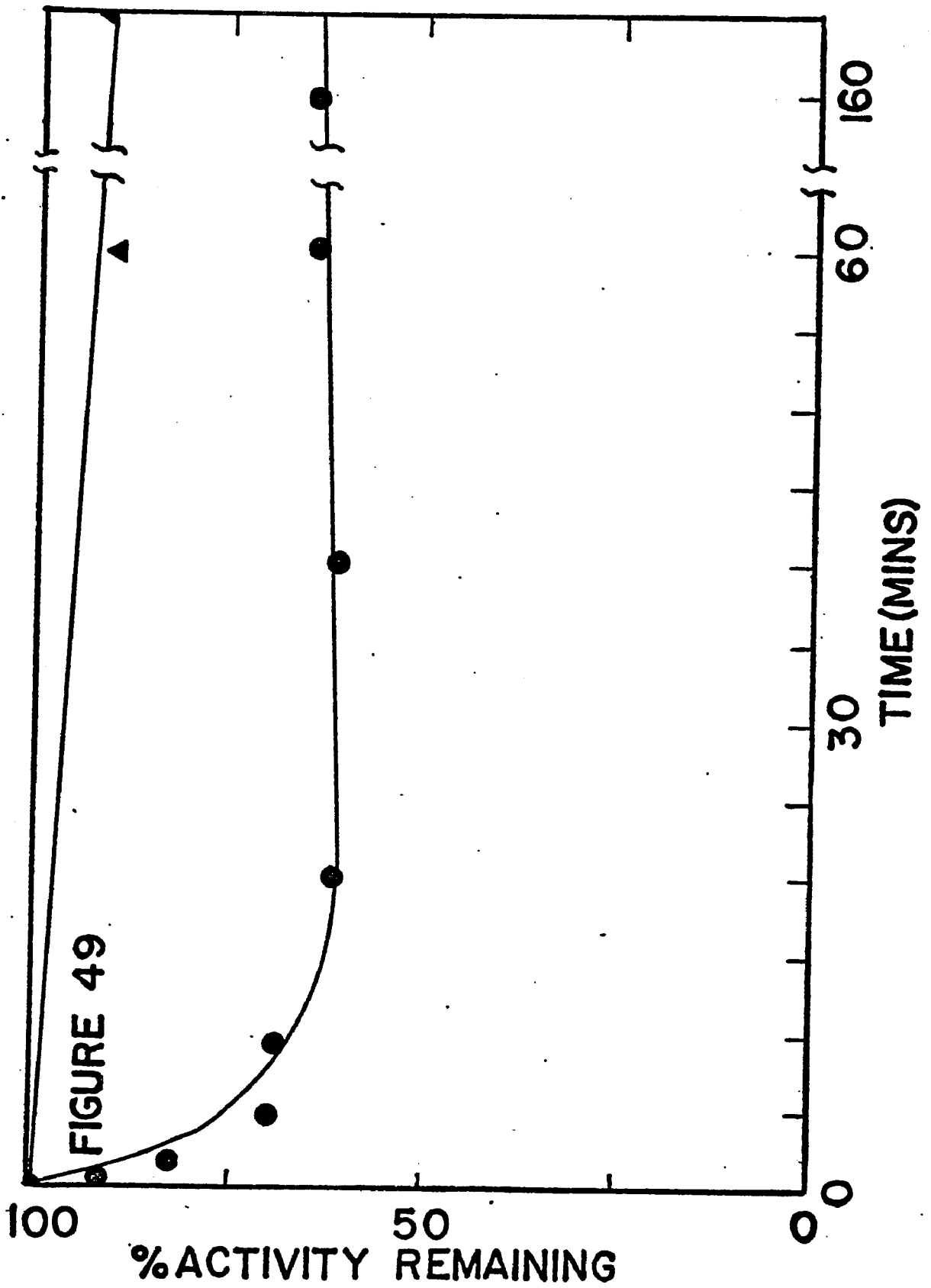
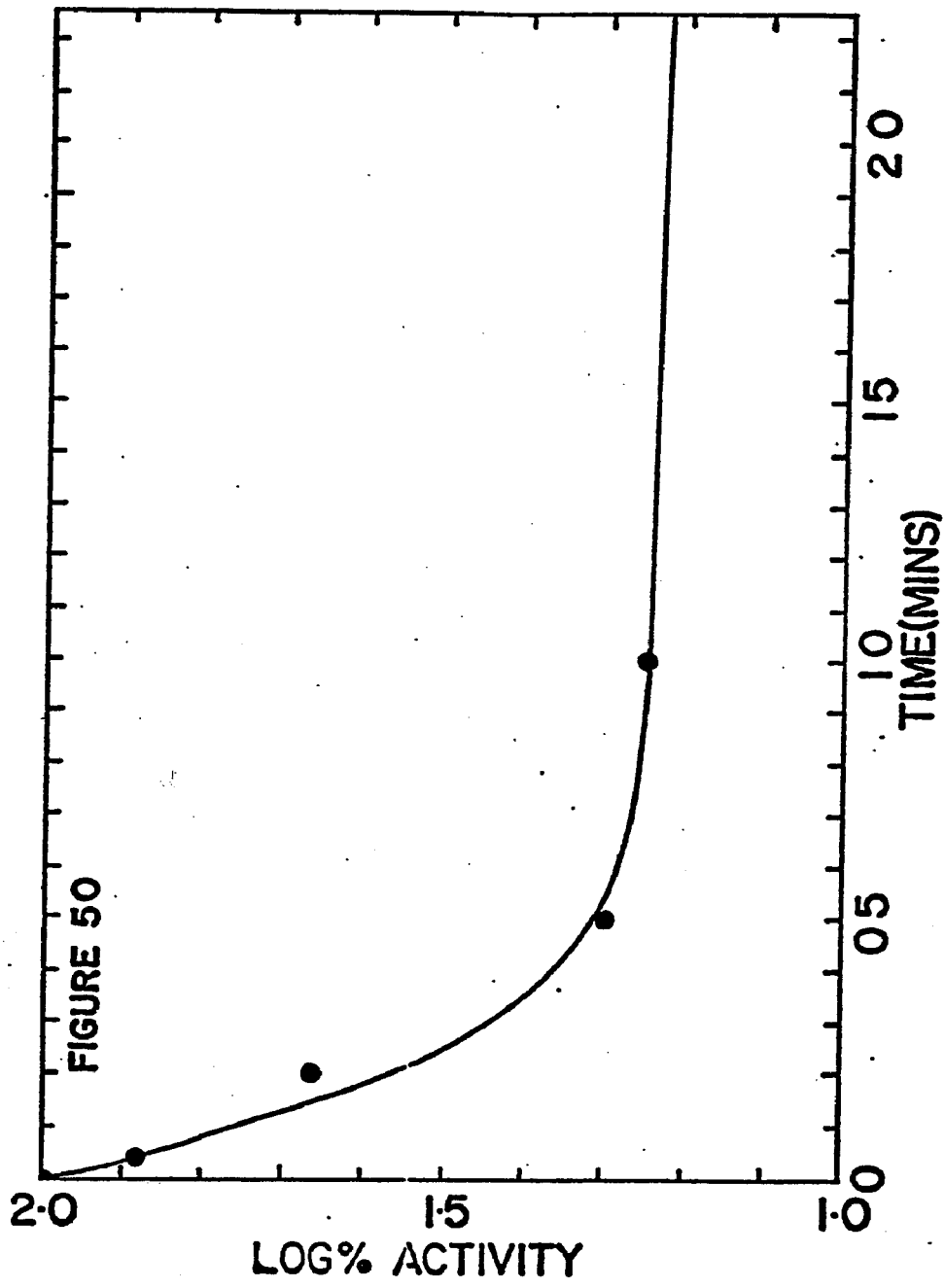


FIGURE 49

Figure 50. Log % Activity Remaining vs. Time for  
200 $\mu$ M Pyridoxal 5-phosphate Inactivation of Liver  
Aldolase



## Discussion

### Stopped Flow - Muscle Aldolase

The first-order replot for the muscle aldolase stopped flow experiment shown in Figure 15 is biphasic in shape. This biphasic shape has previously been interpreted by Wurster and Hess,<sup>17</sup> as well as Schray, et al.,<sup>6</sup> as resulting from rapid utilization of the  $\beta$ -anomer of FBP in the first phase and slow interconversion of the  $\alpha$ -anomer of FBP to the  $\beta$ -anomer of FBP (or open form) in the second phase. Extrapolation of the slow second phase to time zero gives a value of 71% utilization in the rapid initial phase. This is in good agreement with the value of 74% obtained by the previous investigators. This is also in good agreement with the known anomeric composition of FBP in solution. It is also important to point out that the  $t_{1/2}$  for  $\alpha$ -to  $\beta$ -interconversion is 0.1 sec ( $k_{\alpha\rightarrow\beta} = 8.1 \text{ sec}^{-1}$ ). Therefore, one would not expect to see the slow second phase of this curve unless the  $\alpha$ -anomer of FBP is bound very tightly by muscle aldolase and is thereby prevented from spontaneously anomerizing. It is possible to calculate the overall rate for the spontaneous  $\alpha$ -to  $\beta$ -interconversion using the rate constant for this process determined by Midelfort, Gupta, and Rose<sup>19</sup> along with the concentration of  $\alpha$ -FBP present at time

zero ( $20\% \times 12 \mu M = 2.4 \mu M$ ). From the second phase of Figure 15, it is possible to obtain a  $k_{\text{apparent}}^{\alpha \rightarrow \beta}$  of  $0.69 \text{ sec}^{-1}$ . Using this value of  $k_{\text{apparent}}^{\alpha \rightarrow \beta}$  it is then possible to calculate an actual rate for this second phase of the progress curve. The concentration of free  $\alpha$ -FBP is then given by:

$$[\alpha\text{-FBP}]_{\text{free}} = \frac{\text{rate with aldolase}}{\text{spontaneous rate}} \times 2.4 \mu M$$

$$\text{and } [\alpha\text{-FBP}]_{\text{bound}} = 2.4 \mu M - [\alpha\text{-FBP}]_{\text{free}} = [\text{muscle aldolase} \cdot \alpha\text{-FBP}]$$

$$[\text{muscle aldolase}]_{\text{free}} = [\text{muscle aldolase}]_{\text{total}} - [\text{muscle aldolase} \cdot \alpha\text{-FBP}]$$

$$K_{\text{diss}} = \frac{[\text{muscle aldolase}]_{\text{free}} [\alpha\text{-FBP}]_{\text{free}}}{[\text{muscle aldolase} \cdot \alpha\text{-FBP}]}$$

$$K_{\text{diss}} = 1.31 \times 10^{-6} M$$

This value for  $K_{\text{diss}}$  represents a binding of  $\alpha$ -FBP to muscle aldolase which is an order of magnitude tighter than the binding of the substrate,  $\beta$ -FBP, to this enzyme. This system may therefore be an example of a system in which some of the binding energy of the substrate binding is utilized to form a transition state for the catalytic sequence. Hence, the binding of  $\beta$ -FBP appears to be less tight than the unreactive  $\alpha$ -anomer.

Schray et al.<sup>6</sup> demonstrated that yeast apoadolase (formed by removal of the zinc ion), which

is catalytically inactive, can catalyze the anomerization of  $\alpha$ -FBP to  $\beta$ -FBP. Therefore, the yeast enzyme would not give a biphasic progress curve as per muscle aldolase, but rather, would have a straight line utilization of both the  $\alpha$ - and the  $\beta$ -anomer of FBP. In a mixed run containing muscle aldolase plus yeast apoaldolase, the biphasic curve was found to be replaced by a straight line utilization.

#### Stopped Flow - Liver Aldolase

The utilization of FBP by liver aldolase (Figure 16) is clearly not biphasic utilization of the  $\beta$ -anomer followed by a slower  $\alpha$ -to  $\beta$ -interconversion as was the case in the muscle aldolase experiment above. It also is obviously not the opposite possibility:

$\alpha$ -utilization and slow  $\beta$ -to  $\alpha$ -interconversion due to tight binding of the  $\beta$ -anomer. In fact, the anomeric specificity of this enzyme is not resolvable based solely on this experiment. Several possibilities fit the experimental data: 1.)  $\beta$ -utilization with rapid spontaneous or catalyzed  $\alpha$ -to  $\beta$ -anomerization, 2.) open utilization with spontaneous or catalyzed ring opening, 3.)  $\alpha$ -utilization with rapid  $\beta$ -to  $\alpha$ -anomerization, and combinations of these possibilities.

For example, consider the first of the above possibilities,  $\beta$ -utilization with rapid spontaneous

$\alpha$ -to  $\beta$ -anomerization. Rose and co-workers have found a rate constant  $k_{\alpha \rightarrow \beta} = 8.1 \text{ sec}^{-1}$  for the spontaneous  $\alpha$ -to  $\beta$ -interconversion.<sup>19</sup> If the initial concentration of the  $\alpha$ -anomer is  $2.4 \mu \text{ M}$ , the overall rate of the spontaneous  $\alpha$ -to  $\beta$ -process is given by:

$$\frac{d \alpha ( \rightarrow \beta )}{dt} = k_{\alpha \rightarrow \beta} [\alpha\text{-FBP}]$$

$$\frac{d \alpha ( \rightarrow \beta )}{dt} = 8.1 \text{ sec}^{-1} \times 2.4 \mu \text{ M}$$

$$\frac{d \alpha ( \rightarrow \beta )}{dt} = 19.4 \mu \text{ M sec}^{-1}$$

The overall rate for  $\beta$ -FBP only utilization to form product is given by:

$$\frac{d \beta ( \rightarrow \text{Product} )}{dt} = k_{\text{cat}} [\beta\text{-FBP}]$$

The concentration of  $\beta$ -FBP is equal to 80% of the total FBP ( $[\text{FBP}]_{\text{total}} = 12 \mu \text{ M}$ ), therefore,  $[\beta\text{-FBP}] = 9.6 \mu \text{ M}$ .

Using the value of  $k_{\text{cat}}$  determined from the reaction progress curve, the overall rate is then,

$$\frac{d \beta ( \rightarrow \text{Products} )}{dt} = 1.7 \text{ sec}^{-1} \times 9.6 \mu \text{ M}$$

$$\frac{d \beta ( \rightarrow \text{Products} )}{dt} = 16.3 \mu \text{ M sec}^{-1}$$

Since the spontaneous  $\alpha$ -to  $\beta$ -rate is greater than the overall rate of product formation from the  $\beta$ -anomer, the progress curve would be a straight line. Similar calculations for the other possibilities mentioned above show that they are compatible with the straight line utilization of 100% of the FBP found

experimentally. The results of the computer simulations are also in agreement with these calculations.

It is possible to calculate a turnover number from the liver aldolase stopped flow experiment. As will be shown in the computer simulation section of the discussion which follows, the liver aldolase stopped flow experiment was performed under  $V_{\max}$  conditions for  $12 \mu\text{M}$  aldolase catalytic sites. The turnover number is defined as,

$$\text{turnover number} = \frac{k_{\text{cat}}}{\# \text{ active sites}}$$

and

$$V_{\max} = k_{\text{cat}} E_{\text{total}}$$

$$k_{\text{cat}} = \frac{V_{\max}}{E_{\text{total}}}$$

$$\therefore \text{turnover number} = \frac{k_{\text{cat}}}{\# \text{ active sites}} = \frac{V_{\max}}{E_{\text{total}} (\# \text{ active sites})} \quad (1)$$

For the conditions of the stopped flow experiment

$$E_{\text{total}} (\# \text{ active sites}) = 12 \mu\text{M sites}$$

A value of  $k_{\text{cat}} = 1.7 \text{ sec}^{-1}$  is obtained directly from the progress curve of the stopped flow experiment.

From the definition of  $V_{\max}$ , the experimental value is found to be  $V_{\max} = 1.7 \text{ sec}^{-1} \times 12 \mu\text{M}$  and on substitution into (1) above the turnover number is found to be:

$$\text{turnover number} = \frac{V_{\text{max}}}{\text{active sites}} = \frac{1.7 \text{ sec}^{-1} \times 12 \mu\text{M}}{12 \mu\text{M active site}}$$

$$\text{turnover number} = \frac{1.7 \text{ sec}^{-1}}{\text{active site}}$$

This is in agreement with the value found by Rutter<sup>1,44</sup> of 1.8 sec<sup>-1</sup>/active site.

The similarity of the progress curve for the liver aldolase experiment to that obtained for the yeast enzyme, especially in terms of the straight line utilization of both anomers, prompted a mixed stopped flow experiment with both muscle and liver aldolase present.

Stopped Flow - Mixed (Muscle Aldolase Plus Liver Aldolase)

The biphasic reaction curve shown in Figure 17 is the result of stopped flow experiments in which both muscle aldolase and liver aldolase were present under the conditions given in the legend. If the slow second phase is extrapolated to time zero, it is found that the rapid initial phase corresponds to utilization of 50% of the total FBP present. The slow second phase has the same k as is found for the second phase of the muscle aldolase stopped flow experiment. It does not appear that the liver enzyme contains an anomerase activity which can catalyze the conversion of the α-anomer to the

$\beta$ -anomer in the presence of muscle aldolase as per the yeast enzyme. Furthermore, this experiment also does not fully resolve the anomeric specificity of liver aldolase. The possible anomeric specificities given above for the liver aldolase stopped flow experiment must be investigated as possibilities for the mixed stopped flow experiment. As can be seen from Figure 10, this involves the solving of the kinetic expression for a multiple equilibrium, multiple intermediate, multiple substrate reaction. The exact number of equilibria, intermediates, and substrate forms depends on the anomeric specificity of liver aldolase which is assumed in a given instance. In order to solve this convoluted kinetics problem, computer simulation was employed.

#### Computer Simulation

##### Competitive Binding Between Liver Aldolase and Muscle Aldolase in the Absence of Product Formation

The competitive binding of substrate by muscle aldolase and liver aldolase is shown schematically in Figure 51. This simulation shows that within 0.4 milliseconds (Figure 11) virtually all of the substrate is bound to the enzyme. Thus, clearly the system is saturated with enzyme and the conditions of the experiment are such that  $V_{\max}$  is attained for a total of  $12\mu$  M enzyme sites.

Figure 51. Schematic Representation of Simulated  
Competitive Formation of the Michaelis Complex

# FIGURE 51



### Liver Aldolase Only, $\alpha$ -Utilization

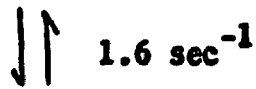
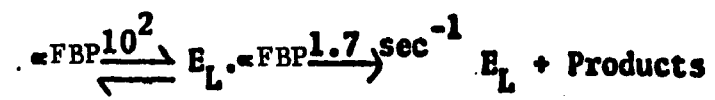
The computer simulation of utilization of the  $\alpha$ -anomer of the FBP shown in Figure 18 is presented schematically in Figure 52. In Figure 18 there is a long lag phase of approximately 400 milliseconds followed by a straight line utilization of the FBP which continues to 100% utilization. The lag is caused by the fact that the  $\beta$ -to  $\alpha$ -bound overall rate is greater than the overall rate for utilization of the  $\alpha$ -anomer to form product. There is therefore a build up of  $E_L \cdot \alpha$ -FBP and a corresponding increase in rate until the steady state is reached. No such lag is seen in the experimental first order replot. Therefore,  $\alpha$ -FBP alone is not the substrate for liver aldolase.

### Liver Aldolase Only, Open Utilization

The corresponding simulation of utilization of only the open form by the enzyme is schematized in Figure 53. The first-order plot for this simulation is given in Figure 19. The shorter lag of about 80 milliseconds in this simulation corresponds to the time required to convert all the  $\beta$ -anomer to the bound open form. The open form is immediately bound by the enzyme causing a build up of  $E_L \cdot$  open FBP and a corresponding increase in the overall rate. Due to problems in mixing the concentrated liver aldolase solution (14.9 mg/ml) in the stopped flow instrument,

Figure 52. Schematic Representation of Simulation  
of Utilization of  $\alpha$ -FBP by Liver Aldolase

# FIGURE 52



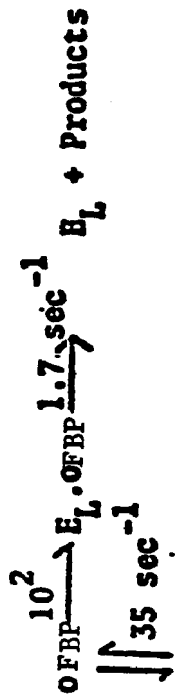
β FBP

Figure 53. Schematic Representation of Simulation  
of Utilization of Open FBP by Liver Aldolase

# FIGURE 53

$\alpha_{FBP}$

$8.5 \text{ sec}^{-1} \int \int$



$\beta_{FBP}$

it is impossible to discern the time course of the early stages of the reaction with accuracy. This substrate utilization is therefore, a viable possibility.

#### Liver Aldolase Only, $\beta$ -Utilization

The computer simulation of  $\beta$ -only utilization by liver aldolase is given in Figures 20 and 54. The first order plot for this anomeric specificity is linear to 100% FBP utilization. Since this is similar to the experimentally determined line, this possibility is also acceptable.

#### Mixed Liver and Muscle Aldolase with Liver Aldolase Utilization of Only the $\alpha$ - Anomer of FBP

In order to verify the previous conclusion that the  $\alpha$ -anomer is not the substrate form utilized by liver aldolase, a computer simulation of a mixed muscle aldolase plus liver aldolase experiment was performed. The muscle enzyme utilizes the  $\beta$ - anomer of FBP and binds the  $\alpha$ -anomer with a dissociation constant  $K_{diss\alpha} = 1 \times 10^{-6} M$ . This utilization-binding pattern for muscle aldolase is employed in all the mixed simulations. The liver enzyme utilization of the  $\alpha$ -anomer is assumed. This system is given schematically in Figure 55. The first order replot for this simulation, shown in Figure 22, is

Figure 54. Schematic Representation of Simulation  
of Utilization of  $\beta$ -FBP by Liver Aldolase

# FIGURE 54

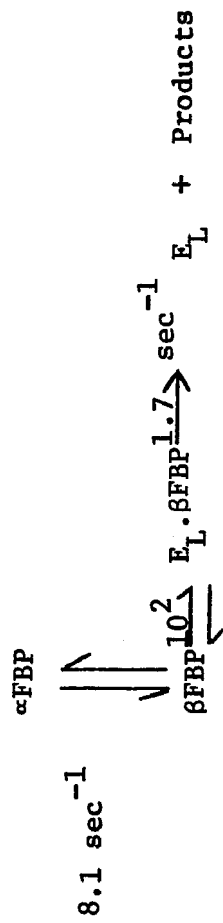
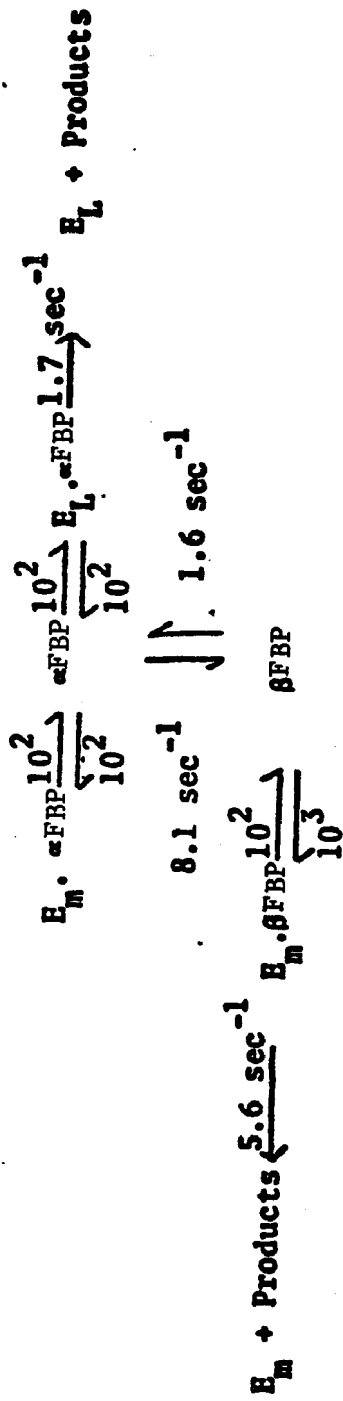


Figure 55. Schematic Representation of Simulation  
of Mixed Liver Aldolase Plus Muscle Aldolase Ex-  
periment with Liver Utilization of  $\alpha$ -FBP

**FIGURE 55**



a linear utilization of 100% of the FBP present. As seen earlier, the experimental result of the mixed muscle aldolase plus liver aldolase stopped flow run is biphasic. The utilization of the  $\alpha$ -anomer of FBP as substrate by the liver enzyme thus can also be ruled out based on this mixed simulation.

Mixed Liver and Muscle Aldolase with Liver Aldolase Utilization of Both  $\alpha$ -and  $\beta$ - Anomers of FBP

The results of the investigation of the possible utilization of both the  $\alpha$ -and  $\beta$ -anomer of the FBP by liver aldolase are shown in Figure 21. This simulation is presented schematically in Figure 56. This simulation results in a straight line and is also not compatible with the experimental results.

Mixed Liver and Muscle Aldolase with Liver Aldolase Utilization of the  $\beta$ -Anomer of FBP

In Figure 23 is shown the first-order plot resulting from the mixed muscle aldolase plus liver aldolase computer simulation with  $\beta$ - FBP utilization by liver aldolase. Figure 57 is the schematic representation of this simulation. The first-order plot from this simulation is biphasic and thus the utilization of exclusively the  $\beta$ -anomer as substrate by liver aldolase is still a viable possibility.

Figure 56. Schematic Representation of Simulation of Mixed Liver Aldolase Plus Muscle Aldolase Experiment with Liver Utilization of  $\alpha$ - and  $\beta$ -FBP

# FIGURE 56

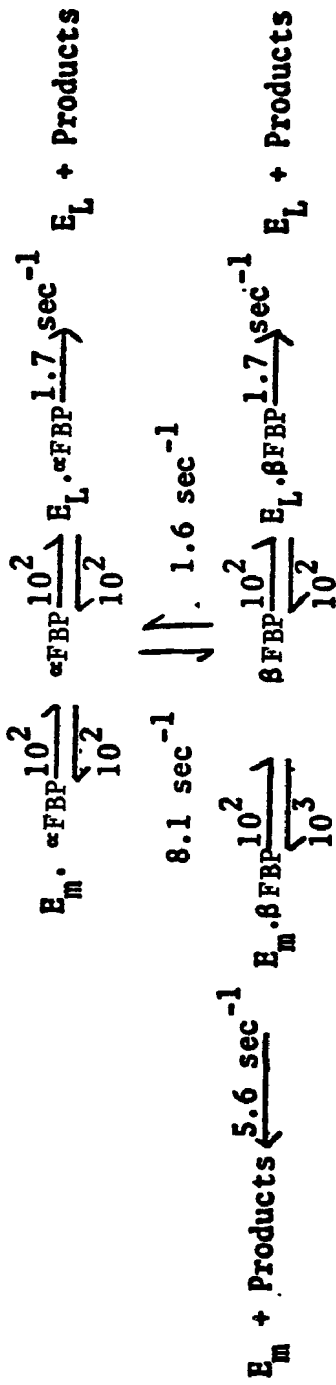
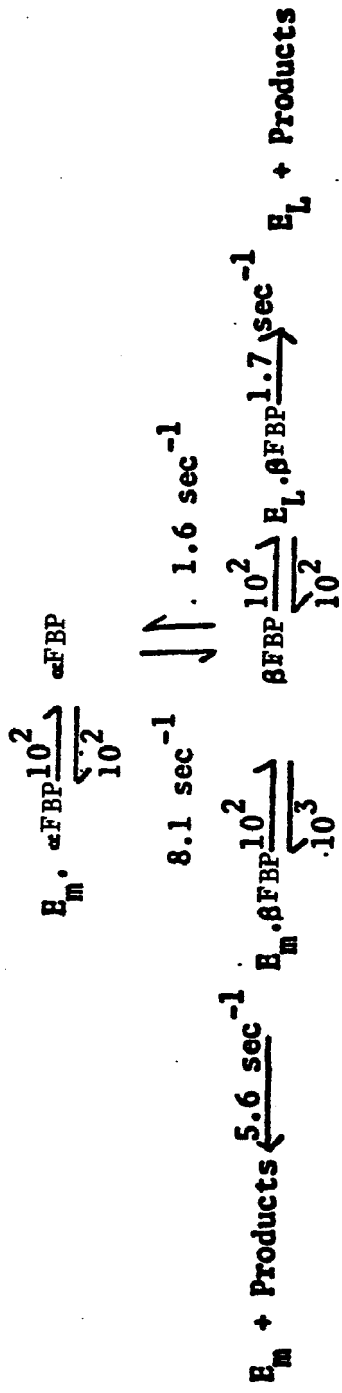


Figure 57. Schematic Representation of Simulation  
of Mixed Liver Aldolase Plus Muscle Aldolase Ex-  
periment with Liver Utilization of  $\beta$ -FBP

# FIGURE 57



Mixed Liver and Muscle Aldolase with Liver  
Aldolase Utilization of the Open Form of FBP

The simulation of a mixed liver aldolase plus muscle aldolase stopped flow experiment with the liver enzyme utilizing only the open form of FBP is shown in Figure 24 and schematized in Figure 58. This simulation also gives a biphasic curve and is compatible with the experimental results.

Summary of Results from Stopped Flow and Computer  
Simulations

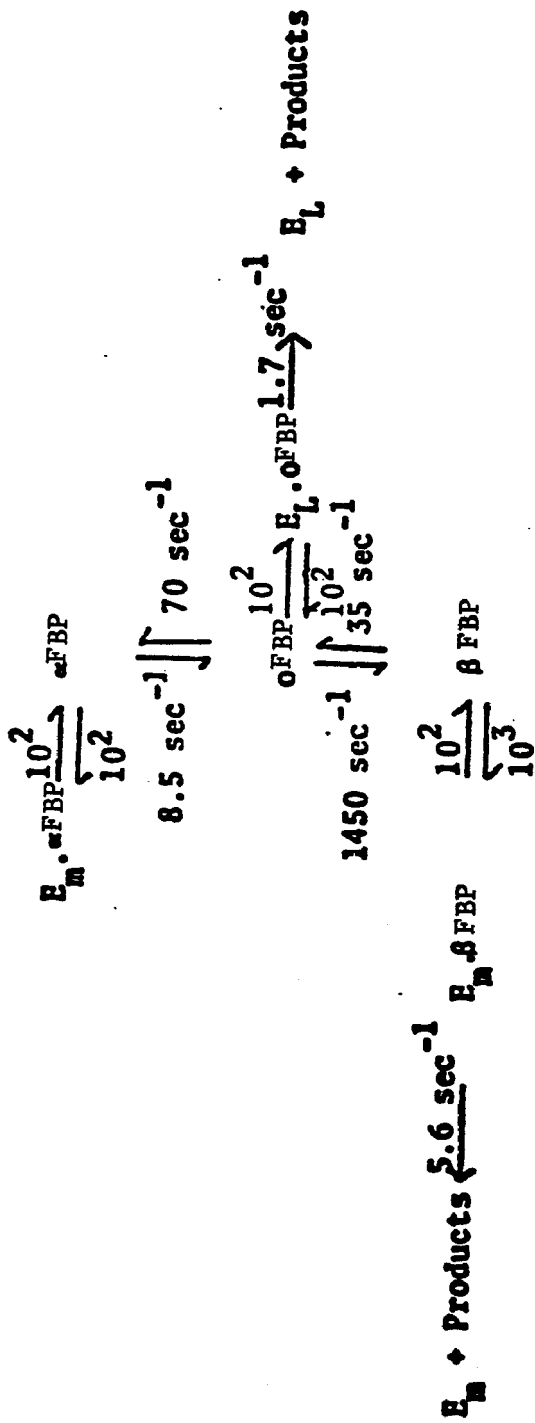
The stopped flow experiment for muscle aldolase is biphasic in nature with rapid utilization of the  $\beta$ -anomer of FBP followed by a slow second phase corresponding to the  $\alpha$ -anomer being slowly anomerized to the  $\beta$ -anomer. The slow rate at which the second phase occurs is the result of tight binding of the  $\alpha$ -anomer by muscle aldolase.

The liver aldolase stopped flow experiment is first-order throughout and hence is not similar to the muscle enzyme in terms of specificity for the anomeric forms of its substrate. The similarity of this experiment to previous work done with yeast aldolase prompted a mixed muscle plus liver aldolase experiment.

The mixed experiment presented a biphasic first order replot. This necessitated computer simulation

Figure 58. Schematic Representation of Simulation  
of Mixed Liver Aldolase Plus Muscle Aldolase Ex-  
periment with Liver Utilization of Open FBP

**FIGURE 58**



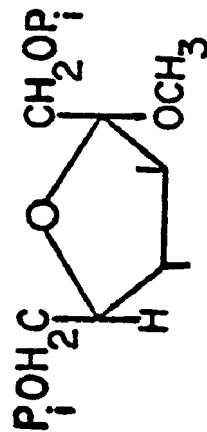
to resolve the anomeric specificity of the liver enzyme. Simulation of the utilization of  $\alpha$ -FBP exclusively by liver aldolase was not consistent with experimental results. To further resolve the specificity, simulations of mixed muscle aldolase plus liver aldolase experiments were performed. These simulations confirmed the inability of the  $\alpha$ -anomer to serve as a substrate for liver aldolase and also were inconsistent with utilization of both the  $\alpha$ - and the  $\beta$ - anomer by the liver enzyme. Simulations which employed utilization of the  $\beta$ -anomer or open form of FBP by the liver enzyme were consistent with the experimental results. A combined  $\beta$ - and open-FBP utilization would also have been consistent with the experimental results.

Inhibition by Substrate Analogues (See Figure 59 for Structures)

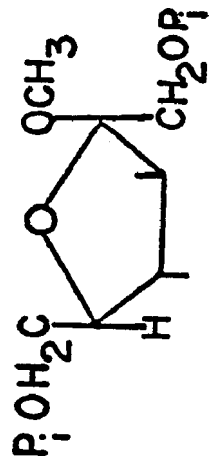
$\alpha$ -,  $\beta$ - methylfructofuranoside is not able to ring open since the hydroxyl on the anomeric carbon has been methylated. Therefore, this substrate analogue provides a molecular probe of the active site for the ability to bind the cyclic form of FBP. The value of  $K_i = 4.6 \times 10^{-5} \underline{M}$  indicates a strong interaction between this analogue and liver aldolase. This same inhibitor is found to have a  $K_i = 2.7 \times 10^{-6} \underline{M}$  for muscle aldolase. This is indicative of an

Figure 59. Structures of Substrate Analogues  
Employed as Inhibitors

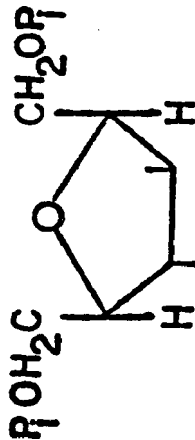
# FIGURE 59



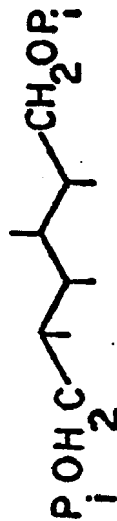
$\alpha$ -methylfructofuranoside  
1,6-bisphosphate



$\beta$ -methylfructofuranoside  
1,6-bisphosphate



$\alpha$ -2,5-anhydroglucitol  
1,6-bisphosphate



glucitol 1,6-bisphosphate

extremely tight binding interaction with the muscle enzyme. The muscle enzyme is known to utilize the  $\beta$ -cyclic form of FBP as substrate and to bind the  $\alpha$ -very tightly. It is interesting to note that the value of  $K_i$  determined for the muscle enzyme is smaller (tighter binding) than the  $K_M$  for its substrate. This may be the result of the fact that muscle aldolase utilizes some of the binding energy to form the transition state for the reaction which follows the binding. This would cause the  $K_M$  value to be larger (less tight) for the substrate. Since the inhibitor can not react, none of the binding energy is siphoned off and the binding constant reflects the entire strength of the binding interaction. It is not clear if this occurs in liver aldolase. Although the value of  $K_i$  determined for  $\alpha$ -,  $\beta$ -methylfructofuranoside does not indicate that this is the case, it is possible that the slightly reduced binding of the inhibitor is the result of unfavorable steric interactions at the active site with the additional methyl group.

When the analogue of the  $\alpha$ -anomer,  $\alpha$ -2,5-Anhydroglucitol 1,6-bisphosphate is used as an inhibitor of liver aldolase, the inhibition is not of a competitive nature. The inhibition is either noncompetitive (parallel lines) or mixed with the lines

intersecting in the  $-x$ ,  $+y$  quadrant. The value of  $K_i$  determined by utilizing the formulas for noncompetitive lines ( $K_i = 1.2 \times 10^{-3}$ ) indicates that this is a fairly weak interaction and may not involve the active site. This is in good agreement with the results of the stopped flow experiments and the computer simulations which are not consistent with utilization of  $\alpha$ -FBP by liver aldolase. Further, since it appears that the  $\alpha$ -analogues of FBP do not bind to liver aldolase to any significant extent, the  $K_i$  value for only the  $\beta$ -form of the methylfructofuranoside 1,6-bisphosphate may be tighter by a factor of two than the value found experimentally.

The open chain FBP analogue, glucitol 1,6-bisphosphate, is seen to be a competitive inhibitor of liver aldolase with  $K_i = 4.3 \times 10^{-6} \text{M}$ . This is expected since it is mechanistically imperative that the furanoside ring open. The requirement for opening arises from the fact that on opening, a ketonic carbonyl is formed which then stabilizes the anionic intermediate. The carbonyl is also necessary for formation of the Schiff's base between the substrate and a lysine on the enzyme.

#### Summary of Anomeric Specificity Determined through Use of Substrate Analogues as Inhibitors

The cyclic analogues of FBP are found to bind

to liver aldolase tightly, albeit not as tightly as they bind to muscle aldolase. This may be the result of steric considerations. Analogues of the  $\alpha$ -anomer bind to liver aldolase less tightly than  $\beta$ -forms by a factor of  $10^2$ . The open chain analogues bind very tightly. This data is consistent with utilization of the  $\beta$ -anomer of FBP as substrate with or without the open form as substrate. The data does not completely rule out the utilization of only the open form of FBP. It does, however, seem unlikely that the cyclic analogues such as the methylfructofuranoside 1,6-bisphosphate would bind with  $K_i = 4 \times 10^{-5} \text{M}$  if only the open chain is the substrate form utilized.

Measurement of the Rate of Liver Aldolase under Conditions of Slow Generation of the  $\beta$ -Anomer of FBP by Phosphofructokinase

In order to further distinguish among the remaining possible anomeric specificities of liver aldolase, the rate of liver aldolase at high aldolase levels relative to the substrate concentration has been measured.  $\beta$ -[5- $^3\text{H}$ ]FBP was slowly generated from [5- $^3\text{H}$ ]F6P by phosphofructokinase (PFK) according to the procedure of Rose and O'Connell<sup>18</sup> as described above.

The results of this experiment are given in

Table 7. The number of counts found in the wash and loading fraction (i.e. in the form of  $^3\text{HOH}$ ) increase relative to the number of counts found in the FBP fraction on going from 9 nanoequivalents of liver aldolase to 56 nanoequivalents of liver aldolase. If all the counts in the F6P fractions are added together, (Figures 32 and 33) it can be seen that ~ 20% of the  $[5\text{-}^3\text{H}]$ F6P still remain at the time the reaction was quenched. Therefore, PFK is indeed the rate limiting enzyme. If liver aldolase utilizes only the open form of FBP as its substrate and, as was seen in the section which preceded, binds cyclic substrate forms (analogues) tightly, the ratio of counts in  $^3\text{HOH}$  to counts in FBP should decrease on going from 9 to 56 nanoequivalents of liver aldolase. This would be caused by the fact that on increasing the level of aldolase present, increased amounts of the nonsubstrate  $\beta$ -anomer are bound to the enzyme and are prevented from opening to the active substrate form. If, in fact, the  $\beta$ -anomer is the substrate for the liver enzyme, the rate would increase as more enzyme is added until the limiting PFK rate is reached. This is observed and the  $\beta$ -anomer is concluded to be the form of FBP utilized by liver aldolase. It should be pointed out that this experiment did not

eliminate the possibility that both the  $\beta$ -anomer and the open form of FBP are utilized. The experiment is only inconsistent with the exclusive use of the open form of FBP and tight binding of the  $\beta$ -anomer. In as much as mechanistic considerations demand ring opening as a step in the reaction sequence, it is most likely the case that both the open form and the  $\beta$ - are utilized as substrates, based on all the experimental evidence presented.

Measurement of the Rate of Exchange from  $^3\text{HOH}$  into DHAP by Liver Aldolase

The results presented in Figures 38 and 39 show that the rate of exchange of tritium from  $^3\text{HOH}$  into DHAP is greater than the overall rate of the liver aldolase cleavage reaction. The value found of 1.41 Moles/min of DHAP undergoing exchange per unit of enzyme is only slightly above the overall rate in the forward direction. One unit of aldolase is defined as the amount of aldolase required to cleave one micromole of FBP/minute. One of the steps in the exchange sequence may be rate limiting to the cleavage reaction; however, based on this data, this does not appear to be the case. However, as can be seen from the equilibrium constant for aldol cleavage of FBP ( $K_{eq} = 8.1 \times 10^{-5}$ ), the overall rate in the reverse direction (i.e. FBP formation) is

much larger than the rate of cleavage. It may therefore be that one of the steps in the exchange reaction is rate determining in the direction of FBP formation. If [ $^3\text{H}$ ]DHAP becomes available, the rate of exchange out of DHAP by liver aldolase should be measured to clarify this point.

Inactivation of Muscle Aldolase by 1-chloro 2,6-dinitrobenzene and 1-chloro 2,4-dinitrobenzene

As mentioned above, 1-chloro 2,4-dinitrobenzene is known to inactivate muscle aldolase at pH  $\geq 9.0$  by alkylating a cysteine group at the active site.<sup>52</sup> The inactivation of muscle aldolase by 1-chloro 2,6-dinitrobenzene shown in Figure 40 is somewhat slower than that found for 1-chloro 2,4-dinitrobenzene under the same conditions (shown in Figure 41). Inactivation by 1-chloro 2,4-dinitrobenzene is 80% complete in 40 minutes. With 1-chloro 2,6-dinitrobenzene, 80% inactivation is not reached until approximately 110-120 minutes. This difference may be due to the bulky nitro group on the six carbon interfering with the nucleophilic displacement reaction occurring at the one carbon. The inactivation curve for 1-chloro 2,4-dinitrobenzene shown in Figure 41 is in good agreement with the previously reported inactivation.

### Inactivation of Liver Aldolase by 1-chloro 2,4-dinitrobenzene

Liver aldolase is inactivated by 1-chloro 2,4-dinitrobenzene as shown in Figure 42. The inactivation is rapid and the enzyme is protected by the presence of substrate. This inactivation was done at pH 9.8 and by analogy to the muscle aldolase inactivation may involve the alkylation of a cysteine group at the active site of liver aldolase.

### Inactivation of Liver Aldolase by 4-hydroxymercuribenzoate

The inactivation of liver aldolase by 4-hydroxymercuribenzoate is consistent with the presence of a cysteine at the active site of liver aldolase. This reagent is well known to be specific for reaction with sulfhydryl groups. The rate of this inactivation is also decreased by the presence of substrate. The inactivation therefore most likely involves a cysteine at the active site.

### Summary of Inactivation Involving Chlorodinitrobenzene and 4-hydroxymercuribenzoate

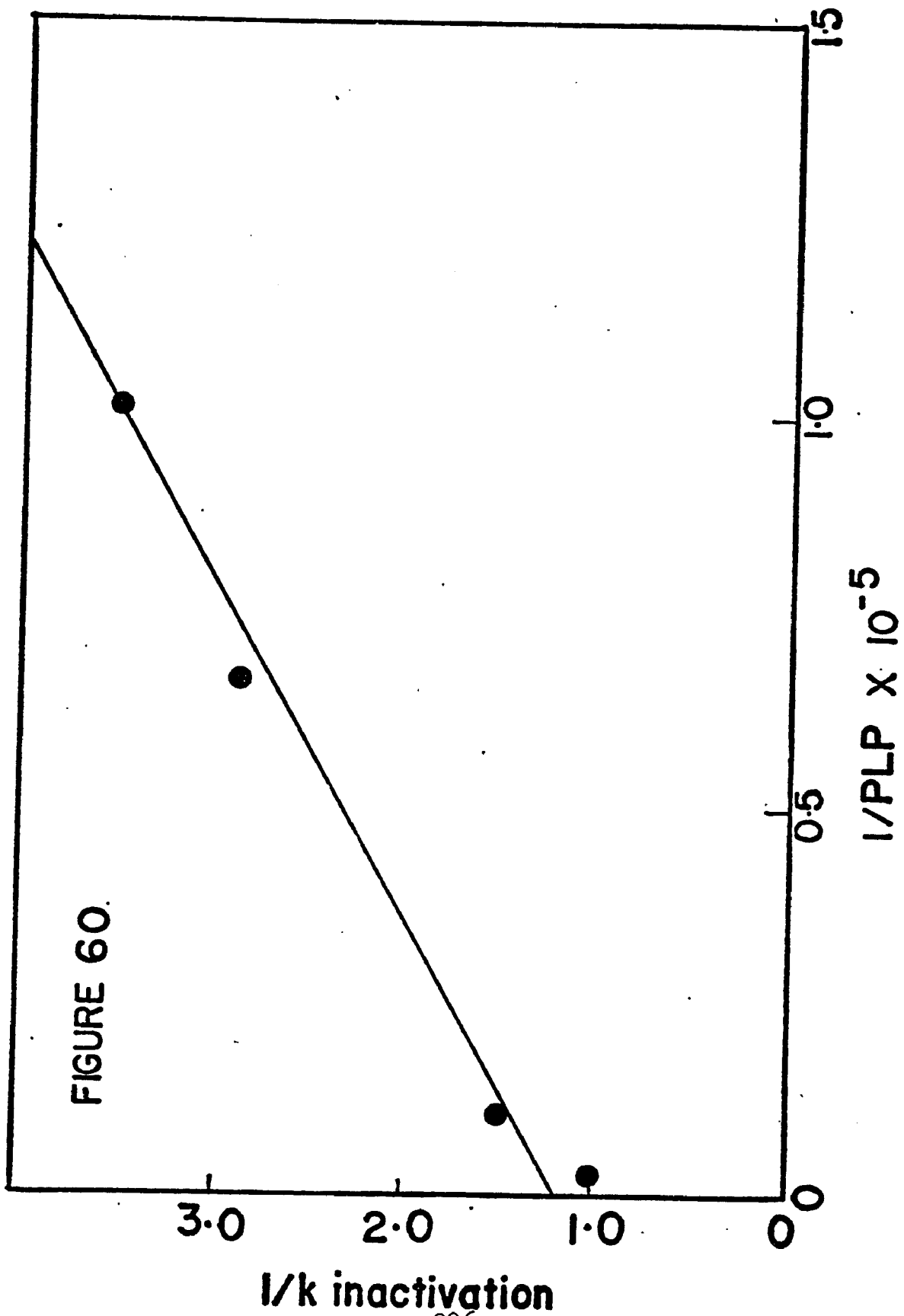
Inactivation of muscle aldolase at pH > 9.0 is found to proceed as reported previously with 1-chloro 2,4-dinitrobenzene. Inactivation of muscle aldolase with 1-chloro 2,6-dinitrobenzene proceeds more slowly

than with 1-chloro 2,4-dinitrobenzene. Liver aldolase is rapidly and completely inactivated by 1-chloro 2,4-dinitrobenzene at pH 9.8. The presence of substrate protects liver aldolase from this inactivation. This is interpreted as involving the alkylation of a cysteine group at the active site of liver aldolase. Inactivation of liver aldolase by 4-hydroxymercuribenzoate, a sulfhydryl specific reagent, agrees with this interpretation.

Inactivation of Muscle Aldolase and Liver Aldolase by Pyridoxal 5-phosphate (PLP)

The inactivation of muscle aldolase by  $10 \mu\text{M}$  PLP shown in Figure 44 is very rapid and in 20 minutes less than 15% of the control activity remains. The previously reported results of Kowal, et al. are similar to the above except that  $400 \mu\text{M}$  PLP is employed rather than  $10 \mu\text{M}$  PLP employed in the present study. The first-order replots of the inactivation for  $10 \mu\text{M}$ ,  $20 \mu\text{M}$ , and  $25 \mu\text{M}$  PLP shown in Figure 45 are clearly nonlinear for all three concentrations. To estimate the strength of the binding interaction, a value for  $K_{\text{inact}}$  is determined from the slope of the first two minutes of the first-order replot. This data is then plotted at  $1/k$  versus  $1/[\text{PLP}]$  as shown in Figure 60. The estimated binding constant for this

Figure 60. Plot of  $1/k$  Inactivation vs.  $1/[PLP]$   
for PLP Inactivation of Muscle Aldolase



interaction is  $K_i = 2.0 \times 10^{-5} \text{M}$ . The binding therefore is a strong interaction.

The nonintegrated first-order replot (Figure 46) is also nonlinear as is the second-order nonintegrated replot (Figure 47). Thus, while the interaction is very strong, the kinetics are not straightforward.

Liver aldolase is also inactivated by PLP, but at much higher concentration. In order to substantially inactivate the liver enzyme, levels of  $200 \mu \text{M}$  PLP are required. At this level inactivation is only 40% complete. At concentrations up to  $2 \text{mM}$  approximately 50% of the initial activity remained at infinite time. The first-order replot of this inactivation (Figure 50) also is linear.

Aldolase B (liver) has been found to be replaced by aldolase A (muscle) in primary hepatomas.<sup>39,40</sup> The aldolase isolated from hepatomas has been shown to be identical in amino acid compositions, electrophoretic mobility, immunological properties, and catalytic properties to aldolase A isolated from normal muscle tissue. Further, it has been shown that a close correlation exists between the amount of aldolase B remaining and the extent of dedifferentiation. That is, in rapidly growing poorly differentiated tumors aldolase A predominated and only traces of aldolase B were found.<sup>40-48</sup>

Hepatomas are among the most lethal malignancies, since there is at present no effective treatment for this type of cancer. Patients diagnosed as having a primary hepatoma have a five year survival rate of <1%. The median survival time is 6 months.<sup>49</sup> Current forms of radiation therapy and chemotherapy are ineffective because these methods do not discriminate sufficiently between healthy and malignant tissue. They would inflict intolerable damage to the liver without eradicating the cancer.

An approach to solving this problem would be to exploit the difference between aldolase isozymes found in the malignant tissue and in the healthy tissue surrounding the hepatoma. As shown herein, vastly larger amounts of PLP are required to inactivate liver aldolase than are required to inactivate muscle aldolase. Even at high concentration, PLP only inactivates liver aldolase to the extent of 50%. Thus, PLP or a suitable derivative could reasonably be expected to enter the active site of aldolase A found in malignant liver cells and inhibit catalytic activity. Benign liver tissue which contains only aldolase B should sustain only limited damage or be unaffected altogether.

Inhibitors as Probes for the Number of Phosphate  
Binding Sites in Liver Aldolase

By employing five carbon mono- and bisphosphate substrate analogues as inhibitors of liver aldolase, it is possible to derive information regarding the number of phosphate binding sites present in this enzyme. Ribulose 1,5-bisphosphate (Figure 29) has a binding constant  $K_i = 2.7 \times 10^{-6} \text{M}$ . This tight binding is probably the result of the 1-phosphate moiety being located in the same position relative to the carbonyl as it is in FBP. When ribose-5-phosphate (Figure 31) is employed as a competitive inhibitor the  $K_i = 1.18 \times 10^{-3} \text{M}$ . The 5-phosphate of ribose 5-phosphate is located at the same relative position to the carbonyl as the 6-phosphate in FBP. This very weak binding interaction is probably the result of the fact that liver aldolase either does not have a 6-phosphate binding site or the position of the binding site is such that the strength of the binding is severely decreased. Ribulose 5-phosphate, in which the 5-phosphate is one carbon closer to the carbonyl than is the case with the 6-phosphate of FBP, has an inhibition which is either uncompetitive or mixed (Figure 30). From the levels of ribulose 5-phosphate necessary to cause this inhibition, it is clear that

this also is not a very strong interaction.

The interpretation of the data for this inhibition as indicative of only one phosphate binding site in liver aldolase (i.e. liver aldolase has no 6-phosphate binding site) is consistent with the 1:1 ratio of activity of liver aldolase toward FBP and F1P. In the muscle enzyme which is known to have both a 1-phosphate and a 6-phosphate binding site, the FBP:F1P ratio is 50:1.

## Conclusions

Based on stopped flow experiments and computer simulations, liver aldolase appears to utilize the  $\beta$ -anomer of FBP as its substrate. The spontaneous rate of  $\alpha$ -to  $\beta$ -interconversion is adequate to give the first-order utilization of 100% of the substrate which was found experimentally. The simulations are found not to be consistent with use of only the  $\alpha$ -anomer as substrate by liver aldolase. The simulation of both  $\alpha$ - and  $\beta$ -utilization also did not fit the experimentally determined curve. Utilization of the open form singly or together with the  $\beta$ -anomer is consistent with experimental results as well. From the results of studies which employ substrate analogues, the same conclusion can be reached: that  $\beta$ -FBP, open FBP, or both can serve as substrate for liver aldolase. However, from the results of measuring the rate of liver aldolase when  $\beta$ -FBP is generated slowly by PFK, it does not appear that only the open form of FBP is employed as substrate. All of these experiments taken together lead to the conclusion that liver aldolase seems to utilize  $\beta$ -FBP and open FBP as its substrate, with no  $\alpha$ -FBP binding and with spontaneous  $\alpha$ -to  $\beta$ -interconversion.

As mentioned in the introductory section, anomeric specificity is thought to be involved in the regulation

of the overall glycolytic and gluconeogenic pathway. Anomeric specificity seems to be particularly important at the molecular level of coupling the reactions of these pathways. The muscle enzyme utilizes only the  $\beta$  - form of the FBP as substrate (Figure 4) and is tightly coupled to glycolysis and is not coupled to the enzymes of gluconeogenesis. Muscle tissue is principally functioning to produce energy via glycolysis and has very limited gluconeogenic activity. On the other hand, yeast, which has both an active glycolytic pathway and gluconeogenic pathway, contains an aldolase which utilizes both  $\alpha$  - and  $\beta$  - FBP. Yeast aldolase also can anomerize the  $\alpha$  - and  $\beta$  - forms of FBP. It is now possible to add to this that liver aldolase can function in both glycolysis and gluconeogenesis, both of which are active in liver tissue. The enzyme is specific for  $\beta$  - FBP; however, the enzyme is slower than muscle aldolase and yeast aldolase and the spontaneous rates of anomerization are faster than the rate of the liver enzyme. It is not clear whether the enzyme contains an anomerase activity. If such anomerase activity exists, it is not sufficient to give a single phase first-order replot in mixed muscle aldolase - liver aldolase experiments. Finally, some investigators now feel that aldolase

is more important in regulating the overall rate of glycolytic flux than had previously been thought.<sup>69</sup> If this proves to be the case, anomeric specificity may prove to be an extremely important part of the molecular mechanism by which glycolysis and gluconeogenesis are regulated.

In terms of the reaction mechanism, it is found that the rate of tritium exchange from  $^3\text{HOH}$  into  $\beta\text{-}^3\text{H}$  DHAP by liver aldolase is greater than the overall rate of the reaction. It can therefore be concluded that none of the steps involved in the exchange process are rate limiting to the overall mechanism of cleavage. However, the rate of exchange was only 1.4 times the overall rate, so this conclusion is not definitive. If the technical problems inherent in production of sufficiently labeled  $3\text{-}^3\text{H}$  DHAP can be overcome, the rate of tritium exchange out of  $^3\text{H}$ -DHAP should be measured to further elucidate this point.

Based on studies employing chlorodinitrobenzene compounds and 4-hydroxymercuribenzoate, it also appears likely that liver aldolase utilizes a cysteine located at the active site in the reaction mechanism. The muscle type enzyme is also known to employ a cysteine in its reaction mechanism.

Pyridoxal 5-phosphate is found to inactivate muscle aldolase at levels much lower than was previously reported. The inactivation goes to greater than 85% completion. Liver aldolase is inactivated by PLP but at levels which are more than an order of magnitude greater than required to inactivate the muscle enzyme. Even at high concentrations, PLP does not inactivate liver to greater than 50%. These results are particularly important since liver aldolase is found to be replaced by muscle type aldolase in hepatomas. These results could possibly lead to a program of chemotherapy based on the use of PLP and its derivatives against hepatomas.

Based on inhibition studies which employed ribulose 1,5-bisphosphate, ribulose 5-phosphate, ribose 5-phosphate, it can be concluded that liver aldolase has only a binding site for the 1-phosphate of FBP and none for the 6-phosphate. It is important to notice that the derivatives employed had the phosphates located at distances from the carbonyl which corresponded to those of FBP. In the earlier study by Hartman and Barker<sup>30</sup> no attempt was made to maintain this similarity and in fact many of the inhibitors used by Hartman and Barker had no carbonyl group at all.

The inactivation of muscle aldolase by PLP is known to involve formation of a Schiff's base between the carbonyl of PLP and the lysine at the 6-phosphate binding site on muscle aldolase. The interpretation of the competitive inhibition data as indicative that liver aldolase lacks a 6-phosphate binding site is consistent with the fact that much higher levels of PLP are needed to inactivate liver aldolase than are required to inactivate muscle aldolase.

Finally, liver aldolase is an interesting case of molecular biological evolution. Because of the necessity of a "flight or fight" response, it seems that muscle tissue must certainly have evolved before such specialized tissues as liver and brain. Therefore, it appears logical that liver aldolase evolved from muscle aldolase. The sequence of liver aldolase varies only slightly from that of muscle aldolase and the differences are all conservative changes. In spite of the apparently modest nature of these changes, several properties of the enzyme are changed. First, the liver enzyme has no 6-phosphate binding site. As a result of this change the ratio of FBP:F1P activity is now 1:1 rather than 50:1 in muscle aldolase. Secondly, the liver enzyme is much slower than the muscle enzyme.

This may be due to a slight shift in the location of one of the catalytic residues making the enzyme function more slowly. This slow rate of reaction may be important to regulation. Finally, and perhaps most importantly, the enzyme can function both in glycolysis and gluconeogenesis which are important to the specialized functioning of the liver. This seems to have been accomplished by liver aldolase not binding the  $\alpha$  - FBP anomer and therefore allowing the spontaneous anomerization to proceed. Thus, very slight changes in the primary sequence of aldolase which occurred during evolution have caused sweeping changes in the molecular properties of the isozymes found in specialized tissues.

## Bibliography

1. Rutter, W.J., Hunsley, J.R., Groves, W.E., Calder, J., Rajkumar, T.V., and Woodfin, B.M. (1966) Methods Enzymol. 9, 479.
2. Kawahara, K., and Tanford, C. (1966) Biochem. 5, 1578.
3. Sia, C.L., and Horecker, B.L. (1968) Arch. Biochem. Biophys. 123, 186.
4. Rutter, W.J. (1964) Fed. Proc., Fed. Am. Soc. Exp. Biol. 23, 1248.
5. Kobes, R.D., Simpson, R.T., Vallee, B.L. and Rutter, W.J. (1969) Biochem. 8, 585.
6. Schray, K.J., Fishbein, R., Bullard, W.P., and Benkovic, S.J. (1975) J. Biol. Chem. 250, 4883.
7. Gibson, Q.H. (1966) Methods Enzymol. 16, 187.
8. Gutfreund, H. (1966) Methods Enzymol. 16, 229.
9. Benkovic, S.J., and Schray, K.J. (1976) Adv. Enzymol. 44, 139.
10. Schray, K.J., and Benkovic, S.J. (1978) Accts. Chem. Res. 11, 136.
11. Salas, M., Vinuela, E., and Sols, A. (1965) J. Biol. Chem. 240, 561.
12. Schray, K.J., Benkovic, S.J., Benkovic, P.A., and Rose, I.A. (1973) J. Biol. Chem. 248, 2219.
13. Wurster, B., and Hess, B. (1974) FEBS Letters 38, 257.
14. Fishbein, R., Benkovic, P.A., Schray, K.J., Siewer, I.J., Steffens, J.J., and Benkovic, S.J. (1974) J. Biol. Chem. 249, 6047.
15. Bartana, J. and Cleland, W.W. (1974) J. Biol. Chem. 249, 1263.

16. Koerner, A.W., Jr., Ashour, A.E., Voll, R.J., and Younathan, E.S. (1973) Fed. Proc., Fed. Am. Soc. Exp. Biol. 32, 668.
17. Wurster, B. and Hess, B. (1973) Biochem. Biophys. Res. Commun. 55, 985.
18. Rose, I.A., and O'Connell, E.L. (1977) J. Biol. Chem. 252, 479.
19. Midelfort, C.T., Gupta, R.J., and Rose, I.A. (1976) Biochem. 15, 2178.
20. Horecker, B.L., Tsolas, O., and Lai, C.Y. (1972) The Enzymes 7, 213.
21. Castellino, F.J., and Barker, R. (1966) Biochem. Biophys. Res. Commun. 23, 182.
22. Ginsburg, A, and Mehler, A.H. (1966) Biochem. 5, 2623.
23. Eagles, P.A.M., Johnson, L.H., Johnson, M.A., McMurray, C.H., and Gutfreund, H. (1969) J. Mol. Biol. 45, 533.
24. Davis, L.C., Brox, L.W., Gracy, R.W., Ribereau-Gayon, G., and Horecker, B.L. (1970) Arch. Biochem. Biophys. 140, 215.
25. Mehler, A.H. (1963) J. Biol. Chem. 238, 100.
26. Penhoet, E.E., Kochman, M., and Rutter W.J. (1969) Biochem. 8, 4396.
27. Gracy, R.W., Lacko, A.G. and Horecker, B.L. (1969) J. Biol. Chem. 244, 3913.
28. Rose, I.A., and O'Connell, E. (1969) J. Biol. Chem. 244, 126.
29. Rose, I.A., and Rieder, S.V. (1958) J. Biol. Chem. 231, 315.
30. Hartman, F.C., and Barker, R. (1965) Biochem. 4, 1068.
31. Kobashi, K., and Horecker, B.L. (1967) Arch. Biochem. Biophys. 121, 178.

32. Riordan, J.F., and Christen, P. (1968) Biochem. 7, 1525.
33. Christen, P., and Riordan, J.F. (1968) Biochem. 7, 1531.
34. Sokolovsky, M., Harell, D., and Riordan, J.F. (1969) Biochem. 8, 4740.
35. Steinman, H.M., and Richards, F.M. (1970) Biochem. 9, 4360.
36. Lai, C.Y., and Horecker, B.L. (1972) Essays in Biochem. 8, 149.
37. Shapiro, S., Enser, M. Pugh, E., and Horecker, B.L. (1968) Arch Biochem. Biophys. 128, 554.
38. Davis, L.C., Ribereau-Gayon, G., and Horecker, B.L. (1971) Proc. Natl. Acad. Sci. 68, 416.
39. Ikehara, Y., Endo, H., and Okada, Y. (1970) Arch. Biochem. Biophys. 136, 491.
40. Matsushima, T., Kawabe, S., Shibuya, M., and Sugimura, T. (1968) Biochem. Biophys. Res. Commun. 30, 565.
41. Adelman, R.C., Morris, H.P., and Weinhouse, S. (1968) Cancer Res. 27, 2408.
42. Sugimura, T., Sato, S., Kawabe, S., and Suzuki, H. (1969) Nature 222, 1070.
43. Criss, W.E. (1971) Cancer Res. 31, 1523.
44. Kawabe, S., Matsushima, T. and Sugimura, T. (1969) Cancer Res. 29, 2075.
45. Sugimura, T., Sato, S., and Kawabe, S. (1970) Biochem. Biophys. Res. Commun. 39, 626.
46. Brox, L.W., Lacko, A.G., Gracy, R.W., Adelman, R.C., and Horecker, B.L. (1969) Biochem. Biophys. Res. Commun. 36, 994.
47. Gracy, R.W., Lacko, A.G., Brox, L.W., Adelman, R.C., and Horecker, B.L. (1970) Arch. Biochem. Biophys. 136, 480.

48. Matsushima, T., Kawabe, S., Shibuya, M. and Sugimura, T. (1968) Biochem. Biophys. Res. Commun. 30, 565.
49. Rubin, P. (ed.) (1974) Clinical Oncology 4th Edition p. 207, University of Rochester, Rochester, N.Y.
50. Chappel, A., Scopes, R.K., and Holmes, R.S. (1976) FEBS Letters 64, 59.
51. Frey, W.A., Fishbein, R., de Maine, M.M., and Benkovic, S.J. (1977) Biochem. 16, 2479.
52. Kowal, J., Cremona, T., and Horecker, B.L. (1965) J. Biol. Chem. 240, 2485.
53. Rowley, P.T., Tchola, G., and Horecker, B.L. (1964) Arch. Biochem. Biophys. 107, 305.
54. Lobb, R.R., Stokes, A.M., Hill, H.A.O., and Riordan, J.F. (1976) Eur. J. Biochem. 70, 517.
55. Lobb, R.R., Stokes, A.M., Jill, H.A.O., and Riordan, J.F. (1975) FEBS Letters 54, 70.
56. Hartman, F.C., and Brown, J.P. (1976) J. Biol. Chem. 251, 3057.
57. Hartman, F.C., Suh, B., Welch, M.H., and Barker, R. (1975) J. Biol. Chem. 248, 8233.
58. Gray, G.R. (1976) Accts. Chem. Res. 9, 418.
59. Gray, G.R. (1971) Biochem. 10, 4705.
60. Gray, G.R., and Barker, R. (1970) Biochem. 9, 2454.
61. Hammes, C.G., and Schimmel, P.R. (1970) The Enzymes 2, 67.
62. Ornstein, L., and Davis, B.J. (1964) Ann. N.Y. Acad. Sci. 121, 321.
63. Clarke, J.T. (1964) Ann. N.Y. Acad. Sci. 121, 428.
64. Weber, K., and Osborn, M. (1968) J. Biol. Chem. 214, 4466.

65. Reisfeld, R.A., Lewis, U.J., and Williams, D.E. (1962) Nature 195, 281.
66. Ripa, M. and Pontremoli, S. (1969) Arch. Biochem. Biophys. 133, 112.
67. Kan, R.O. (1966) Organic Photochemistry, p. 213, McGraw-Hill, New York, N.Y.
68. Chapman, O. (1969) Org. Photochem. 2, 51.
69. Master, C.J. (1977) Current Topics in Cellular Regulation 12, 75.

## Vita

John Martin Waud, the son of Claire T. Waud and the late Ira B. Waud, was born on August 9, 1949 in Sellersville, Pennsylvania. Mr. Waud received his elementary and secondary education in the Pennridge School District, Perkasie, Pennsylvania.

Mr. Waud received his undergraduate education from Lehigh University, Bethlehem, Pennsylvania. While he was at Lehigh University, he was active in the Student Affiliates of the American Chemical Society and was president of this organization from 1969-1970.

Mr. Waud received his B.S. in Chemistry from Lehigh University in June 1971.

Mr. Waud was then employed as an Environmental Protection Specialist by the Pennsylvania Department of Environmental Resources from January 1972 to August 1975. During this time Mr. Waud also attended the University of Pennsylvania in Philadelphia, Pennsylvania. He received the M.S. in Chemistry from the University of Pennsylvania in December 1974. While at the University of Pennsylvania, he was elected to  $\Phi\Lambda\Gamma$  Chemistry Honorary Society.

Mr. Waud began his graduate work at Lehigh University in September 1975. His publications from his research performed at Lehigh University include:

Anomeric Specificity of Liver Aldolase (E.C. 4.1.2.13,  
John M. Waud and Keith J. Schray, 12th ACS MARM, Hunt  
Valley, Maryland.

Phosphomannose Isomerase: Isomerization of the Pre-  
dicted B-D-Fructose 6-Phosphate, Keith J. Schray,  
John M. Waud, and Elizabeth E. Howell, accepted for  
publication - Archives of Biochemistry and Biophysics.